Visual and Non-visual Effects of Light on Health in Neonatal Intensive Care Units (NICU)

Zining Cheng

A thesis submitted in partial fulfillment of the

requirements for the degree of

Master of Science in Architecture

University of Washington

2022

Committee:

Mehlika Inanici

Marty Brennan

Heather Burpee

Program Authorized to Offer Degree:

Architecture

University of Washington

Abstract

Visual and Non-visual Effects of Light on Health in Neonatal Intensive Care Units (NICU)

Zining Cheng

Chair of the Supervisory Committee:

Associate Professor Mehlika Inanici

Department of Architecture

Only in recent years, scientists have uncovered the importance of lighting design, beyond facilitating vision. Human eyes function in a dual manner, and the second function is to facilitate healthy circadian rhythms. The photobiological research is still evolving, but preliminary findings show that light-sensing opsins within the retina interact with genes oscillating to circadian rhythms. Photoreceptors photopsin (OPN1), melanopsin (ONP4) and neuropsin (OPN5) send information that impacts health, vision, and circadian rhythms.

Research in neonatal intensive units (NICU) shows that circadian light regimes can exert a positive influence on a baby's brain and eye development, and metabolic body functions. It is necessary to design, control, and manage the intensity and spectra of light in NICU settings to support the healthy

development for premature babies. Currently, design guidelines for circadian lighting in healthcare settings are not well established; and there are not any tools that can simulate the neuropic light levels in built environments. Hence, this thesis addresses to a need for a tool that can predict the visual and non-visual effects of lighting decisions within a design workflow.

LARK Multi-Spectral Lighting simulation tool was developed in 2015 as a Rhino Grasshopper plugin to simulate the non-visual effects of lighting. The objectives of this research are i) to further develop LARK to quantify the recently discovered non-visual opsin neuropsin along with photopsin and melanopsin, and ii) to demonstrate simulation workflows for NICU settings to perform robust and accurate daylighting and electric lighting analyses for occupants including patients, clinicians, and patient families.

Sample workflows are exemplified to study the role of daylight and electric lighting in a NICU setting with the goal of improving design decisions. Different date, time, and weather conditions, spectral properties of glazing, surface materials, and electric light sources are simulated, and the resulting photopic, melanopic, and neuropic light levels are analyzed. The results of this thesis show that healthy lighting recipes, which satisfy the criteria for all three opsins, can be prescribed through dynamic commissioning practices for shading and tunable electric lighting systems, in addition to thoughtful design decisions such as appropriate glazing and material selections.

Acknowledgments

It is never an easy decision for me to choose architecture and design computing and it definitely changes the path of my career and life. I want to thank myself for the courage and insist on chasing dreams.

I am incredibly grateful for my committee chair, Mehlika Inanici, for giving me an opportunity to study with her. I aspire to the excellent guidance and helpful comments as I studied the wonderful world of architectural lighting, design computing, and healthcare design, which are always where my passion is. I am lucky to have a professional, knowledgeable, and patient instructor who is passionate about research. I will never forget her encouraging words and precise advice. She always kept me on track through all the stages of this thesis.

Besides my committee chair, I would like to convey my heartfelt gratitude towards my other committee member, Marty Brennan, who gave valuable advice, professional support, and encouragement to me on coding and debugging throughout my studies. Heather Burpee provided timely feedback and support for my thesis and presentations. My committee made sure that I was headed in the right direction. I also appreciate all the helps from other instructors and faculties for the past four years.

My sincere thanks go to Renee Cheng, the Dean of the College of Built Environments, for providing me the opportunity to join the Applied Research Consortium (ARC) program. I would also like to express my gratitude to ZGF Architects, the firm partner in the ARC program, for providing me the financial support throughout my ARC Fellowship. I thank Todd Stine, Victoria Nichols, and Kelly Chanopas from ZGF Architects for sharing their healthcare design expertise with me. I also thank Dr. Richard Lang, Dr. James Greenberg, and Yuying Cao from Cincinnati Children's Hospital Medical Center for sharing their knowledge and innovative research findings with me. We had many hybrid meetings during the pandemic years, thank you all for overcoming the technical issues and challenges of

an unusual year. I would like to thank the developers of LARK 1.0: Mehlika Inanici, Marty Brennan, and Ed Clark for letting me have the chance to use this free, open-source, and powerful tool.

Lastly, I would like to thank my beloved friends and family. My roommate, Karen Wong, spent time being my mock-up presentation audience and cheered me up during the pandemic years. My friends from different cities all over the world gave their love and confidence to my architecture career. I also thank Jianfei Li for all his care, love, and support despite the distance from the other side of the earth. Finally, I thank my parents and grandparents for their enduring love and affirmation in me. I cannot stand here without their self-giving support, and I wish to share this moment with you.

Table of Contents

Chapter 1 Introduction and Objectives 1

Chapter 2 Background 3

2.1 Visual and Non-visual Responses 3

2.1.1 Overview of the Visual System 3

2.1.2 Non-Visual Photoreceptors 5

2.1.2.1 Melanopsin 7

2.1.2.2 Neuropsin 8

2.1.3 Metrics 9

2.1.3.1 Photopic Lux 9

2.1.3.2 Equivalent Melanopic Lux 11

2.1.3.3 Equivalent Neuropic Lux 11

2.1.3.4 Photon Flux 12

2.2 Neonatal Intensive Care Unit (NICU) 13

2.2.1 NICU Design 14

2.2.2 NICU Lighting Requirements 14

2.2.3 Opsin Influences on NICU Infants 16

2.3 Simulation Tools to Calculate Visual and Non-visual Effects of Lighting 17

2.3.1. Physical Stimuli and their Simulation 17

2.3.2 Radiance 19

2.3.3 LARK and ALFA 20

2.3.4 Electric Light 23
Chapter 3 Methodology 25
3.1 Simulation Workflow 25
3.2 Simulation Tool 26
3.2.1 Multi-Spectral Lighting Channel Divisions and Calculation 26
3.2.2 Grid Simulations (Illuminance) 28
3.2.2.1. Grids and Views 28
3.2.2.2. Evaluation Criteria 29
3.2.2.3 Visualization 30
3.3 Simulation Setup and Model 31
3.3.1 Location 31
3.3.2 Weather, Date and Time 31
3.3.2.1 Point-in Time Simulation 31
3.3.2.2 Time Periods Simulation 32
3.3.3 Electric Light 37
3.3.4 NICU Model and Simulation Grids 37
3.3.5 Glazing 39
3.3.6 Surface Materials 40
Chapter 4 Result and Discussion 42
4.1. Point In Time Analysis with CIE sky 42
4.1.1 Changes at Different Time of the Year (Clinician/ Family View) 45

4.1.1.1 March 21st , Intermediate Sky, 5000K, 12 p.m. 45

4.1.1.2 June 21st , Clear Sky, 25000K, 12 p.m. 47

4.1.1.3 December 21st , Overcast Sky, 7000K, 12 p.m. 48

4.1.2 Daylight with Supplement of Electric Light and Shade Fabric (Patient View) 42

4.1.2.1 June 21st , Clear Sky, 25000K 42

4.1.2.2 December 21st , Overcast Sky, 7000K 44

4.1.3 Glazing 49

4.1.4 Surface Material 53

4.2 Period Analysis with Measured Sky Parameters 54

4.2.1 CCT and Irradiance 55

4.2.1.1 Irradiance 55

4.2.1.2 CCT 57

4.2.2 Change Over a Day 60

4.3 Analysis 64

4.3.1 Comparison of Change of Over Months, Clinician View 64

4.3.2 Comparison of Clinician/Family Facing Different Direction 65

4.3.3 Comparison with Shade Fabric and the Supplement of Electric Light 66

4.3.4 Comparison of the Patient View and Clinician/Family View 67

4.3.5 Selection of Glazing 69

4.3.6 Selection of Surface Material 70

4.3.7 Effects by Irradiance and CCT 71

4.3.8 Comparison with the Measured Sky Data 72

Chapter 5 Conclusion 74

5.1 Summary of Thesis 74

5.2 Contributions 74

5.3 Future Work 75

Bibliography 76

List of Figures

Figure. 2.1 Schematic View of Human Visual System [4]

Figure. 2.2 Diagram Representation of the Retina and Its Three Layers of Cells (the Retina with Its Specialized Cells) [5]

Figure. 2.3 Wavelength Sensitivity of the Cones and Rods Cells

Figure.2.4 Photopic, Melanopic and Neuropic Spectral Curve

Figure.2.5 For same light Intensity, Blue Light Requires Fewer Photons [48]

Figure 2.6 CIE 1931 (2°) and 1964 (10°) Standard Colorimetric Observers $x(\lambda)$, $y(\lambda)$, $z(\lambda)$ [57]

Figure 2.7 An Example on the Calculation of the CIE XYZ Tristimulus System [57]

Figure 2.8 CIE 1931 Chromaticity Coordinates [57]

Figure 2.9 CIE 1931 Best-Fit Colorimetric Epicenters x_e, y_e and Constants for Eq. (4) [59]

Figure 2.10 Comparison of HDR and Mathematical Models for A Cloudy Sky and A Clear Sky Condition [68]

Figure 2.11 ALFA Interface for Displaying Melanopic Vertical Illuminance and Hyperspectral Renderings [77]

Figure 3.1. Examples of Grid Simulation Results

Figure 3.2. Criteria and Legend Bars for (a) Photopsin, (b)Melanopsin, and Neuropsin

Figure 3.3. Demo of the Grid Simulation Result of Photopsin, Melanopsin and Neuropsin

Figure 3.4. Sky Rendering in Lark, False Color Graph and Spectral Curve of CIE Intermediate (5000K) for March 21st, Clear Sky (25000K) for June 21st and Overcast Sky (7000K) for December 21st. Diagrams by Mehlika Inanici.

Figure 3.5. A Spectrometer on the Roof of a Gould Hall is Measuring the Spectrum of Daylight in Seattle. Photo by Mehlika Inanici.

Figure 3.6. Scatter Diagram of CCT and Irradiance Data Per Minute June 9th, 2021

Figure 3.7. CCT and Irradiance Data Per Minute June 9th, 2021, Over Time (per Minute)

Figure 3.8 (a) NICU Light by BIOS (b)Normalized Spectra Power Distribution Curves of Bios Light with 3500K Comparing with CIE 5000K, 7000K and 25000K Sky

Figure 3.9. (a)NICU Single Family Patient Room of Cincinnati Children Hospital, ZGF. Photo by Ryan Kurtz and (b) Diagram based It

Figure 3.10. (a) Single Family Patient Room Floor Plan (b) Grid Distribution of the Single-Family Patient Room

Figure 3.11. Normalized Spectra Power Distribution Curves of Selected Glazing.

Figure 3.13. Normalized Spectra Power Distribution Curves of Selected Wall Surfaces.

Figure 4.1 Photopic, Melanopic, and Neuropic Light Simulation Results for June 21st, 12 p.m., Clear Sky, 25000K, Seattle, with South facing and White Wall Surfaces: (a) Daylight Only (b) with Shade Fabric from A Patient View

Figure 4.2 Photopic, Melanopic, and Neuropic Light Simulation Results for December 21st, 12 p.m., Overcast Sky, 7000K, Seattle, South Facing Glazing and White Wall Surfaces: (a) Daylight Only (b) with 3500K Electric Light Source (Wall Light 5600.8 Lumens and Ceiling Lights 7695.9 Lumens) from A Patient View

Figure 4.3 Photopic, Melanopic, and Neuropic Light Simulation Results for March 21st, 12 p.m., Intermediate Sky, 5000K, Seattle, with South facing and White Wall Surfaces with Daylight Only from A Clinician/Family View

Figure 4.4 Photopic, Melanopic, and Neuropic Light Simulation Results for June 21st, 12 p.m., Clear Sky, 25000K, Seattle, with South facing and White Wall Surfaces with Daylight Only from A Clinician/Family View

Figure 4.5 Photopic, Melanopic, and Neuropic Light Simulation Results for December 21st, 12 p.m., Overcast Sky, 7000K, Seattle, South Facing Glazing and White Wall Surfaces with Daylight Only from A Clinician/Family View

Figure 4.6 Selected Grids Points to Compare for Glazing

Figure 4.7 Grid Simulations for 4 Selected Glazing for (a) Photopic, (b) Melanopic, and (c) Neuropic Light Simulation Results

Figure 4.8 Horizontal Grid Simulation and Illuminance Curve of Selected Grids to Compare the Impact of Four Glazing Types for (a) Photopic, (b) Melanopic, and (c) Neuropic Light Simulation Results

Figure 4.9 (a)Fisheye Rendering of the Room using White, Blue and Red Wall Surfaces (b)Grid Simulations for Comparing the Effect of Surface Materials on Photopic, Melanopic, and Neuropic light

Figure 4.10 Selected Grid Point for Comparison

Figure 4.11 Selected Time Point with Varying Measured Sky Irradiance Value (CCT Values Are Relatively Constant)

Figure 4.12 (a) Photopic, (b) Melanopic, and (c) Neuropic Light Simulation Results of One Select Point with Varying Measured Sky Irradiance Value (CCT Values Are Relatively)

Figure 4.13 Grid Simulations for Comparing the Effect of Sky Irradiance Value on (a) Photopic, (b) Melanopic, and (c) Neuropic Light Simulation Results

Figure 4.14 Selected Time Point with Varying Sky CCT Value (Irradiance Value Are Relatively Constant)

Figure 4.15 (a) Photopsin, (b) Melanopsin, and (c) Neuropsin Simulation Results of a Select Point with Varying Sky CCT Value (Irradiance Value Are Relatively Constant)

Figure 4.16 Grid Simulations for Compare the Impact of CCT on (a) Photopic, (b) Melanopic, and (c) Neuropic Light Simulation Results

Figure 4.17 Curve Graphs of Measured Hourly CCT and Irradiance on June 9, 2021

Figure 4.18 Percentage of the Room Area Under the Criteria of (a) Photopsin, (b) Melanopsin, and (c) Neuropsin Using Measured Sky Spectral Data on June 9, 2021

Figure 4.19 Grid simulations to Compare Changes Over a Day for (a) Photopic, (b) Melanopic, and (c) Neuropic Light Simulation Results on June 9, 2021

Figure 4.20 Grid simulations to Compare Changes Over Months: March 21st, June 21st , and December 21st

Figure 4.21 Photopic, Melanopic, and Neuropic Light Grid simulations to Compare Difference When Clinician/Family Facing Different Direction on (a) March 21st, 12 p.m., Intermediate Sky, 5000K, (b) June 21st, 12 p.m., Clear Sky, 25000K, (c) December 21st, 12 p.m., Overcast Sky, 5000K, Seattle, with South facing and White Wall Surfaces with Daylight Only

Figure 4.22 Comparison of Photopic, Melanopic, and Neuropic Light Simulation Patient and Clinician/Family View on June 21st, Clear Sky (25000K)

Figure 4.23 Comparison of Photopic, Melanopic, and Neuropic Light Simulation Patient and Clinician/Family View on June 21st, Clear Sky (25000K)

Figure 4.24 Summary of Grid Simulations and Curve Graphs of Selected Grids Points that Compare Glazing for Photopic, Melanopic, and Neuropic Light Simulation Results

Figure 4.25 Grid Simulation to Compare Increasement of CCT for Photopsin, Melanopsin, and Neuropsin Light Simulation Results

Figure 4.26 Grid Simulation to Compare CIE Clear Sky Model (25000K) and Measured Sky on June 21st, 2021

List of Tables

Table 1. Spectral Intervals and Coefficients for 3 Channels

Table 2. Spectral Intervals and Coefficients for 9 Channels

Table 3. Transmissivity, U-Value and Solar Heat Gain Coefficients of Selected Glazing

Table 4. Reflectance Value of Surface Materials

Table 5. Percentage of the Room Area Under the Criteria of Photopsin, Melanopsin and Neuropsin on March 21st, 12 p.m., Intermediate Sky, 5000K, Seattle, with South facing and White Wall Surfaces with Daylight Only from A Clinician/Family View

Table 6. Percentage of the Room Area Under the Criteria of Photopsin, Melanopsin and Neuropsin on June 21st, 12 p.m., Clear Sky, 25000K, Seattle, with South facing and White Wall Surfaces with Daylight Only from A Clinician/Family View

Table 7. Percentage of the Room Area Under the Criteria of Photopsin, Melanopsin and Neuropsin on December 21st, 12 p.m., Overcast Sky, 7000K, Seattle, South Facing Glazing and White Wall Surfaces with Daylight Only from A Clinician/Family View

Table 8. Irradiance, CCT and One-point Opsin Values that Compare the Effect of Irradiance.

Table 9. Irradiance, CCT and One-Grid Opsin Stimulation Value of Selected Points to Compare the Effect of CCT

Table 10. Measured Hourly CCT, Irradiance, and Percentage of the Room Area Under the Criteria of Photopsin, Melanopsin and Neuropsin on June 9, 2021

Chapter 1 Introduction and Objectives

The human eye can detect electromagnetic wavelengths between 380 to 700 nanometers. The eyes function in a dual manner, the first function is vision, and the second function is to facilitate the internal body clock (aka circadian rhythms). Visual photoreceptors include cones (opsin 1, aka OPN1) and rods (opsin 2, aka OPN2). Cones are responsible for colored photopic vision with daylight, while rods are responsible for uncolored scotopic vision at a low light level. Melanopsin (OPN4) and Neuropsin (OPN5) are the photoreceptors that regulate the circadian rhythms.

Research in neonatal intensive units (NICU) shows that circadian light regimes can exert a positive influence on babies' brains, eyes, and other development. A NICU environment is designed to provide the right environment for premature infants. Every year, 15 million preterm infants are born as reported by the World Health Organization. Most premature infants grow up with a variety of chronic conditions, ranging from damaged eyesight to underdeveloped immune systems that require delicate care in the NICU. Hospitals have traditionally strived to maintain a dark environment like a mother's womb. However, practices are changing. Some countries continue to have dim conditions, while others are experimenting with bright NICUs. Contemporary NICU design practices in the United States are oriented towards single-family rooms that meet the needs of the patients and parents who stay with their babies. Compared to multi-patient rooms, private (single-family) rooms provide a better potential to create a healing environment that can enhance newborn development and family. The study of circadian rhythms in healthcare environments is still limited. There is a need to study healthcare environments for patients, clinicians, and families' perspectives. It is necessary to control and manage the wavelengths, intensity and duration, and the spectra of light in neonatal care. Previous researchers have explored the visual response and circadian response of light, but there is not any research in the field of architecture that focuses on quantifying the non-visual response from neuropsin (OPN5).

The objectives of this thesis are i) to further develop LARK Multispectral Lighting simulation tool to quantify the recently discovered neuropsin along with photopsin and melanopsin, and ii) to

determine simulation workflows for NICU settings to perform daylighting and electric lighting analyses for NICU settings. Simulations are exemplified to compare parameters such as surface materials and glazing in the context of NICU.

The methodology of this research is to utilize a multi-spectral simulation-based approach to study the impact of surface colors and materials in the room (including walls, floors, and ceilings), along with glazing and shading system alternatives. The electric lighting system, which supplements the daylighting in the room, is studied to provide the targeted range of wavelengths and intensities. A parametric study approach is employed to inform design decisions based on date and time, surface materials, glazing, and bed location in the context of NICU design. The simulation workflow is developed to quantify opsin (photopic, melanopic, and neuropic) illuminance and luminance values to study the role of daylight and electric lighting in delivering the right lighting recipes for newborn development. The quantities are evaluated based on available standards: (Illuminating Engineering Society (IES) recommended photopic illuminances, the melatonin suppression at an hourly time scale for compliance with the Recommend NICU Standard 2020, WELL Building Standard, and other emerging research results.

Chapter2 summarizes the literature review on the impact of light on visual and non-visual systems, NICU design guidelines, and the simulation tools available to architects and lighting designers. Chapter 3 summarizes the methodology, revisions implemented to Lark, and the simulation setting. Results are presented and discussed in Chapter 4. Chapter 5 summarizes the thesis findings.

Chapter 2 Background

This chapter discusses the current research on human visual and nonvisual responses to light. Most of the scientific knowledge regarding the subject of spectral changes comes from photobiology. Although it is still in its early stages to provide a comprehensive understanding of its impact on humans, a considerable body of knowledge has accumulated to help architects make informed decisions. This chapter starts with an overview of the visual and non-visual responses of the human ocular system to light, followed by a discussion on NICU design settings from a lighting design and analysis perspective, and concludes with a comparison of the existing lighting simulation software that can calculate the visual and non-visual effects of light.

2.1 Visual and Non-visual Responses

2.1.1 Overview of the Visual System

The ocular system is a complex system of networks connecting the eye and the brain (Figure 2.1). The human eye can be subdivided into two systems: ocular (i.e. lens and sclera) and neural (i.e. retina) systems (Figure 2.2). [1] Light is first received at the ocular system and transmitted to the back of the retina, which is an extension of the brain. In the retina, optical signals are absorbed and converted to electric signals. Ganglion cell axons pass the electric signals from the eyes to various parts of the brain for further processing.[2]

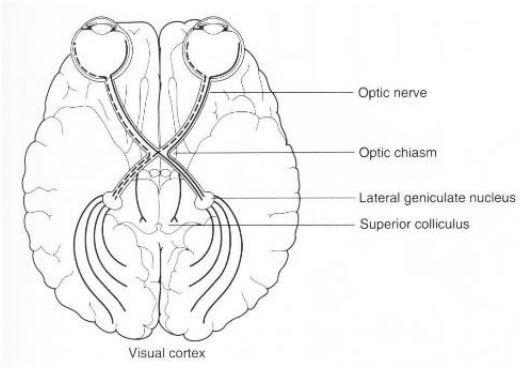

Figure 2.1 Schematic View of Human Visual System [4]

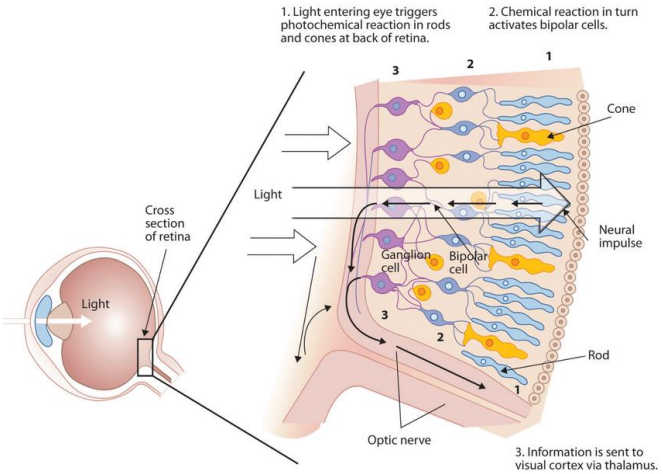

Figure 2.2 Diagram Representation of the Retina and Its Three Layers of Cells (the Retina with Its Specialized Cells) [5]

Humans have opsins as the light-sensitive photoreceptors in the retina.[3] Light passes through the ganglion layer and cells in the inner retina to the predominant visual photoreceptors in the eye. Visual photoreceptors are the cones (opsin 1, aka OPN1) and rods (opsin 2, aka OPN2). Cones are responsible for colored photopic vision, they are concentrated in the center of the retina, with an angular extent in the field of view of approximately two degrees. The three different kinds of cones are the short (S-), medium (M-), and long (L-) wavelength cones. The S-cones contain the visual photopigment cyanolabe and are maximally sensitive to wavelengths at 448 nm; the M-cones contain the visual photopigment chlorolabe and have a peak spectral sensitivity at 541 nm; the L-cones contain the visual photopigment erythrolabe and are maximally sensitive to wavelengths at 569 nm. [6] Color vision is initiated in the distal retina by combining the outputs from these three cone types into two spectrally opponent mechanisms, red versus green and blue versus yellow. The photopic curve represents the visual sensitivity of the human eye. [6] As shown in Figure 2.3, it is the combined spectral sensitivity of the S, M, L cones. It peaks at 556 nm and is defined by 1931 and 1964 as the CIE Standard photopic observer for 2° and 10° field of views, respectively. [7]

Rods contain the visual photopigment rhodopsin with a peak sensitivity at 495nm. They are responsible for uncolored scotopic vision at low light levels. They are almost entirely distributed in the

retinal angular field of view regions not covered by the cones.[3] When rods begin to saturate in response to higher light levels, cones become the dominant photoreceptor for photic input to the ganglion cells and, subsequently, to different parts of the brain. The visual message leaves the retina as ganglion cell axon spike discharges that occur either when a spot of light stimulates the retina, or when the spot of light is extinguished. This visual pathway facilitates how humans perceive shape, color, movement, and even complex geometries such as faces from different angles. [3]

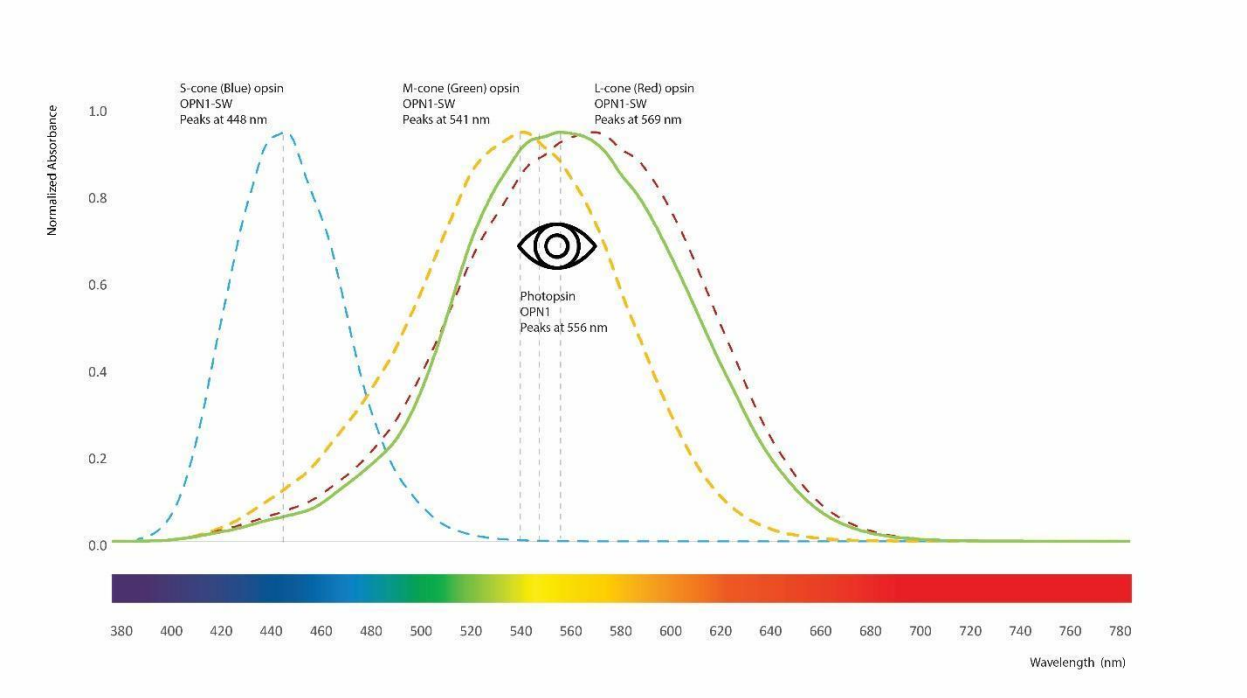

Figure. 2.3 Wavelength Sensitivity of the Cones and Rods Cells

2.1.2 Non-Visual Photoreceptors

Until recently it was accepted that the ocular system is used for vision only, but since 2001 it is known that it has both visual and non-visual functions. [3] The studies found the non-imaging response of the retina is adjusted by the rods and cones of cells and a new class of photoreceptors known as intrinsically photosensitive retinal ganglion cells (ipRGCs).[8] ipRGCs can synchronize the circadian rhythm of the human biological clock to the natural environment.

In addition to understanding how the retina converts light signals to neural signals for the visual system, it is necessary to determine the photic pathways involved in circadian, neuroendocrine, and neurobehavioral responses. Through synapses with the ipRGCs, whose axons comprise the retinohypothalamic tract that directly innervates the suprachasmatic nucleus (SCN), neurons can supply photic input to the circadian system.

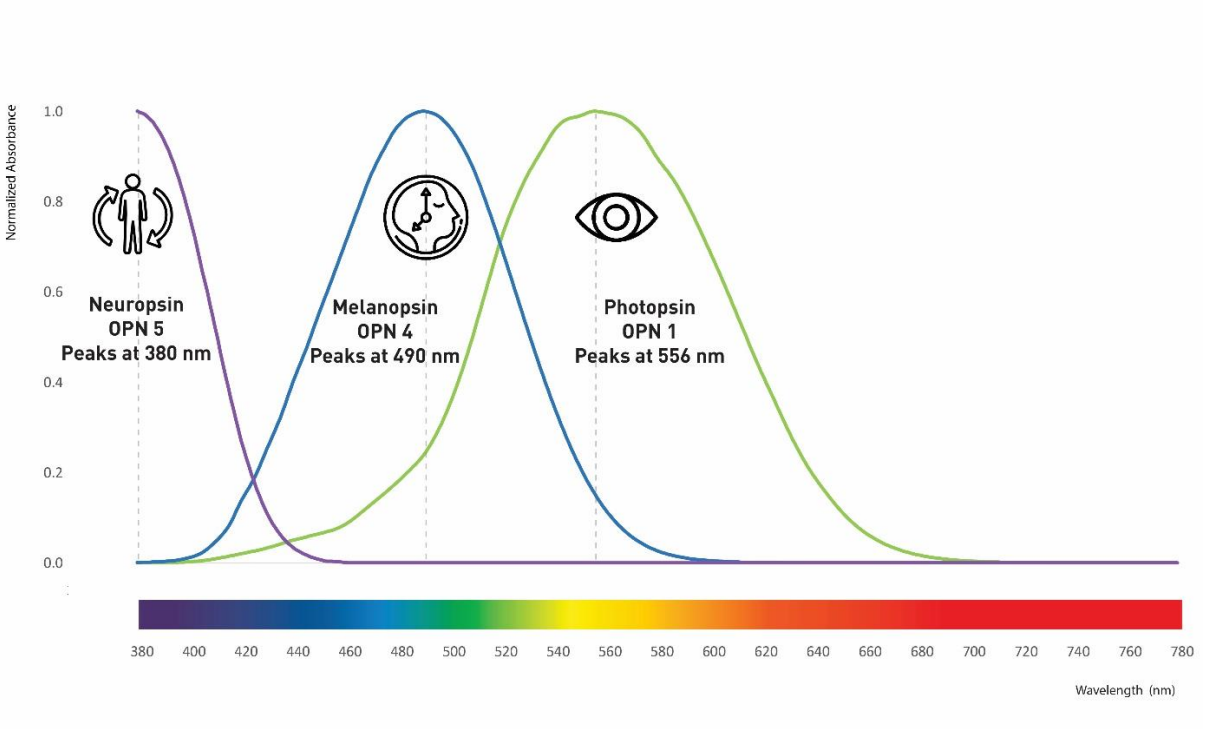

Figure.2.4 Photopic, Melanopic and Neuropic Spectral Curve

Humans have evolved to base their circadian rhythms around the natural light-dark patterns associated with daytime and night-time. Well timed light and dark cycle can provide the right environmental cues to synchronize it with the local time. However, with humans being indoors for extended periods of time, exposure to adequate levels of light have been compromised as typical indoor electric light levels often do not equate to the amount of light the human body traditionally receives outdoors. [1] Light deficiencies affecting the circadian rhythms include periods of wake and sleep, activity and rest, hunger

and eating, and variations of hormone release and body temperature. Disruption of circadian rhythm has been linked with obesity, diabetes, depression and metabolic disorders.[21][22]

2.1.2.1 Melanopsin

Melanopsin, known as Opsin 4 or OPN4, is a blue-light-responsive opsin for the mammalian circadian photopigment of ipRGCs. The available data indicate that the spectral sensitivity of melanopsin is similarly invariant with λ_{max} at approximately 480 nm. [10][11][12][13][14]

Although melanopsin phototransduction is only activated at moderate light levels (when rods are saturated), ipRGCs and their downstream responses can be activated at considerably lower light levels. [15] Cones transfer signals to ipRGCs during abrupt light shifts at these light levels, whereas melanopsin registers light signals when the light is steady. It was once assumed that 2500 lux of illumination was necessary to inhibit nocturnal melatonin in humans. [16] Later investigations have demonstrated that under some situations, ipRGCs and non-visual systems can be sensitive to considerably lower amounts of light, as low as 1 lux or less, in a carefully controlled environment, suppressing melanopsin. [17]

Melanopsin is involved in melatonin release, phase shifting, the functioning of the human body's biological clock, entrainment of circadian rhythms, hormone production, mood regulation, and cognitive and emotional processes, among other non-image-forming visual activities. [18] [19] [20] Melatonin secretion is lower during the day and keeps the body alert; it is higher at night and makes people feel weary and drowsy.

Blue light exposure during the day was beneficial in avoiding light-induced melatonin suppression at night, but blue light exposure before sleep had the reverse effect [23] Exposure to light at night has also been associated with negative health effects, such as breast cancer, circadian phase disruption and sleep disorders.[24][25] Both at night and during the day, bright blue light can boost human attentiveness and

performance. It was also more effective in raising body warmth and pulse rate, as well as reducing tiredness. [22][23]

Furthermore, several recent pieces of research have looked at the connection between artificial light and circadian rhythms, and other processes. The timing of the light intervention, on the other hand, is critical. The use of light via closed eyelids during sleep has been shown to increase circadian alignment and sleep wellness. [27] The time it takes to fall asleep is lengthened, the circadian clock is delayed, levels of the sleep-promoting hormone melatonin are repressed, the amount and timing of REM sleep are reduced and delayed, and the following morning alertness is diminished, according to studies.[27][28][29][30] Blocking blue light dramatically decreased LED-induced melatonin suppression in the evening, lowering attentive attention and subjective alertness, increasing sleep quality, and even treating the seasonal affective disorder, according to some research (SAD). [24] [32] [33]

2.1.2.2 Neuropsin

Melanopsin and neuropsin have both been shown to control circadian rhythms. [34][36][37] Rods, cones, and melanopsin-expressing, intrinsically photosensitive ganglion cells in the retina synchronize animals' behavioral circadian rhythms to light/dark cycles. The mammalian retina's molecular circadian rhythms are also synced to light/dark signals. Nearly all mammalian tissues contain working, autonomous circadian clocks that must be synced to the 24-hour day.[34] Neuropsin is required for retinal photoentrainment of the local circadian oscillator, according to recent studies. [38]

While previous studies have suggested that humans might express opsin proteins outside the eye, there was little information on what functions they might influence. It was assumed that, when humans evolved, the brain took over informing all organs of the body if it was day or night. Neuropsin is found in the retina and skin of mice, but it is also found in the brown adipose tissue through a light-sensing mechanism. Animals like squids, octopuses, cuttlefish, amphibians, and chameleon lizards may change

their skin color in the blink of an eye. [34] Their skin has photoreceptors that work independently of their brain. According to recent research, skin produces its photoreceptors.

Neuropsin, commonly known as Opsin 5 or OPN5, is an opsin with a low degree of homology to other opsins. [35] It has a peak sensitivity in the UV region. OPN5 is highly conserved and sensitive to visible violet light, with an absorption peak at 380 nm. [36] With violet light, they suppress brown adipose tissue activity and maintain a constant body temperature. The research actively demonstrates that OPN5 allows brown adipose tissue to create heat and elevate body temperature in the absence of violet light. This obstructs the body's ability to break down lipids and carbohydrates, potentially leading to metabolic disorders. In addition, neuropsin-expressing retinal ganglion cells appear to have a significant role in reducing myopia development in humans, according to current studies. Both the time of day and the retinal expression of the violet light-sensitive atypical opsin were factors in the violet light effect. [37]

Although the neuropic spectral response was not explicitly discovered in CIE S 026/E:2018 as an opsin linked to human ipRGC-influenced reactions, it remains an intriguing aspect of the scientific inquiry into human physiological and psychological responses to light.

2.1.3 Metrics

2.1.3.1 Photopic Lux

Illuminance is the amount of light incident on a surface per unit area and is calculated using the CIE spectral luminous efficiency V(λ) which represents the relative spectral response of the human eye for photopic vision (Photopsin, OPN1). The unit of illuminance is Lux (Lx, lumens per square meter) or footcandles (lumens per square foot). 1 foot candle = 10.76391 lux. Luminance is the amount of light coming from a light source or a reflecting or transmitting surface, in a given direction, and is calculated using the CIE spectral luminous efficiency V(λ). The units of luminance are candela per square meter, cd/m2. [2]

Providing the appropriate lighting levels is necessary for health care providers and patients. WELL Building Standard, the first building certification system to focus exclusively on health and wellbeing, provides general recommendations for all building typologies. Lighting Guidelines from WELL are mainly for human general health. What has yet to be explored is the specific metrics for children and the right tool for lighting designers, architects, and engineers to quantify the impact of lighting on health.

The Recommended Design Standards for Advanced Neonatal Care provides constraints of current practices, after meeting the prerequisites of energy code and visual comfort objectives. Several variables drive the study: (1) light sources, (2) source spectrum, and (3) views.[43] Recommended light values for the general exam are 500 Lx on the horizontal surface and 200 Lx on a vertical target. [40] Based on the NICU Design Guidelines the recommended range of ambient illumination levels of any plane at each bedside needs in the range of 10- 600 lux (1 to 60 foot candles). However, this guideline may not be appropriate when considering daylit rooms as daylit rooms have higher light levels. The supplemental electric lighting must be able to provide at least 2000 lux at the baby bed's plane, and it must be framed so that no more than 2% of the luminaire's light output goes beyond its illumination field. [42]

Anderson et al.[44] and Mardaljevic et al.[45] used a threshold but divided the day into three distinct periods to accommodate changing biological effects depending on exposure time: “circadian resetting” from 6:00-10:00, “alerting” from 10:00-18:00, and “light avoidance” from 18:00-6:00.

For night lighting at healthcare facilities, below 300 lux can still provide adequate light for achromatic visual tasks (e.g., reading black font on a white paper). Very modest light levels, no more than 60 lux on horizontal surfaces using warm white light, 2700 K is enough for minor visual tasks without circadian disruption but may not provide alertness. [39] The Illuminating Engineering Society (IES) RP-29-16 recommends [41] that patient room night lighting consider using a low level, less than 5 lux of warm, 2700 K light sources. This suggests that a dim-to-warm strategy that decreases the correlated color temperature of the light and the luminous flux could benefit circadian entrainment at night. [39]

2.1.3.2 Equivalent Melanopic Lux

Lux has always been an essential consideration in lighting design for visual tasks. Light also affects the release of an essential hormone, melatonin, which helps regulate sleep and wakefulness cycles. Thus, "melanopic lux" is a new metric that more accurately quantifies how the lighting in an interior space affects the melanopic response of occupants in a given environment.

Based on the standard of WELL, melanopic lux is the light measurement by quantifying the stimulus degree of light source response to Melanopsin. The higher the melanopic lux, the lower the secretion of melatonin. The higher the melanopsin, the more the secretion of melatonin, and the more likely it is to feel sleepy. The Illuminating Engineering Society (IES) RP-29-16 recommends the use of controls for task lighting that are kept in sync with light or increasing illumination in the blue spectrum during daytime. [43]

Equivalent Melanopic Lux (EML) is a measure of light's effect on stimulating the circadian system compared to the visual system. It is weighted to the melanopic response curve instead of to the photopic response curve (a.k.a. lux or photopic lux). [46] EML is typically measured on the vertical plane at the eye level of the occupant. [43] Based on the WELL v2 Q1 2022, electric lighting should reach at least 275 EML for workstations utilized during the daytime, and at least 180 EML for projects with enhanced daylight. For all workstations in frequently inhabited places, the light levels are reached for at least four hours (beginning by noon at the latest) at a height of 18 inches above the work plane. Electric illumination is essential for residential units to achieve the same aim. Furthermore, the light levels can be dimmed. Specifically, if automated lighting is used, it is automatically dimmed after 8:00 pm. [47]

2.1.3.3 Equivalent Neuropic Lux

To compare with photopic lux ad melanopic lux, neuropic lux was defined as the light measurement by quantifying the stimulus degree of light source response to neuropsin. Equivalent Neuropic Lux, ENL is a measure of light's effect on stimulating UV-induced productions of melatonin compared to the visual

system. It is a proposed alternate metric that is weighted to the neuropic curve, as defined in ENL is measured in the vertical plane at the occupant's eye level.[35] Due to the absence of established recommended ENL ranges, this research decided to use the melanopsin criterion, which is 275-1100 comparable neuropic lux. The maximum value was set as the light levels are reached for at least four hours.

2.1.3.4 Photon Flux

Photon flux, commonly used in biology studies, is the number of photons (in µmol) per second and unit area on a surface is given in µE (µEinstein; 1 Einstein Equals energy of 1 mole of photons/m^2s). [48] As shown in figure 2.5, blue light requires fewer photons for the same light intensity since each photon has a higher energy content. The photon flow is crucial in determining the number of electrons produced by a solar cell. As the photon flux does not give information about the energy or wavelength of the photons, the energy or wavelength of the photons in the light source must also be specified. [48]

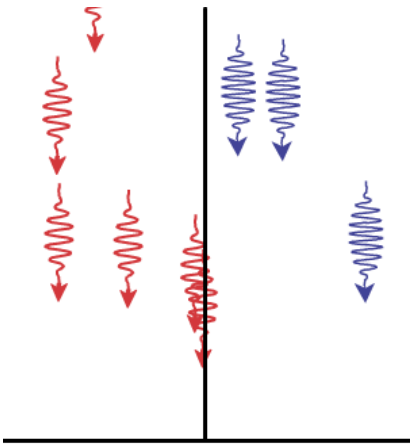

Figure.2.5 For same light Intensity, Blue Light Requires Fewer Photons [48]

A photon has a distinct energy Ep which is defined with Planck constant h = 6.63 x 10^34 (J•s); speed of light c = 2.998 x 108 (m/s); frequency f (s^-1); wavelength λ (m).[49] Irradiance in photon flux is

converted using Equation 1. Thus, the energy of a mole of photons of a given wavelength is $E_p \cdot N_A$, where N_A=6.022 x 1023 mol^-1. [49]

$$E_P = h\,f = \frac{h\,c}{\lambda}$$

Equation 1

The spectral irradiance, the most common way of characterizing a light source, can be determined by converting the photon flux at a given wavelength. [48][49] The photon flux can be determined by converting the number of photons to µmoles of photons using Equation 2, where Np is the number of photons per second and surface unit and can be calculated from the irradiance (I) by the nm value for λ. In summary, Equation 3 applies to the conversion of irradiance [W/m²] into quantum flux [µE] when wavelength is expressed in nm.[49][50]

$$E_{QF} = \frac{N_p}{N_A \times 10^{-6}}\,[\mu mol/(m^2\,s)]$$

Equation 2

$$E_{QF} = \frac{I \times \lambda \times 5.03 \times 10^{15}[m^{-2}\,s^{-1}]}{6.02 \times 10^{17}[\mu mol^{-1}]} = I \times \lambda \times 0.836 \times 10^{-2}\,[\mu mol/(m^2\,s) = \mu E]$$

Equation 3

2.2 Neonatal Intensive Care Unit (NICU)

Every child born before 28 weeks of pregnancy is considered extremely premature. Many grow up with a variety of chronic conditions, ranging from damaged eyesight to under-developed lungs and immune systems that make them prone to poor outcomes even when routine infections occur [36][37][38]. They might spend months in the hospital as medical staff tries to get them closer to a normal-term birth at 40 weeks. Newborn intensive care is described as the treatment of medically unstable or severely ill newborns who require 24-hour nursing, complex surgical procedures, continuous breathing support, or other intense treatments.[50]

2.2.1 NICU Design

The NICU is designed to protect the physical safety of infants, families and staff and designed to minimize the risk of infant abduction. Contemporary designs contain sufficient single-family rooms to meet the needs of parents who expect to stay with their babies. compared to multi-patient rooms, private (single-family) rooms provide for a better potential to create tailored and private surroundings for each newborn and family. However, to provide appropriate space at the bedside for both caregivers and families, these rooms must be larger than an infant space in an open multi-bedroom design, with extra bedside storage and communication capabilities to minimize caregiver isolation or excessive movement. A private patient room intended for a single baby and his or her family should have a minimum size of 180 square feet (16.7 square meters) of unobstructed floor area, according to the 9th edition of the Recommended Standards for Newborn ICU Design.[50] Each room is intended to provide the newborn and family with visual and speech privacy, as well as a comfortable reclining chair for skin-to-skin care and a reclined sleep surface for at least one parent. When feasible, a second parent's sleep surface, a bathroom, a shower, and lockable storage for parents should be given. The purpose of giving parents sleep space is to remove impediments to their engagement and enhance connection.[50]

To improve the quality of cleaning, durability, a desirable ambient sound level, and high indoor air quality, the room's comprehensive design should include the flooring, wall finish material, and acoustic ceiling as a system. [50] Only flooring materials with a light reflectance value of less than 30% are advised.[2][51]

2.2.2 NICU Lighting Requirements

Traditional approach and existing NICU standards believe that hospitals strive to maintain sterile, quiet, and dark environments to mimic conditions in the womb by given ambient lighting levels in infant spaces shall be adjustable through a range of at least 10 to no more than 600 lux and it also does not require outside the window. [50] Also, the two existing NICU design standards recommend having windows only

intended to encourage and support family engagement. [50] [52] The goal was to establish an environment that encouraged early mother-infant bonding by providing family accommodations and amenity areas across the unit and inside patient rooms. [50] [51][52] [53]

If exterior windows are available, they should be placed carefully to minimize direct sunlight reaching the child and causing glare. Where a window or skylight is provided, external windows in infant spaces or infant rooms must be glazed with a maximum U value of 0.50 and must be located at least 2 feet (0.6m) away from the infant bed.[50]

Many hospitals and offices' glazing systems typically are composed of laminated glass might not provide proper light since having coatings that block crucial wavelengths, the penetration of the violet range of light. [53] Thus, just bringing neonates closer to windows might not provide the full range of spectrum environments for healing. Also, it is necessary to control and manage the amount and the spectra of light in neonatal care, and determine what intensity, quantity, spectrum, timing, duration, spatial distribution, and adaptation photic history are most important for supporting premature infants' development.

Control of electrical illumination in infant areas should be capable of adjustment across the recommended range of ambient illumination levels, as measured on any plane at each bedside. [50] Separate procedure lighting shall be mounted at each infant bed. Furthermore, as mentioned previously, just placing newborns closer to windows may not offer adequate light since many hospital and workplace windows have coatings that exclude important wavelengths. Likewise, delivering daylight light that can't be fine-tuned for individual patient needs isn't enough. Electrical lighting in baby spaces should also be adjustable over the appropriate range of ambient lighting levels, as measured on any plane at each bedside. [50] Temporary increases in illumination needed to check a newborn or execute a treatment should be possible without impacting other newborns if it is a twin patient room.

Controls for both natural and electric light sources should allow for instant dimming of any bed position. Since bright light may be both uncomfortable and detrimental to the growing retina, every effort should be taken to keep direct light out of the eyes of infants. Shading devices should be simple to use so

that they may be used at different times of the day. Procedure lights that can be adjusted for intensity, field size, and direction will assist shield the infant's eyes from direct exposure while also providing the best visual support for the staff. Instead of a floor stand, the process light should be positioned on the headwall, ceiling, or incubator. [50]

The spectral properties of the light, brightness levels, duration, and time of exposure should all be addressed since the circadian reaction of people to light is reliant on the light that enters the eye. To simulate light entering the user's eye, the light levels must be attained on the vertical plane, at the eye level of the occupant.[47] It is also important to consider the duration of exposure to light, as well as the timing of exposure. Bright light stimulation of the circadian system at night might have a detrimental influence on sleep quality.

2.2.3 Opsin Influences on NICU Infants

Recent research demonstrated that circadian light had a favorable impact on newborn development, including the brain, eyes, immune systems, and other metabolic processes. [34][35][36][37][38] Newborn light exposure affects the development of the retina, many preterm infants raised under the artificial lighting of a NICU do not experience normal eye development. Opsins deep within the brain directly sense specific wavelengths of light that are found in daylight but not typically in artificial lights. Also, in 2013, their research shows that newborn light exposure affects the development of the retina, explaining that partially explains why so many preterm infants raised under the artificial lighting of a NICU do not experience normal eye development.

2.3 Simulation Tools to Calculate Visual and Non-visual Effects of Lighting

2.3.1. Physical Stimuli and their Simulation

CIE Standard Colorimetric Observers 1931 and 1964 are two sets of standard color matching functions adopted by the CIE for color vision as shown in figure 2.6. The main premise of color matching functions is to modify the respective radiant powers to match the color of any light stimulus with additive combinations of three primary stimuli. Humans are trichromats, meaning they see color through three different types of cones in their retinas. That is, at the retina, the complete spectrum of incident stimulus is condensed to three signals. As a result, presenting color stimuli in three dimensions is both possible and practicable. [54][55][56]

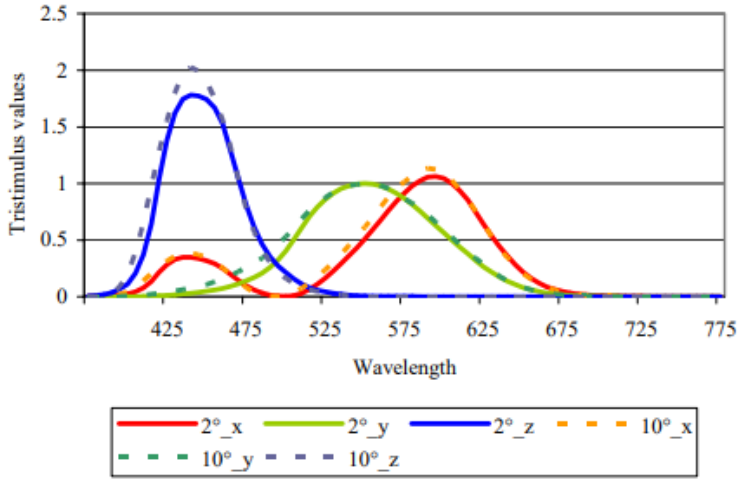

Figure 2.6 CIE 1931 (2°) and 1964 (10°) Standard Colorimetric Observers x(λ), y(λ), z(λ). [57]

CIE uses CIE XYZ color space to define standard colorimetric observer. The XYZ system was designed for 2° viewing fields and is used by the CIE 1931 Standard Colorimetric Observer. The color matching functions, x(λ), y(λ), and z(λ), weight the spectral power distribution of any stimuli to produce the CIE XYZ values. It's worth noting that y has been chosen to match the spectral luminous efficiency function for photopic vision, OPSN1, which is the CIE 1924 Standard Observer, Standard Observer response curve, V(λ). Cone vision and brightness levels of more than 3cd/m2 are relevant. As a result, the

1931 Standard Colorimetric Observer integrates color matching and heterochromatic brightness matching qualities into a single system.[54][55]

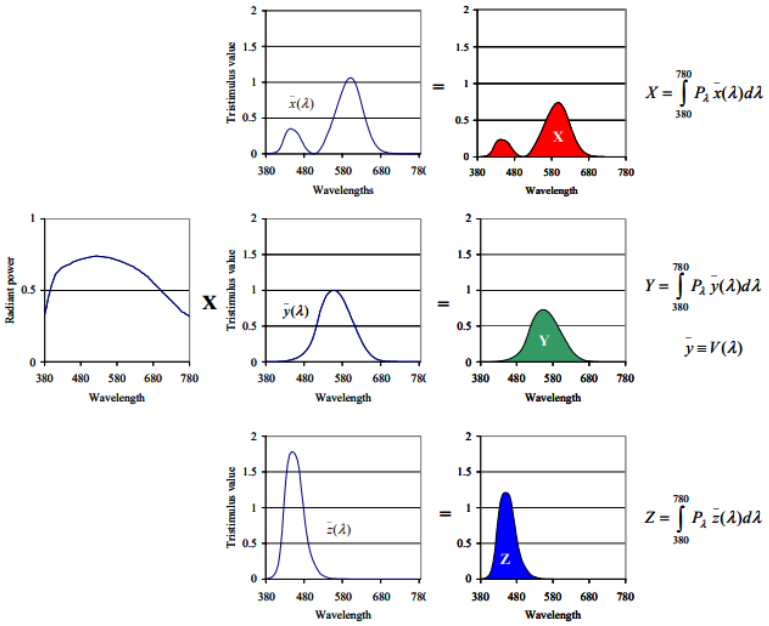

Figure 2.7 An Example on the Calculation of the CIE XYZ Tristimulus System. [57]

Color can be represented in a two-dimensional space using CIE Chromaticity Coordinates. CIE chromaticity coordinates, x, y, and z are the fractions of CIE X, Y, and Z values to their summation, respectively. Because the total of x, y, and z equals unity, it is possible to get a two-dimensional representation by removing the z value. The CIE Chromaticity diagram (x,y), which is presented in a rectangular coordinate system (Fig.2.8), is used to establish chromaticity coordinates by convention. [54][58]

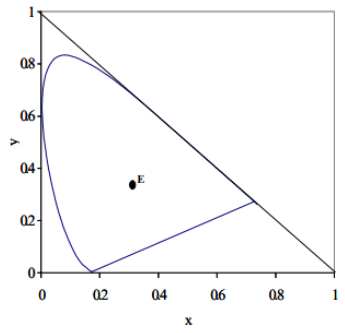

$$x = \frac{X}{X+Y+Z}$$

$$y = \frac{Y}{X+Y+Z}$$

$$z = \frac{Z}{X+Y+Z}$$

$$x + y + z = 1$$

Figure 2.8 CIE 1931 Chromaticity Coordinates. [57]

The correlated color temperature (CCT), which approximates the absolute temperature of a blackbody whose chromaticity is closest to that of the light source, is often used to assess the color attributes of light sources. Iso-temperature lines, which are short straight lines that cross the Planckian locus, make calculating the CCT for any light source that is not on the Planckian locus easier. As the chromaticity of the light source moves away from the Planckian locus, the metric becomes inefficient. Hernandez uses chromaticities calculated from our measurements of nearly 7000 daylight and skylight spectra to test an equation that accurately maps CIE 1931 chromaticities x and y into CCT in Equation 4, where the coefficients are listed in Figure 2.9 and n is defined by in Equation 5.[59]

$$CCT = A_0 + A_1 \exp(-n / t_1) + A_2 \exp(-n / t_2) + A_3 \exp(-n / t_3) \quad \textit{Equation 4}$$

$$n = (x - x_e) / (y - y_e) \quad \textit{Equation 5}$$

	Valid CCT Range (K)	
Constants	3000–50,000	50,000–8×10^5
x_e	0.3366	0.3356
y_e	0.1735	0.1691
A_0	−949.86315	36284.48953
A_1	6253.80338	0.00228
t_1	0.92159	0.07861
A_2	28.70599	5.4535×10^{-36}
t_2	0.20039	0.01543
A_3	0.00004	
t_3	0.07125	

Figure 2.9 CIE 1931 Best-Fit Colorimetric Epicenters x_e, y_e and Constants for Eq. (4) [59]

2.3.2 Radiance

Radiance is a suite of tools for performing photopic lighting simulation for the calculation of optical properties of optically complex window products including lighting, daylighting, and solar control design to improve the energy efficiency of buildings.[60] It includes a renderer and other tools for quantifying the simulated light levels. It uses ray tracing to perform all lighting calculations, accelerated by the use of an

octree data structure. Radiance offers complete flexibility in terms of scene geometry and materials and has been validated using detailed measurements.[61]

2.3.3 LARK and ALFA

Lark multi-spectral lighting (LARK) and Adaptive Lighting for Alertness (ALFA) are the two currently available spectral daylight simulation platforms that use spectral data of skies and materials to perform multi-spectral, photopic, and melanopic quantities.[62][63][64] Lark is a free and open-source tool that was initially developed by a collaboration of the University of Washington and ZGF Architects LLP in 2015, while ALFA is a licensed tool that was released by Solemma LLC & Alertness CRC, in 2018.[64] Both systems, which run directly as Grasshopper plugin in Rhinoceros 3D, were designed to calculate circadian lighting metrics, but they can also provide visual spectrum representations of the simulated settings. [62][63][64][65]

When compared to RGB (Red, Green, Blue) 3 channels lighting simulations, the multispectral simulation tools have more channels, and therefore more accurate color in format. ALFA uses 81-color channels while Lark uses 3- or 9-channels simulations, however, it is possible to increase the number of channels at a higher computational cost. Photopic and equivalent melanopic illuminance or luminance are provided in their output. [68][69][70][71] Compared to RGB (Red, Green, Blue) 3 channels lighting simulations, the multispectral simulation tools have more channels, and therefore more accurate color in format. ALFA uses 81-color channels while Lark uses 3- or 9-channels simulations, however, it is possible to increase the number of channels at a higher computational cost. Photopic and equivalent melanopic illuminance or luminance are provided in their output. [68][69][70][71]

Lark's spectral resolution allows users to plan and study lighting while taking into account local sky, outdoor context, glazing optics, surface materials, interior design, and viewer position. [69][70] It uses an N-step method based on the physically realistic Radiance rendering engine.[67][68] It achieves a spectral

resolution in three steps: first, it divides the spectrum of simulated light sources into three or nine consecutive wavebands, then it runs a standard RGB simulation for each triplet of consecutive wavebands, and finally, it combines the outputs of the three or nine-channel simulation. [69] For every location in ALFA's database, the spectral sun and sky are precomputed in a radiative transfer library called libRadtran. [72] It involves employing Radiance's backward raytracing method to go back toward the sensor position, accounting for spectral reflectance and transmittance at each material contact. [68] [69]

To model the daylight spectrum, Lark and ALFA take quite different methodologies. ALFA utilizes libRadtran to produce colorful skies and calculate spectral irradiance for different places and times based on atmospheric parameters or sky luminance. [68] ALFA creates skies based on the user's location, date, and time, and allows users to pick between different sky conditions (clear, overcast, hazy, heavy rain clouds). [70] The normal mid-latitude summer profile of the US Air Force Geophysics Laboratory (AFGL) was utilized in libRadtran to create spectral sun and sky for ALFA. [45][70] It replicates point-in-time occurrences, and annual simulations are not possible owing to the requirement of entering user-specified sky types. [68] However, because this method depends on historical atmospheric data and uses radiative transfer models, it takes specialized knowledge, and its photopic illuminances differ from normal Radiance8 simulations that employ CIE or Perez sky models. [68]

LARK models the spectral sky with an observed or assumed global horizontal sky spectra or CCT, encompassing the sky and the sun. The skydome is colored with the global horizontal spectra. The default sunlight in LARK is simulated as 5,455 Kelvin equal-energy white, however, it may be changed to a certain spectral power distribution (SPD) or CCT. [68][70] Lark may employ CIE and Perez skies, with an user input or measured global horizontal CCT. CCTs are not part of standard weather files but they can be recorded using a spectroradiometer or colorimeter. [68][71] Based on direct and diffuse global horizontal irradiance, an improved LARK weighs the CCT of the sun and sky. When a user specifies a CCT, it must be converted to spectral irradiance data using the Wyzsecki and Stiles formula, which is a proven approach to create full-spectrum data for CCTs ranging from 4,000 to 25,000 K. [68] [70] In the realm of architecture and daylighting,

Inanici et al. used spectral sky from observed CCT values to examine interior settings for circadian and photopic lux.[63] [70] The precision of measured spectrum irradiance data is higher than that of the CIE illuminants, which reflect standard sky conditions. [70] This approach needs in situ observations from an unobstructed site and does not depict color change over the sky-dome. [71] In general, the sky color spectrum proved difficult to manage in our simulations since, unlike ALFA, Lark relies on the extra input parameters. [71]

A few studies have used LARK and ALFA to perform multi-spectral simulations under measured and computed spectral skies experienced exterior and interior, respectively. [68] [69][70][71] ALFA simulates the spectra of direct and diffuse radiation independently by modeling the sun using the alien solar spectrum and traveling through an atmospheric profile.[68][70] In comparison to measurements, Balakrishnan et al. found that Lark generates the closest color coordinates to HDR captures, richer color information, and the most accurate SPD for dim morning and evening sky represents, whereas ALFA works best for clear skies. [70] ALFA and Lark simulations produced similar results for sensitivity to material reflectance spectrum and glass transmittance spectrum. [69][70][71]

Figure 2.10 Comparison of HDR and mathematical models for a cloudy sky and a clear sky condition [68]

2.3.4 Electric Light

Although daylighting has better performance than electric light in terms of circadian efficacy, the ability to incorporate electric lighting into a model is critical because all buildings have electric lighting and daylight may not provide sufficient light levels depending on the building design and daylight availability outside. [73] The pattern of the normal daily cycle has changed dramatically in contemporary times. According to the data from the Environmental Protection Agency (EPA), 96 percent of adult human life is spent inside. [74] Daylight may not be sufficient, and electric lighting can be harmful when light stimulus is provided at biologically disruptive times. Most threshold-based evaluation criteria that do not account for time of light exposure continue to have this restriction.[45]

Electric light sources are included in simulation software through IES file format. IES format represents measured luminous intensity values in three dimensions; however, IES files do not include spectral information. [75][76] ALFA and Lark overlay the IES luminous intensity data with manufacturer-provided spectral power distribution (SPD), resulting in color corrected presentation that retains the same luminous flux as the original IES data.

Electric light sources are included in ALFA through import of IES files, an industry standard format for representing measured luminous intensity information in three-dimensions; however, IES files do not include spectral information. ALFA applies a user-settable spectral power distribution (SPD) on top of the IES luminous intensity data, and the result is a spectral intensity adjusted to maintain the same luminous flux as the original IES data.[64] Based on its spectral computations, ALFA calculates melanopic illuminance, photopic illuminance, and M/P ratios, which it may display over a work plane sensor grid or a vertical sensor grid.[64] The whole spectrum irradiance of the work plane and vertical sensor data can be exported as a comma separated value (CSV) file and the analysis result can be only available in ALFA as shown in figure 2.11.[64]

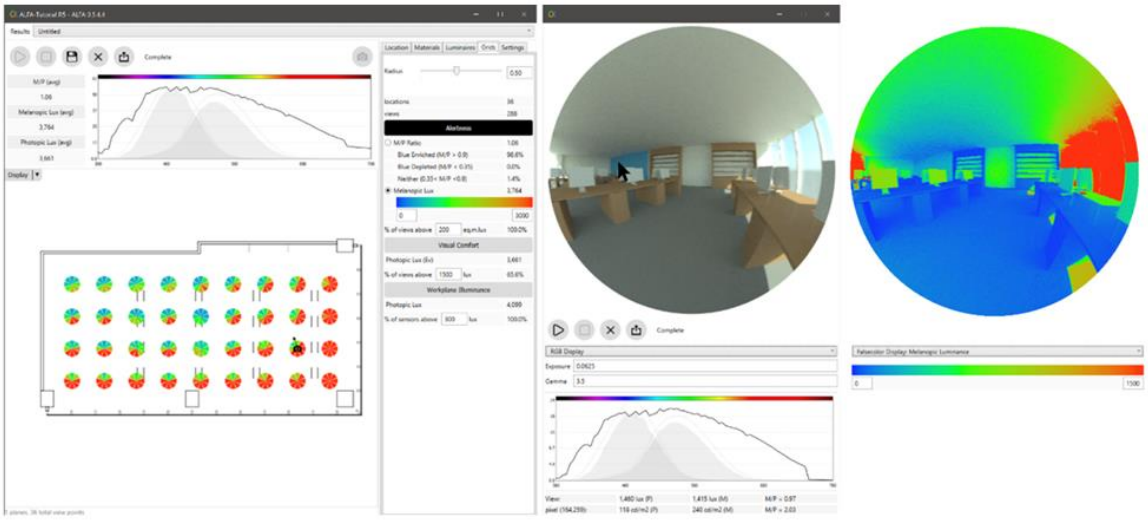

Figure 2.11 ALFA Interface for Displaying Melanopic Vertical Illuminance and Hyperspectral Renderings [77]

LARK can simulate electric lighting sources by using spectral candle power distribution curves to simulate light distribution and spectral power distribution curves to simulate color content.

Chapter 3 Methodology

The workflow described in this section combines spatial grid simulation across a 2D surface which can provide an accurate value for each test spot and a human-centric approach that represents an immersive evaluation of space with hemispherical fisheye images. These simulations have been developed to assess daylight and electric light to predict health potential, visual and non-visual impact within different occupants' views, and other related design and operational parameters in NICU. The simulation workflow is intended to help designers and researchers to perform a holistic assessment of the luminous environment in NICU as it impacts intended functional use and design.

Section 3.1 will describe the integration of the general simulation workflow of this research. Section 3.2 will introduce the Grasshopper grid tool, revised based on LARK 1.0, which allows users to perform conventional spatial grid-based illuminance simulations and luminance maps. The NICU patient room setup is introduced in Section 3.3. This room models an existing NICU, and selected parameters are explored through simulation and analysis. In Section 3.4, the threshold values for the various performance indicators are determined using the three opsins described in the previous section. The evaluation criteria (minimum, maximum, or recommended values are discussed.

3.1 Simulation Workflow

The main technique is a grid-based simulation of the room space, and it is based on two sets of NICU occupants: i) clinicians or families and ii) patients. For each time and date specified for the study, a series of grid simulations and hemispherical fisheye renderings are generated from these view spots. The fisheye rendering images are created from a single viewpoint. The hemispherical fisheye images with a 180-degree view range provide a full human field of view in a given direction and provide a more direct sense of space. The grid simulation result focuses on the quantity of light for opsin stimulations; the values are evaluated using the threshold values provided in Section 3.4.

3.2 Simulation Tool

The original version of the Lark Multi-spectral Lighting system (beta versions and Lark 1.0) was initially adopted for this study, but a new version has been developed to accommodate changes. The authors modified the coefficients for multi-channel calculation based on information from Dr. Inanici [81], added electric lighting simulation based on information from ZGF Architects [82]. The grid simulation and visualizations are customized based on NICU settings. The sections that follow outline the changes made to Lark 1.0 as part of the thesis work.

3.2.1 Multi-Spectral Lighting Channel Divisions and Calculation

In typical lighting simulations, the full spectrum is reduced to 3 channels (red, green, and blue, which is also what is known as RGB) for computational efficiency. In Radiance software, these intervals correspond to 586-780 nm for red, 498-586 nm for green, and 380-498 nm for blue (Table 1). These channels determine the color and reflectance properties of surface materials, and the color and luminance flux of electric light sources. Table 1 and Equations 6-8 show the coefficients used in Lark (version to be released) for 3 channels to calculate OPN1, OPN4, and OPN5. Therefore, to calculate radiance channel divisions, for 3-channel:

Table 1. Spectral Intervals and Coefficients for 3 Channels

Channels	λ (nm)	λ (nm)	OPN1	OPN4	OPN5
R	568	780	0.049591265	0.000061	0
G	498	568	0.081085718	0.000296	0
B	380	498	0.130177072	0.0017	0

*OPN 1, Illuminance = 179 * (0.265 * R + 0.67 * G + 0.065 * B)* *Equation 6*

*OPN4, EML = 179 * (0.021 R + 0.3911 * G + 0.6068 B)* *Equation 7*

*OPN 5, ENL = 179 * (1 * B)* *Equation 8*

The multi-spectral rendering approach allows us to increase the channels so that the color simulations are more accurate. 9-channel designation further divides the RGB channels into 3 channels each, which have 3 channels for blue, 3 channels for green, and 3 channels for red. In the revised version, the spectral intervals were rearranged for efficient distribution of coefficients for each channel, shown in Table 1. Equations 9-11 give the calculation of the new 9 channels method for each opsin.

Table 2. Spectral Intervals and Coefficients for 9 Channels

Channels	λ (nm)	λ (nm)	OPN1	OPN4	OPN5
R3	630	780	0.049591265	0.000061	0
R2	608	630	0.081085718	0.000296	0
R1	587	608	0.130177072	0.0017	0
G3	558	587	0.259754249	0.019	0
G2	529	558	0.250355905	0.1033	0
G1	499	529	0.164071102	0.268843	0
B3	459	499	0.055590209	0.4165	0.00007
B2	419	459	0.009098397	0.1784	0.0948
B1	380	419	0.0003	0.0119	0.905131

*OPN 1, Illuminance = 179 *(0.130177072 * R_1 + 0.081085718 * R_2 + 0.049591265 * R_3 + 0.164071102 * G_1 + 0.250355905 * G_2 + 0.259754249 * G_3 + 0.0003 * B_1 + 0.009098397 * B_2 + 0.055590209 * B_3)* *Equation 9*

*OPN4, EML = 179 * (0.0017 * R_1 + 0.000296 * R_2 + 0.000061 * R_3 + 0.268843 *G_1 + 0.1033 * G_2 + 0.019 * G_3 + 0.0119 * B_1 + 0.1784 * B_2 + 0.4165 * B_3)* *Equation 10*

*OPN5, ENL = 179 * (0.905131 * B_1 + 0.0948 * B_2 + 0.00007 * B_3)* *Equation 11*

There are no restrictions on the number of channels that can be simulated, but simulation time increases with more channels. Studies show that a 9-channel approach is sufficient for daylighting, and for most electric light sources. [68]

3.2.2 Grid Simulations (Illuminance)

3.2.2.1. Grids and Views

In this revised tool, testing grids can be set up by selecting a 2D surface, (usually the floor of the space for horizontal illuminance measurements) and offsetting the grid plane to match the task surface (such as a table or patient bed). For vertical tasks, users can offset the height of the simulation surface to an eye level and grid orientation to the direction of eye gaze.

The tool allows the view to be set up in two options as shown in Figure 3.1. One is from clinician and family views with four or eight vertical directions at human eye level, presenting the field of view when they look around. The other is from the patient's view lying in the bed and looking up to the ceiling. The human eye level was set up as 5’4’’ (1.67m) from the floor and the patient’s eye level was approximately equal to the infant incubator height, 4’ (1.22m)

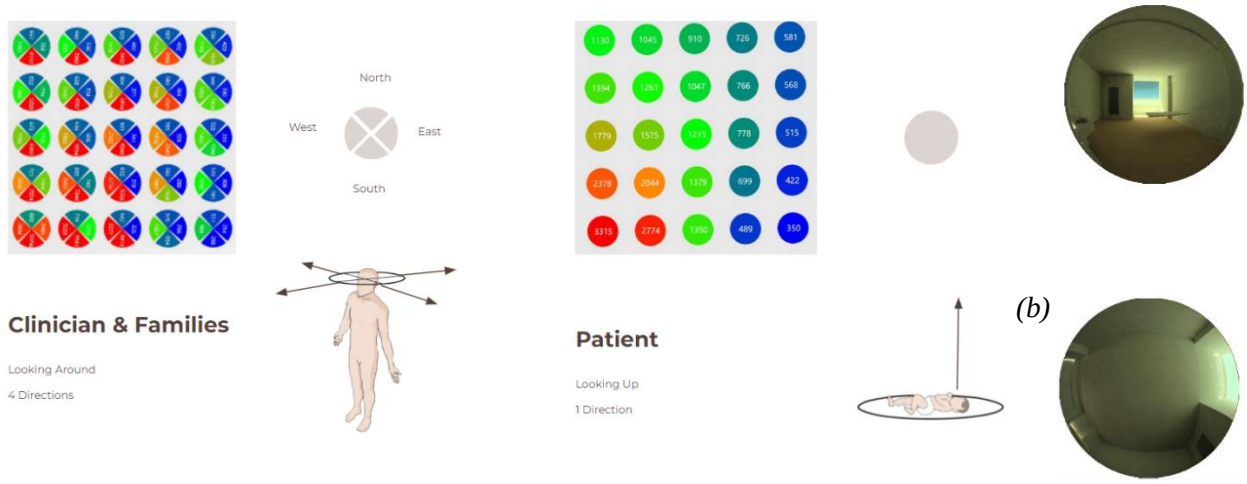

Figure 3.1. (a) Examples of Grid Simulation Results for Clinician and Families View of Four Directions and for Patient View with One Direction (b) Examples of Fisheye Rendering of Clinician/Families View facing South and (c) Patient View Facing the Ceiling.

3.2.2.2. Evaluation Criteria

Computed metrics included photopsin (OPN1), melanopsin (OPN4) and neuropsin (OPN5) to compare the visual and nonvisual effects of light on health in Neonatal Intensive Care Units.

Based on LEED v4.1 IEQ-DAYLIGHT (option 2), the criteria for photopsin (OPN1) were required to demonstrate illuminance levels between 300 lux and 3,000 lux. And according to the standard of WELL, V2, Q1 2022, for space used during the daytime, electric lighting is used to achieve for at least 275 Equivalent Melanopic Lux (EML) [43] at least four hours (beginning by noon at the latest) at a height of 18 inches above the work-plane for all workstations in regularly occupied spaces. And the light levels are achieved on the vertical plane at eye level to simulate the light entering the eye of the occupant. The maximum value of melanopsin (OPN4) is set as getting it for four hours, which is 1100 EML in this study. This value does not mean that values above 1100 EML are excessive, it means that the lower value will entrain the system in four hours, and the upper value will suffice after one-hour exposure. Values

above 1100 EML do not cause discomfort, they simply do not offer further benefit. For neuropsin (OPN5), due to the absence of established criteria, the criteria of melanopsin is adopted, resulting in a range of 275 - 1100 Equivalent Neuropic Lux (ENL).

3.2.2.3 Visualization

The color of the legend bar uses a typical false color for photopsin (OPN1) which represents the visual stimuli, Gray to dark blue legend is adopted for melanopsin (OPN4), and gray to violet for neuropsin (OPN5). The different false color ranges for OPN4 and 5 were purposefully selected to differentiate the metrics from the visual response. Blue and violet were chosen to remind the audience of the peak sensitivities of OPN4 and 5. A similar approach was not adopted for OPN1, as a typical false color for visual response includes multi-range colors as shown in Figure 3.2.

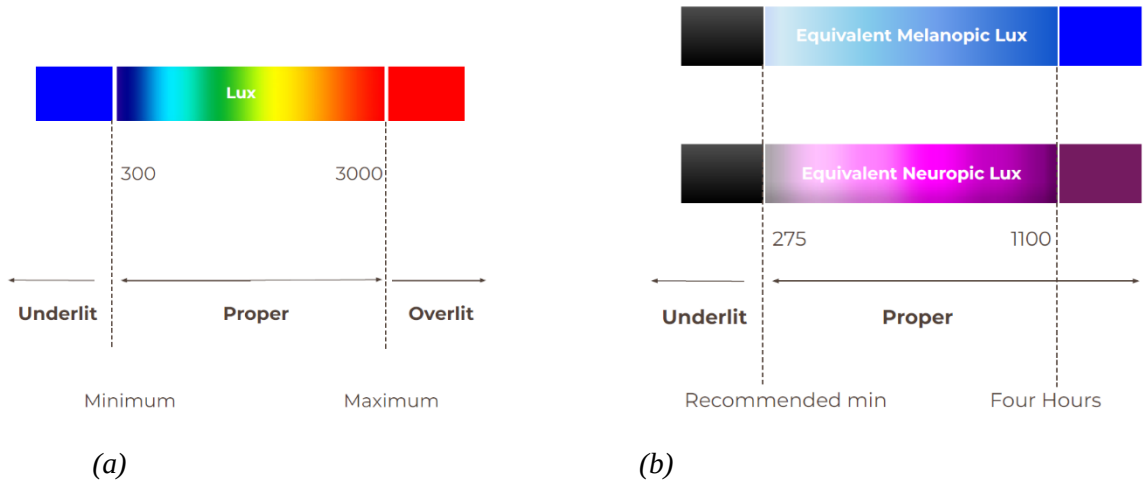

(a) *(b)*

Figure 3.2. Criteria and Legend Bars for (a) Photopsin, (b)Melanopsin, and Neuropsin.

The visualization of the tool, shown in Figure 3.3, provides a 2D dots graph with numeric values with colors on each dot for patient view or each piece for clinician views. False color is used to represent for OPN1, measurement points shown in red are over lit, and all of the other dark blue measurement points do not receive good lighting. For melanopsin and neuropsin results, the gray color corresponds to the minimum recommended levels, darker blue, and darker violet represents higher circadian stimulation

and black means that the value is lower than the criteria. Users can switch the bar to show the percentage of room area higher, under, and lower than the criteria mentioned in Section 3.1.2.3. Test points' location, values for each opsin, and percentage information is automatically written in an excel file that can be saved by the users.

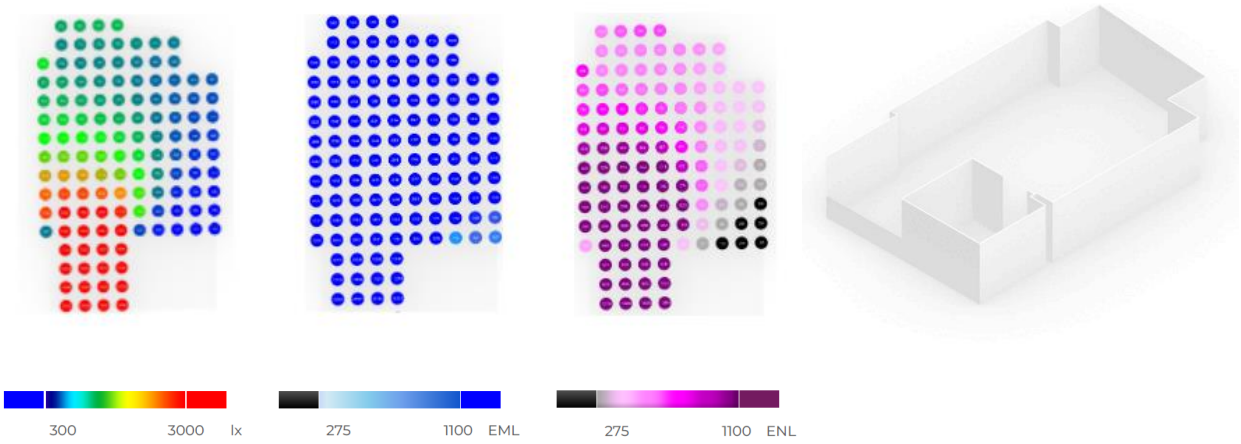

Figure 3.3. Demo of the Grid Simulation Result of Photopsin, Melanopsin and Neuropsin.

3.3 Simulation Setup and Model

3.3.1 Location

The location was selected in Seattle (latitude: 47.6062° N, longitude: 122.3321° W). The sky spectral data were collected at the roof of Gould Hall, University of Washington.

3.3.2 Weather, Date and Time

3.3.2.1 Point-in Time Simulation

To give a method for calculating sky luminance in daylighting design procedures, CIE has mathematically developed 15 different universal basis sky conditions. The initial simulations used the solstices and equinox with CIE sky models and a probable CCT value associated with the sky type. Among these sky conditions, intermediate, overcast, and clear skies have been widely used in

daylighting simulations all over the world. In LARK, the sky uses measured spectral sky irradiance, and the sky condition is determined by the global horizontal irradiance input to Radiance gensky or gendaylit commands. The skies in standard lighting simulation tools are grayish white but in real life, the sky color ranges from gray to blue, and there is variability across the sky dome. In Lark, the color of the sky is based on Correlated Color Temperature, CCT, which is a measure of light source color appearance defined by the proximity of the light source's chromaticity coordinates to the blackbody locus. March 21 was modeled as an intermediate sky with a CCT of 5000K, June 21 as a clear sky with a CCT of 25000K, and December 21 as an overcast sky with a CCT of 7000K as shown in Figure 3.4.

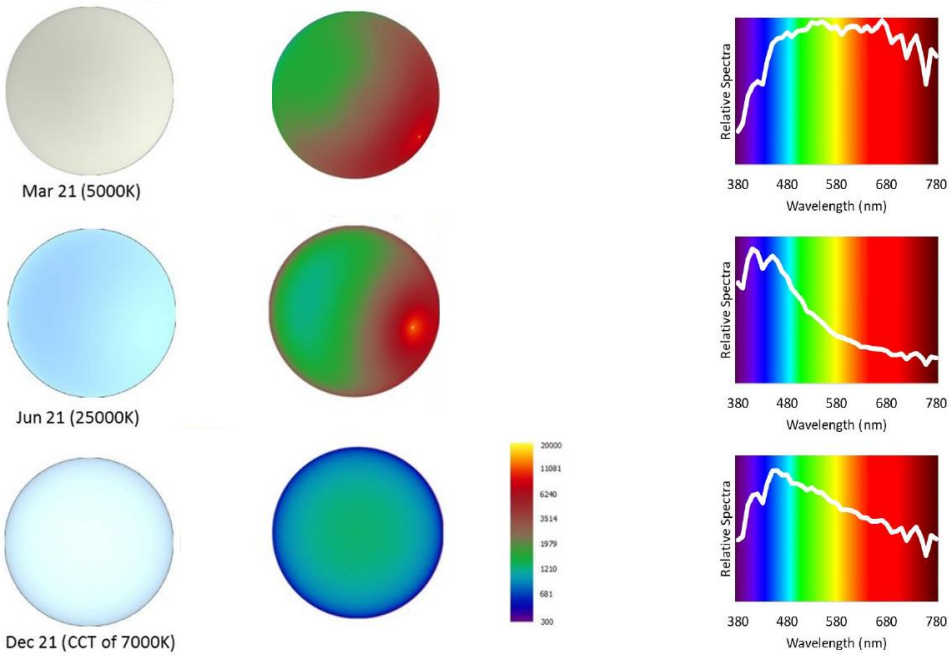

Figure 3.4. Sky Rendering in Lark, False Color Graph and Spectral Curve of CIE Intermediate (5000K) for March 21st, Clear Sky (25000K) for June 21st and Overcast Sky (7000K) for December 21st. Diagrams by Mehlika Inanici.

3.3.2.2 Time Periods Simulation

In the second phase of simulations, instead of using assumed CCT values, sky spectral and irradiance measurements collected under naturally occurring skies are utilized. This approach is useful for

quantifying the impact of actual sky spectra on visual and non-visual light metrics. The measured sky-spectra is modeled based on the data collected from a cosine-corrected spectrophotometric sensor, mounted on the roofs of Gould Hall, which measures the spectrum of daylight in Seattle (Figure 3.5).

Figure 3.5. A Spectrometer on the Roof of a Gould Hall is Measuring the Spectrum of Daylight in Seattle. Photo by Mehlika Inanici

To get the full-wavelength sky spectra data and sky CCT, the raw data is calibrated through a Python script and processed with Colour, which is a Python-based color science package. [78] This package implements color theory transformations and algorithms, to calculate CIE XYZ, xy chromaticity coordinates, and CCT. [78] The author utilized the Hernandez et al. method to quantify CCT from spectra. [59] The calculations steps include:

1. The time stamps are organized.

	time	337.71	338.17	338.63	339.09	339.55	340	340.46	340.92	341.38	...	819.89	820.39	820.89	821.39	821.89	822.39	822.89	823.39	823.89	time_cvt
0	20210604161252	20.0	19.0	21.0	13.0	25.0	17.0	22.0	23.0	25.0	...	919.0	933.0	948.0	959.0	952.0	934.0	930.0	892.0	885.0	2021-06-04 16:12:52
1	20210604161353	22.0	18.0	22.0	23.0	25.0	28.0	19.0	22.0	24.0	...	910.0	935.0	945.0	957.0	954.0	941.0	918.0	894.0	887.0	2021-06-04 16:13:53
2	20210604161454	21.0	17.0	24.0	31.0	21.0	22.0	23.0	23.0	26.0	...	913.0	934.0	949.0	953.0	953.0	939.0	931.0	892.0	878.0	2021-06-04 16:14:54
3	20210604161555	21.0	25.0	26.0	20.0	17.0	23.0	27.0	21.0	26.0	...	913.0	930.0	948.0	950.0	952.0	933.0	925.0	897.0	879.0	2021-06-04 16:15:55
4	20210604161656	20.0	20.0	20.0	26.0	23.0	19.0	21.0	27.0	19.0	...	913.0	933.0	955.0	961.0	960.0	942.0	924.0	899.0	880.0	2021-06-04 16:16:56

2. The irregular wavelength columns are converted to extrapolated into integers.

```
import numpy as np

for col in col_delta:
    df[col] = np.nan
df.head()
```

	time	337.71	338.17	338.63	339.09	339.55	340	340.46	340.92	341.38	...	771	772	773	774	775	776	777	778	779	780
0	20210604161252	20.0	19.0	21.0	13.0	25.0	17.0	22.0	23.0	25.0	...	NaN	NaN	NaN	NaN	NaN	NaN	NaN	NaN	NaN	NaN
1	20210604161353	22.0	18.0	22.0	23.0	25.0	28.0	19.0	22.0	24.0	...	NaN	NaN	NaN	NaN	NaN	NaN	NaN	NaN	NaN	NaN
2	20210604161454	21.0	17.0	24.0	31.0	21.0	22.0	23.0	23.0	26.0	...	NaN	NaN	NaN	NaN	NaN	NaN	NaN	NaN	NaN	NaN
3	20210604161555	21.0	25.0	26.0	20.0	17.0	23.0	27.0	21.0	26.0	...	NaN	NaN	NaN	NaN	NaN	NaN	NaN	NaN	NaN	NaN
4	20210604161656	20.0	20.0	20.0	26.0	23.0	19.0	21.0	27.0	19.0	...	NaN	NaN	NaN	NaN	NaN	NaN	NaN	NaN	NaN	NaN

3. Eliminate duplicate Full wavelength.

```
col_needed = [str(i) for i in range(380,781,1)]
print(len(col_needed))
col_old = df.columns
col_existed = []
for a in col_old:
    if  '.' not in a:
        col_existed.append(a)
# 340,793,time,time_cvt doesn't count
print(len(col_existed))
col_existed
```

```
401
13
['time',
 '340',
 '433',
 '452',
 '514',
 '529',
 '617',
 '639',
 '677',
 '692',
 '753',
 '793',
 'time_cvt']
```

4. Sort and filter out the range between 380-780 nm.

```
df = df.reindex(columns=sorted(df.columns))
df.columns
```

```
Index(['337.71', '338.17', '338.63', '339.09', '339.55', '340', '340.46',
       '340.92', '341.38', '341.84',
       ...
       '820.39', '820.89', '821.39', '821.89', '822.39', '822.89', '823.39',
       '823.89', 'time', 'time_cvt'],
      dtype='object', length=1418)
```

```
df[col_delta].head()
```

	380	381	382	383	384	385	386	387	388	389	...	771	772	773	774	775	776	777	778	779	780
0	NaN	NaN	NaN	NaN	NaN	NaN	NaN	NaN	NaN	NaN	...	NaN	NaN	NaN	NaN	NaN	NaN	NaN	NaN	NaN	NaN
1	NaN	NaN	NaN	NaN	NaN	NaN	NaN	NaN	NaN	NaN	...	NaN	NaN	NaN	NaN	NaN	NaN	NaN	NaN	NaN	NaN
2	NaN	NaN	NaN	NaN	NaN	NaN	NaN	NaN	NaN	NaN	...	NaN	NaN	NaN	NaN	NaN	NaN	NaN	NaN	NaN	NaN
3	NaN	NaN	NaN	NaN	NaN	NaN	NaN	NaN	NaN	NaN	...	NaN	NaN	NaN	NaN	NaN	NaN	NaN	NaN	NaN	NaN
4	NaN	NaN	NaN	NaN	NaN	NaN	NaN	NaN	NaN	NaN	...	NaN	NaN	NaN	NaN	NaN	NaN	NaN	NaN	NaN	NaN

5. The full-length wavelength value is calculated based on two nearest wavelengths by linear approximation using Linear Method
6. CCT value is calculated using Colour-science package

```
# cct calculation Test
import colour

# sd_to_XYZ By default : CIE 1931 2 Degree Standard Observer
sd = colour.SpectralDistribution(df_fullwave.iloc[1][0:-2].to_dict())
xy = colour.XYZ_to_xy(colour.sd_to_XYZ(sd))
colour.temperature.xy_to_CCT_Hernandez1999(xy)
```

```
from tqdm import tqdm
df_cct = df_fullwave.copy()
tqdm.pandas()

df_cct['CCT'] = df_cct.progress_apply(getCCT, axis=1)
df_cct.head()
```

```
  1%|▉                                                                | 358/37141 [00:03<04:39, 131.47it/s]D:\Anaconda3\lib\site-packages\colour\temperature\hernandez1999.py:95: Run
timeWarning: overflow encountered in exp
  + 5.4535e-36 * np.exp(-n / 0.01543),
  1%|▉                                                                | 456/37141 [00:03<04:38, 131.95it/s]D:\Anaconda3\lib\site-packages\colour\temperature\hernandez1999.py:94: Run
timeWarning: overflow encountered in exp
  + 0.00228 * np.exp(-n / 0.07861)
  1%|▉                                                                | 498/37141 [00:04<04:37, 131.84it/s]D:\Anaconda3\lib\site-packages\colour\temperature\hernandez1999.py:86: Runt
imeWarning: overflow encountered in exp
  + 0.00004 * np.exp(-n / 0.07125)
 16%|██████████                                                       | 6015/37141 [00:46<03:53, 133.11it/s]D:\Anaconda3\lib\site-packages\colour\temperature\hernandez1999.py:84: Run
timeWarning: overflow encountered in exp
  + 6253.80338 * np.exp(-n / 0.92159)
D:\Anaconda3\lib\site-packages\colour\temperature\hernandez1999.py:85: RuntimeWarning: overflow encountered in exp
  + 28.70599 * np.exp(-n / 0.20039)
 21%|█████████████                                                    | 7709/37141 [00:58<03:42, 132.41it/s]D:\Anaconda3\lib\site-packages\colour\temperature\hernandez1999.py:85: Run
timeWarning: overflow encountered in double_scalars
  + 28.70599 * np.exp(-n / 0.20039)
100%|████████████████████████████████████████████████████████████████| 37141/37141 [04:43<00:00, 131.11it/s]
```

7. CCT Standard deviation is calculated for each day and different periods
8. Average values are calculated.

```
mean_10m = df_cct_time.groupby('date').resample('10Min')['CCT'].mean()
mean_30m = df_cct_time.groupby('date').resample('30Min')['CCT'].mean()
mean_60m = df_cct_time.groupby('date').resample('60Min')['CCT'].mean()
```

```
mean_10m
```

```
date        time_cvt
2021-06-04  2021-06-04 16:10:00    3764.236511
            2021-06-04 16:20:00    3851.489918
            2021-06-04 16:30:00    3929.987039
            2021-06-04 16:40:00    3856.309288
            2021-06-04 16:50:00    3801.884931
```

In this thesis, data from June 9th, 2021, was selected to represent a day with variable CCTs calculated from spectra data. Figures 3.6 and 3.7 compare the CCT value for every minute from 7:00 a.m. to 8:50 p.m. with the solar irradiance value got from the University of Washington, Department of Atmospheric Sciences. [83] CCT and irradiance together define the characteristics of the sky: i) CCT

values define the color appearance of the light source in Kelvin; and ii) irradiance defines the intensity of daylight (power per unit area).

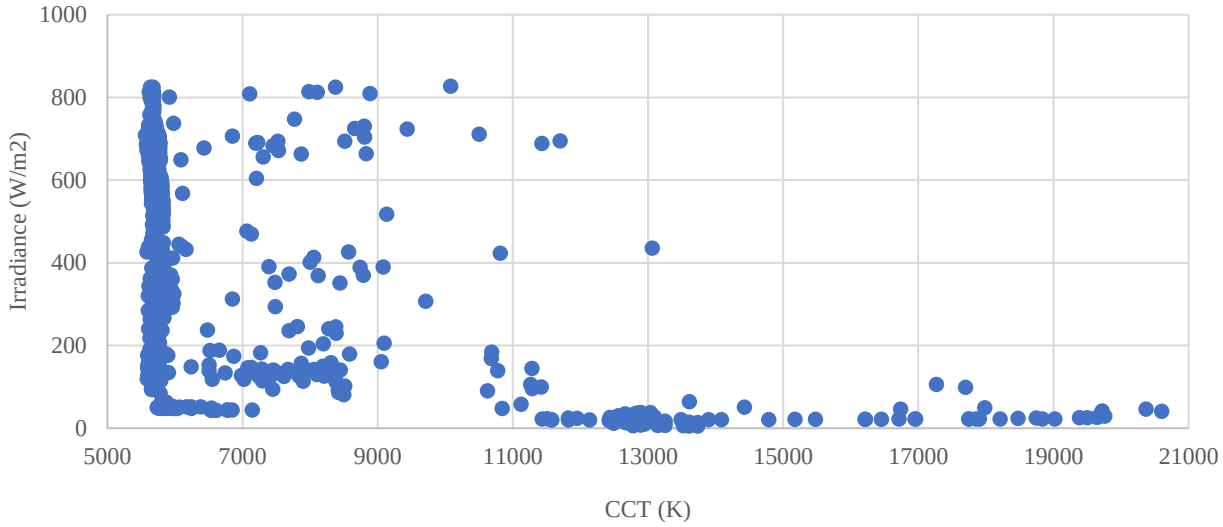

Figure 3.6. Scatter Diagram of CCT and Irradiance Data Per Minute June 9th, 2021

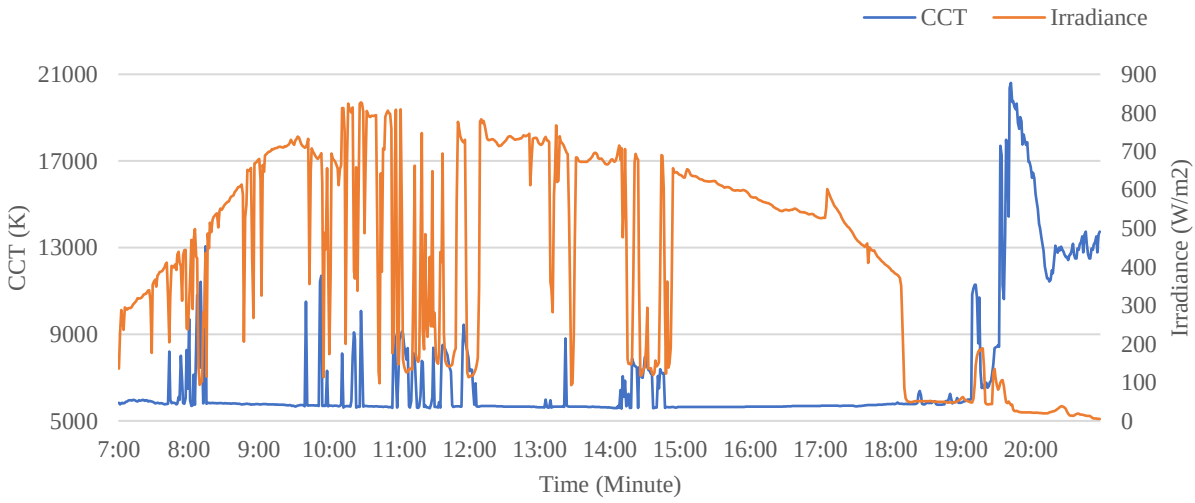

Figure 3.7 CCT and Irradiance Data Per Minute June 9th, 2021, Over Time (per Minute)

3.3.3 Electric Light

The Electric was selected from an existing children's hospital, which is manufactured by BIOS. It has several channels for different time periods and in this research, the author selected the daytime scenario, which is 3500K. Comparing its normalized spectra curve with the 5000K, 7000K, and 25000K skies, as shown in Figure 3.8, it is obvious that this electric light has a lower level for the violet range and a higher level for the blue (490nm) and red range (630nm).

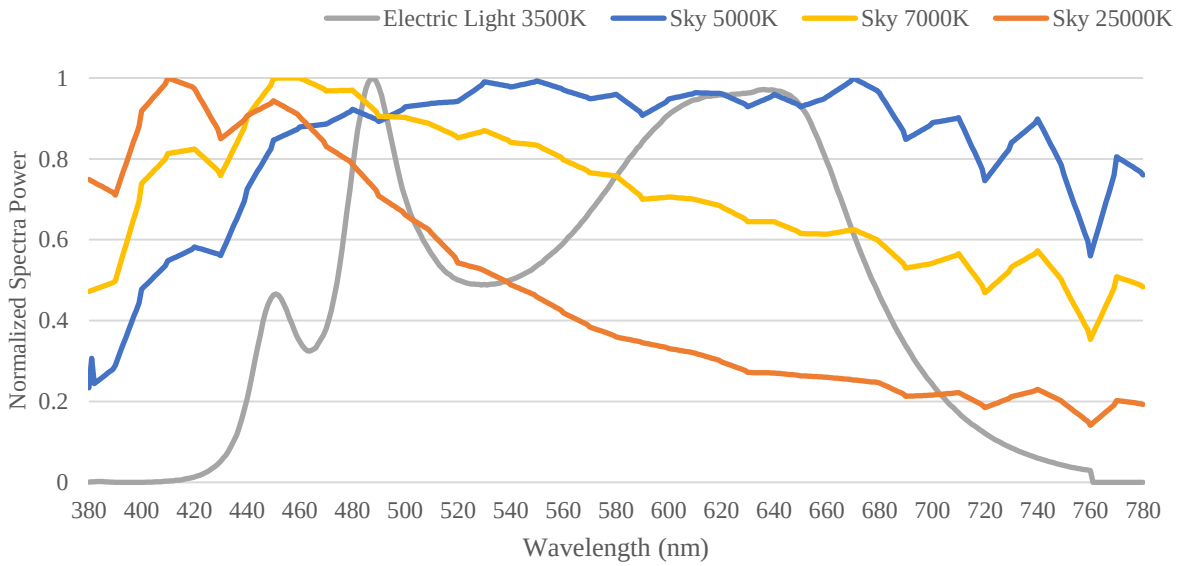

Figure 3.8 (a) NICU Light by BIOS (b)Normalized Spectra Power Distribution Curves of Bios Light with 3500K Comparing with CIE 5000K, 7000K and 25000K sky.

3.3.4 NICU Model and Simulation Grids

The author selected a single-family patient room based on an existing children's hospital designed by ZGF Architects, shown in Figure 3.9. It was chosen as a representative example of contemporary typical NICU patient room design in the United States, where daylight and an understanding of its dynamics have played an important role in its design. The single-family patient room has the patient bed in the middle and a family resting area near the window as shown in the plan (Figure 3.10 (a)). Using an

existing typical NICU patient room where now daylight considerations were central to the architect's design intent allows us to discuss the role of lighting on human responses to light stimuli within the interior. The window is oriented to the south orientation, which receives the higher light levels among the four cardinal directions. The simulation grids in this study were set up for every 0.6 meters, as illustrated in Figure 3.10 (b).

(a)

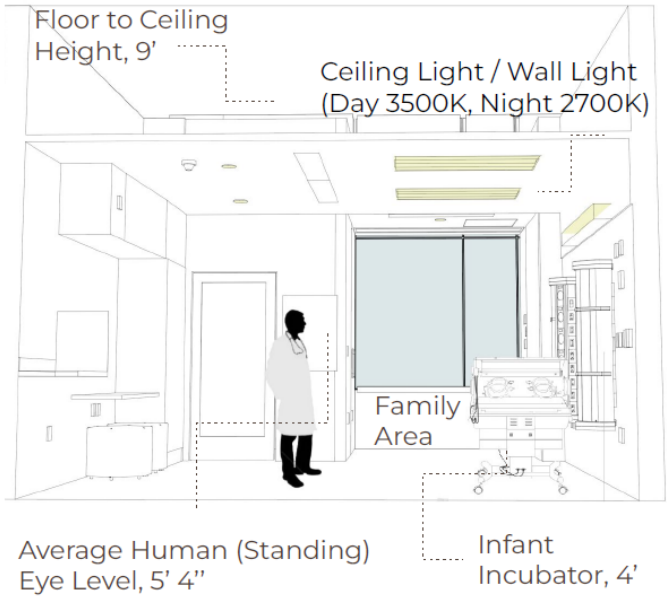

(b)

Figure 3.9. (a)NICU Single Family Patient Room of Cincinnati Children Hospital, ZGF. Photo by Ryan Kurtz and (b) Diagram based It

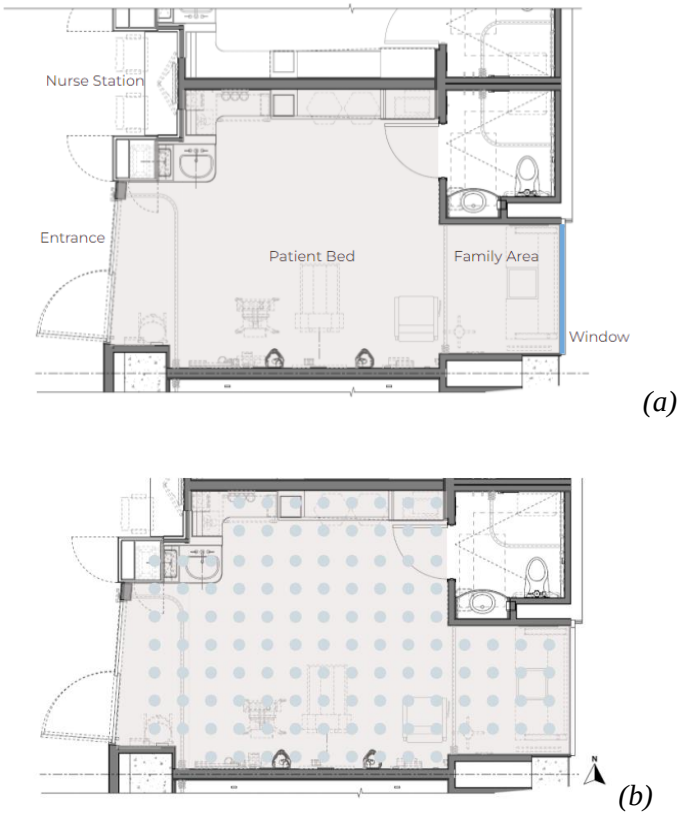

Figure 3.10. (a) Single Family Patient Room Floor Plan (b) Grid Distribution of the Single-Family Patient Room

3.3.5 Glazing

To investigate the influence of the impact of different glazing systems on three opsins, glazing options that filter sunlight and provide framed views of the surrounding landscape were identified from existing children's hospital projects. Their spectral data was checked using Optics 6, a program for creating glazing layers and computing spectral data for different stacks of components from the integrated International Glazing Database (IGDB).[79] Selected four glazing with very different performances are aimed to compare how it can influence the transmission of different spectrum ranges of light. Figure 3.11 and Table 3 depict the normalized spectral power distribution curve, transmissivity, u-value, and solar heat gain coefficient of the four glass alternatives.

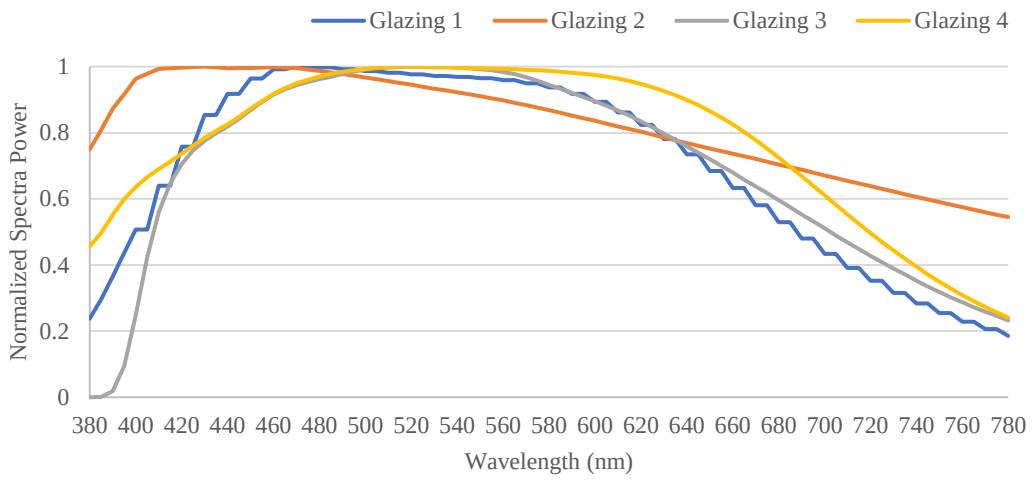

Figure 3.11. Normalized Spectra Power Distribution Curves of Selected Glazing.

Table 3. Transmissivity, U-Value and Solar Heat Gain Coefficients of Selected Glazing.

	Glazing 1	Glazing 2	Glazing 3	Glazing 4
Transmissivity	46.8%	45.9%	35.5%	58%
U-Value/Summer (Btu/Hr*Sqft* ^{o}F)	0.25	0.34	0.34	0.29
U-Value/Winter (Btu/Hr*Sqft* ^{o}F)	0.28	0.31	0.34	
Solar Heat Gain Coefficients (SHGC)	0.22	0.25	0.27	0.28

3.3.6 Surface Materials

To compare how surface material color can influence the performance of each opsin, the author selected three wall surface materials, white, blue, and red walls from the Spectra Material Database. [80] Figure 3.13 shows the rendering of using these three wall materials and their normalized spectra power distribution curve. Other surface materials that include floor, ceiling and shade fabric (Transmissivity = 72%) were fixed. The reflectance value for opaque surfaces is shown in Table 4.

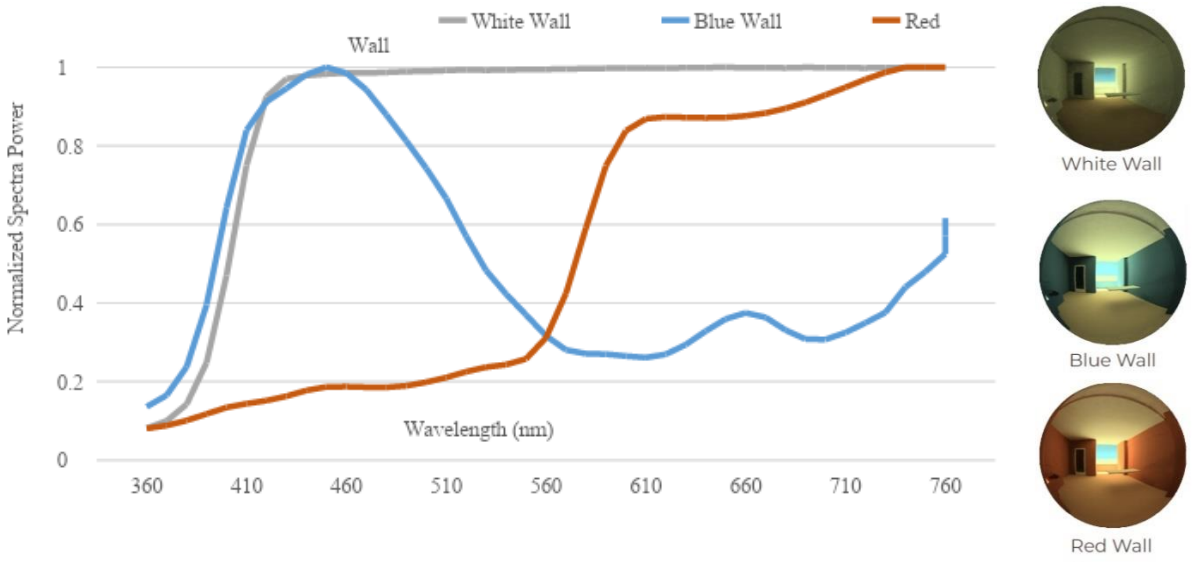

Figure 3.13. Normalized Spectra Power Distribution Curves of Selected Wall Surfaces.

Table 4. Reflectance Value of Surface Materials

Material	V(λ)Reflectance	M(λ)Reflectance	M/P Ratio
White Wall	0.93	0.92	0.99
Blue Wall	0.19	0.35	1.91
Red Wall	0.31	0.14	0.45
Ceiling	0.89	0.88	0.98
Floor	0.52	0.41	0.78

Chapter 4 Result and Discussion

Architectural features such as weather, orientation, glazing transmittance, surface materials, view directions, shades, and electric light sources are design decisions that impact the luminous environment. The resulting building shapes the lighting experience for its occupants and determines both the photopic and circadian light exposure.

This chapter demonstrates the application of the eight scenarios for daylight and electric light assessment using the NICU single-family patient room introduced in Section 3.3. The results for each scenario are presented using 2D grid simulation, graphs, and fisheye rendering images to enable the comparison of the effect of luminous environment on opsins. These results are analyzed for each indicator and then compared and discussed with each other.

4.1. Point In Time Analysis with CIE Sky

In environments where daylight is the main source of light, multiple analyses are performed to simulate date, time, and sky type. In this section, June, and December are selected to explore the clear, and overcast sky scenarios. The base cases simulate using clear and CIE skies with CCT values of 25000K and 7000K, respectively. The base cases are compared to scenarios where shade fabric is used to control glare, and electric lighting is used to supplement daylight.

4.1.1 Daylight with Supplement of Electric Light and Shade Fabric (Patient View)

4.1.1.1 June 21st , Clear Sky, 25000K

Figure 4.1.a shows a fisheye rendering from the patient view (i.e. patient lying on the bed) and June horizontal grid simulation throughout the room for OPN1, OPN4, and OPN5 under daylight only conditions on June 21, at 12 p.m., with clear skies (25000K). The wall surfaces are white. At this time, the family resting area and part of the patient bed area nearby the window are glary; 20% of the room area is over 3000 lux and 80% area of the room is between the desired range of 300 to 3000 lux. The grid points across the entire room satisfy the minimum required Equivalent Melanopic Lux (EML) and

Equivalent Neuropic Lux (ENL). This scene shows the potential of daylight as a primary light source in delivering adequate light intensity and spectra to the circadian system. However, there is a glare issue in the vicinity of the window, and it is necessary to address the problem through shade controls. Figure 4.1.b shows that adding shade fabric decreases photopic illuminance by 16.8%, melanopic (OPN4) and neuropic (OPN5) illuminance by 15.1% and 16.8%.

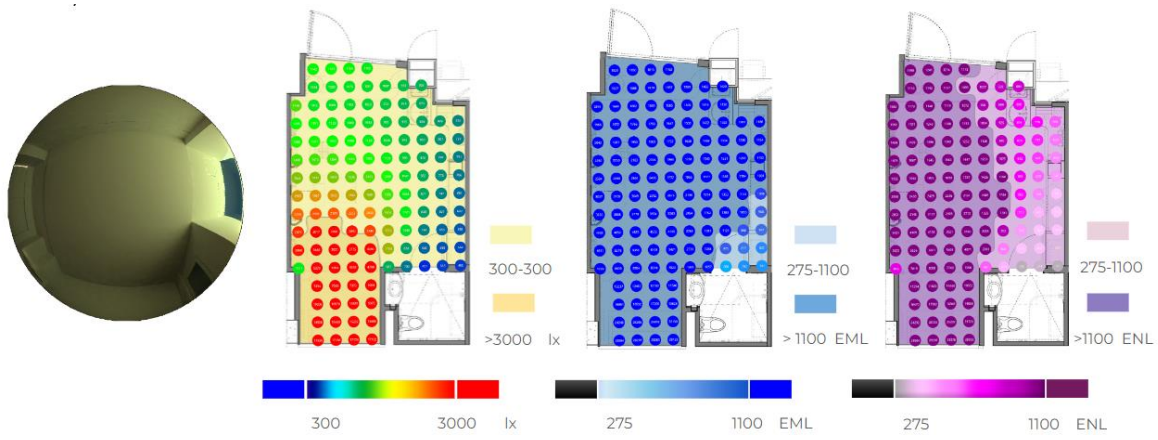

(a)

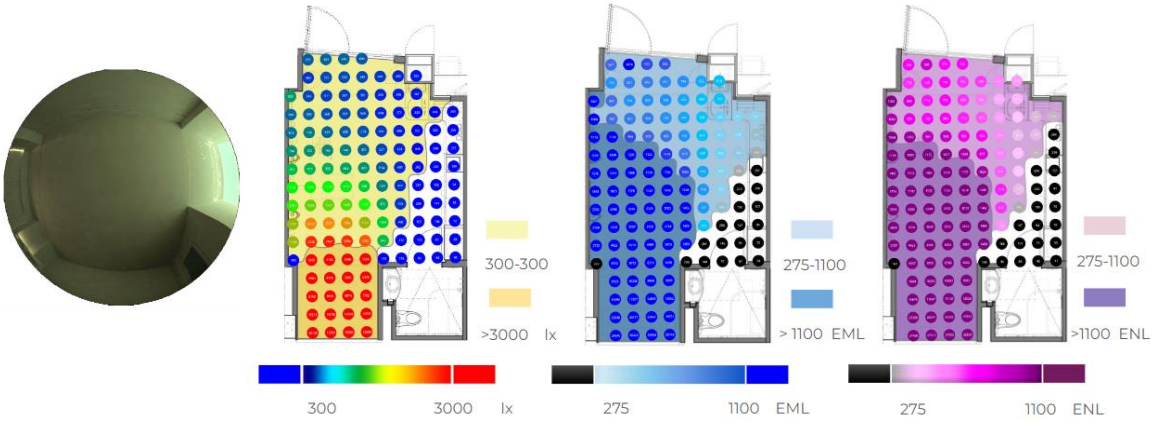

(b)

Figure 4.1 Photopic, Melanopic, and Neuropic Light Simulation Results for June 21st, 12 p.m., Clear Sky, 25000K, Seattle, with South facing and White Wall Surfaces: (a) Daylight Only (b) with Shade Fabric from A Patient View

4.1.1.2 December 21st, Overcast Sky, 7000K

Under an overcast sky (7000K) on December 21st, at 12 p.m., the daylight only setting leaves the majority area of the room too dim and it is not sufficient for appropriate melanopic (OPN4) and neuropic (OPN5) stimulation (Figure 4.2.a). After adding the electric lighting composition given in Section 3.3.3, all three opsin levels improve (Figure 4.2.b). The supplementary electric light, with its higher intensity and blue rich spectra, raises the visual and non-visual light levels to acceptable ranges. Comparing all three optic systems, this electric lighting recipe increases illuminance for the photopic system from 12.8% to 100%, melanopic system stimulation from 16% to 100%, and neuropic system from 9.6% to 66%.

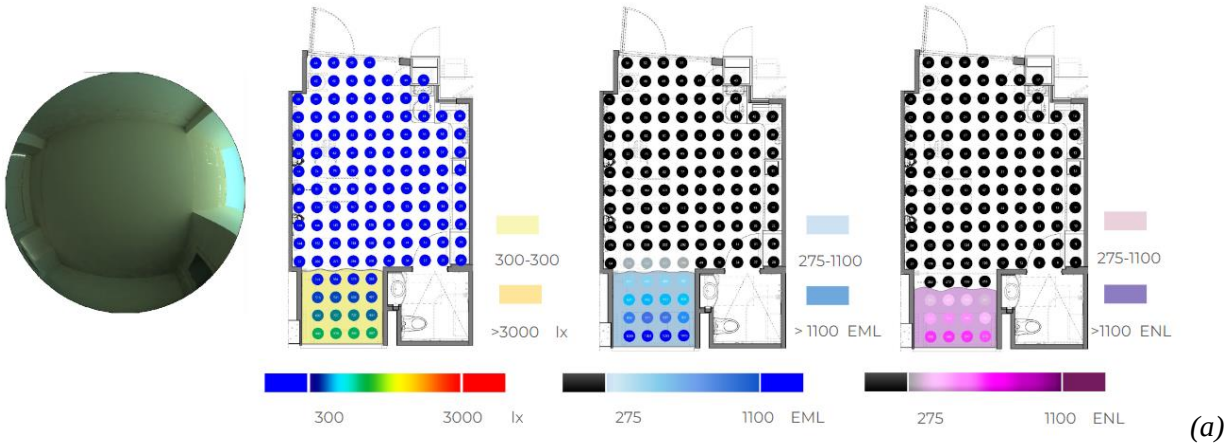

(a)

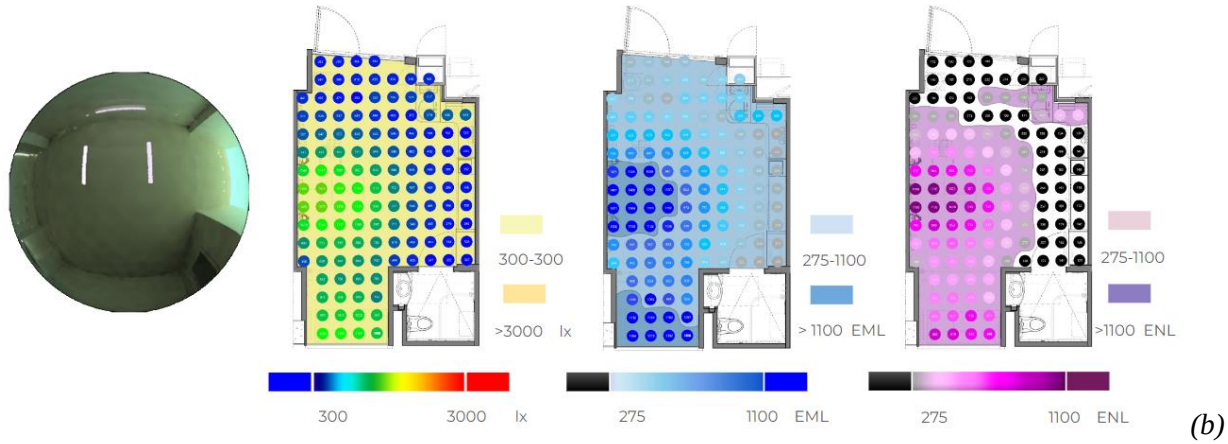

(b)

Figure 4.2 Photopic, Melanopic, and Neuropic Light Simulation Results for December 21st, 12 p.m., Overcast Sky, 7000K, Seattle, South Facing Glazing and White Wall Surfaces: (a) Daylight Only (b) with 3500K Electric Light Source (Wall Light 5600.8 Lumens and Ceiling Lights 7695.9 Lumens) from A Patient View

4.1.2 Changes at Different Time of the Year (Clinician/ Family View)

4.1.2.1 March 21st, Intermediate Sky, 5000K, 12 p.m.

Figure 4.3.a shows a fisheye rendering from the clinician view, standing next to the entrance door and facing to the window. Figure 4.3.b shows vertical grid simulation throughout the room for OPN1, OPN4, and OPN5 under daylight only conditions for March 21st, at 12p.m., with intermediate skies (5000K). The wall surfaces are white. At this time, the family resting area is glary towards the south orientation; 9.4% (south) of the room area is over 3000 lux. Areas nearby the entrance and cabins are dim.

11.1% (gaze oriented to north), 78.6% (east), 31.6% (south), and 68.4% (west) area of the room is between the desired range of 300 to 3000 lux. (Table 5)

When looking at north, east and south directions, only 11.1% (north), 24.8% (east), and 43.6% (west) of the room area satisfy the minimum required Equivalent Melanopic Lux (EML). Looking at south, where the window is located, 74.4% (south) of the room area is adequately lit. For Equivalent Neuropic Lux (ENL), only 0.9% (gaze oriented to north), 14.5% (east), and 16.2% (west) of the room area achieve the 275 Equivalent Neuropic Lux (ENL) goal. Similar to melanopsin stimulation, 64.1% (south) of the room area satisfy the minimum required Equivalent Neuropic Lux (ENL). (Table 5)

This scene shows that the potential of daylight as a primary light source is able to give adequate light intensity to perform visual tasks but cannot provide enough circadian entrainment unless facing to the window (south) in March. However, there is a glare issue in the vicinity of the window for clinicians and families when they are facing west, east and south but it is acceptable when they are facing the patient bed direction (north).

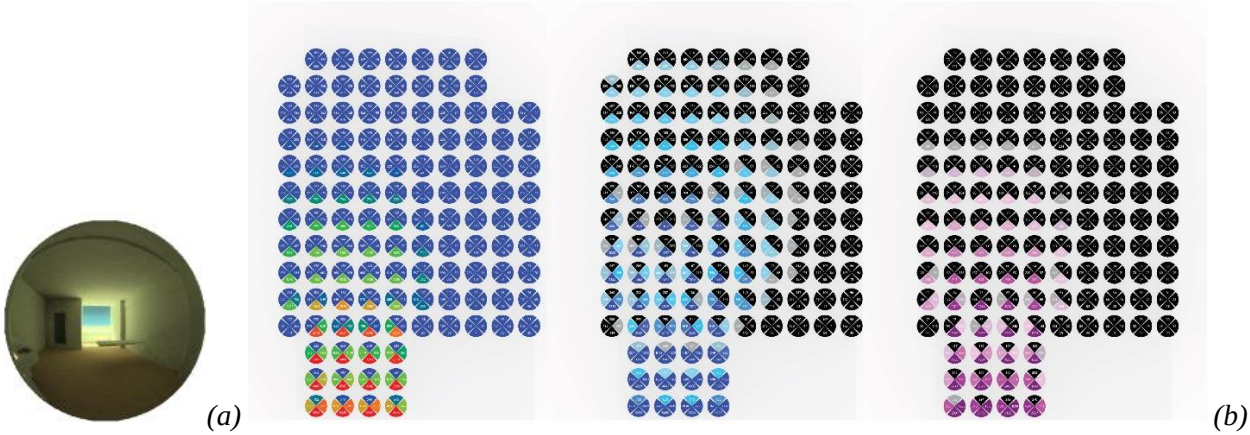

(a) *(b)*

Figure 4.3 Photopic, Melanopic, and Neuropic Light Simulation Results for March 21st, 12 p.m., Intermediate Sky, 5000K, Seattle, with South facing and White Wall Surfaces with Daylight Only from A Clinician/Family View

Table 5. Percentage of the Room Area Under the Criteria of Photopsin, Melanopsin and Neuropsin on March 21st, 12 p.m., Intermediate Sky, 5000K, Seattle, with South facing and White Wall Surfaces with Daylight Only from A Clinician/Family View

		North	East	South	West
OPN 1 (Lux)	300- 3000	11.1	78.6	31.6	68.4
	> 3000	0	0	9.4	0
OPN 4 (EML)	>= 275	11.1	24.8	74.4	43.6
OPN 5 (ENL)	>= 275	0.9	14.5	64.1	16.2

4.1.2.2 June 21st, Clear Sky, 25000K, 12 p.m.

Figure 4.4.b shows vertical grid simulation throughout the room for OPN1, OPN4, and OPN5 under daylight only conditions on June 21, at 12 p.m., with clear skies (25000K). The wall surfaces are white. At this time, the family resting area has a glare problem; 0% (gaze oriented towards north), 11.1% (east), 30.8% (south), and 11.1% (west) of the room area is over 3000 lux and 98.3% (north), 59.8% (east), 59.8% (south), and 88.9% (west) area of the room is between the desired range of 300 to 3000 lux (Table 6).

The grid points across the entire room satisfy the minimum required Equivalent Melanopic Lux (EML) when facing north, south, and west in general. 32.5% (east) and 9.4% (south) of the room area, where it is blocked by the bathroom in the corner, is lower than 275 Equivalent Melanopic Lux (EML). For Equivalent Neuropic Lux (ENL), most of the grid points across the entire room satisfy the minimum required Equivalent Melanopic Lux (EML), with only 24.8% (east) and 13.7% (south) area of the room does not achieve the 275 Equivalent Melanopic Lux (EML) goal. (Table 6)

This scene shows the potential of daylight as a primary light source in June for delivering adequate light intensity for occupants standing in the patient room and looking around. Daylight can also provide the intensity and spectra to stimulate the circadian system in June. However, there is a glare issue in the vicinity of the window for clinicians and families when they are facing south, possibly when they walk into the patient room to check the patient and talk to the families.

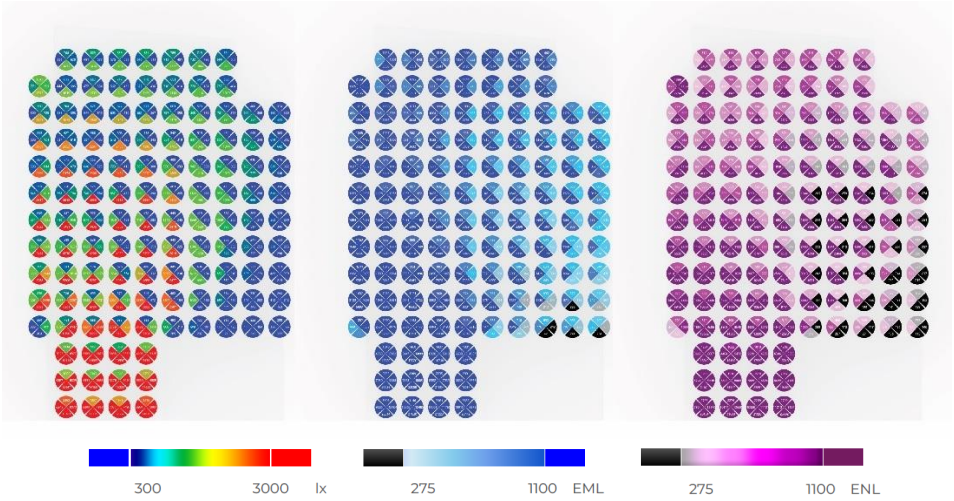

Figure 4.4 Photopic, Melanopic, and Neuropic Light Simulation Results for June 21st, 12 p.m., Clear Sky, 25000K, Seattle, with South facing and White Wall Surfaces with Daylight Only from A Clinician/Family View

Table 6. Percentage of the Room Area Under the Criteria of Photopsin, Melanopsin and Neuropsin on June 21st, 12 p.m., Clear Sky, 25000K, Seattle, with South facing and White Wall Surfaces with Daylight Only from A Clinician/Family View

		North	East	South	West
OPN 1 (Lux)	300- 3000	98.3	59.8	59.8	88.9
	> 3000	0	11.1	30.8	11.1
OPN 4 (EML)	>= 275	100	67.5	90.6	100
OPN 5 (ENL)	>= 275	100	75.2	86.3	100

4.1.2.3 December 21st, Overcast Sky, 7000K, 12 p.m.

Under an overcast sky (7000K) on December 21st, at 12 p.m., the daylight only setting leaves the majority area of the room too dim with only 0% (north), 6.8% (east), 18.8%(south) and 6% (west) area of the room are between the desired range of 300 to 3000 lux. It also cannot stimulate appropriate melanopic (OPN4) and neuropic (OPN5) of most area of the room except family resting space. (Figure 4.3.b and Table 7).

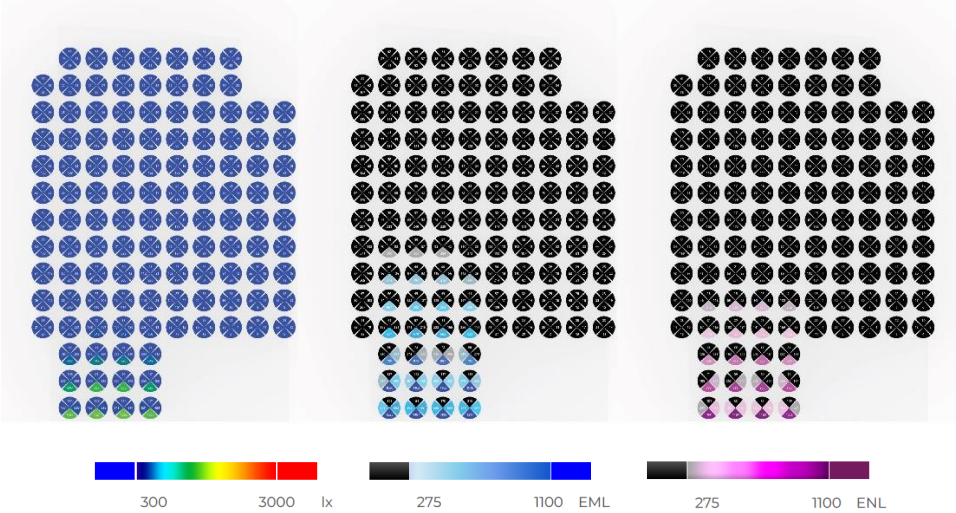

Figure 4.5 Photopic, Melanopic, and Neuropic Light Simulation Results for December 21st, 12 p.m., Overcast Sky, 7000K, Seattle, South Facing Glazing and White Wall Surfaces with Daylight Only from A Clinician/Family View

Table 7. Percentage of the Room Area Under the Criteria of Photopsin, Melanopsin and Neuropsin on December 21st, 12 p.m., Overcast Sky, 7000K, Seattle, South Facing Glazing and White Wall Surfaces with Daylight Only from A Clinician/Family View

		North	East	South	West
OPN 1 (Lux)	300- 3000	0	6.8	18.8	6
	> 3000	0	0	0	0
OPN 4 (EML)	>= 275	0	9.4	17.9	8.5
OPN 5 (ENL)	>= 275	0	5.1	15.4	5.1

4.1.3 Glazing

The impact of the spectral selectivity of glazing on the photopic, melanopic, and neuropic lighting quantities is studied based on 4 glazing types given in 3.3.5. The results are reported for 10 points spaced every 0.6-meters from one side of the patient bed near the rear wall to the glazing as shown in Figure 4.6.

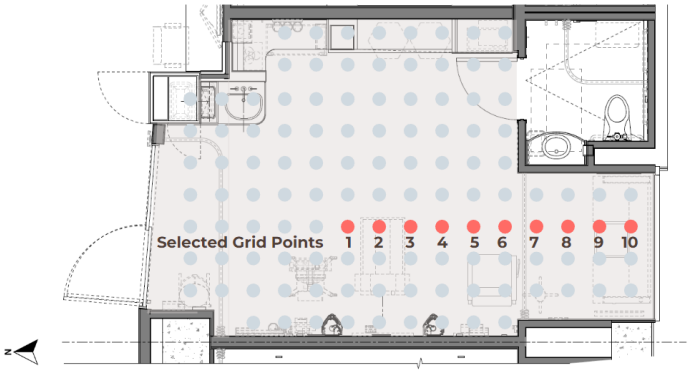

Figure 4.6 Selected Grids Points to Compare for Glazing

Figure 4.7 shows the three sets of results for three opsins simulated at noon for different glazing options on June 21st with a clear day, 25000K (white wall and the glazing facing South). The grid simulation results clearly show that the light level drops progressively with increasing distance to the window, however without any shading controls the main issue is not daylight availability, it is glare. Glazing 4 leads to a higher coverage to glare area compared to other glazing. This is to be expected as it has higher visible transmissivity. All four glazing (which were selected among existing healthcare design buildings) provide satisfactory, stimulation results for melanopsin (OPN4), but note that the shading control is not applied to the glazing. Given the high photopic illuminances, and the resulting glare, the OPN4 results should be considered preliminary. Glazing 3 results in low stimulation for neuropsin (OPN5) at the cabin, sink, and workstation for clinicians, where were located across from the patient bed zone. This is a direct result of its spectral composition that prohibits the admission of the violet range of daylight.

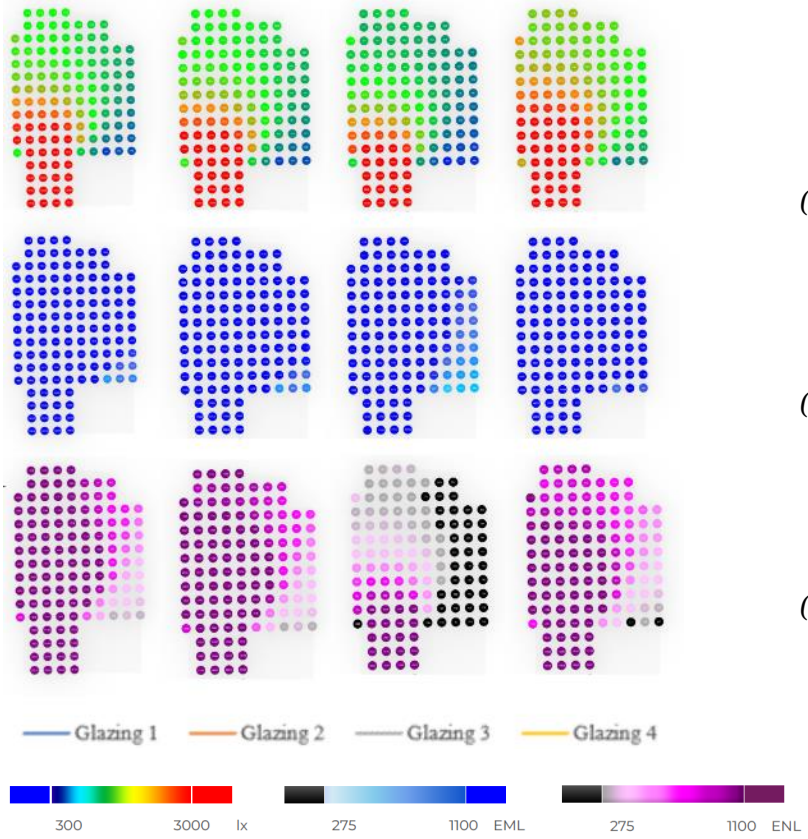

Figure 4.7 Grid Simulations for 4 Selected Glazing for (a) Photopic, (b) Melanopic, and (c) Neuropic Light Simulation Results

Figures 4.8.a and 4.8.b show that glazing 4 transmits photopic and melanopic light while glazing 1 and 2 have similar performances. Looking at the horizontal grid simulation for the entire space, it does not differ for melanopsin (OPN4) stimulation. Glazing 2 has the best neuropic (OPN5) performance followed by glazing 4 and 1 (Figure 4.8.c). All glazing options satisfy the minimum requirement at the location of the bed.

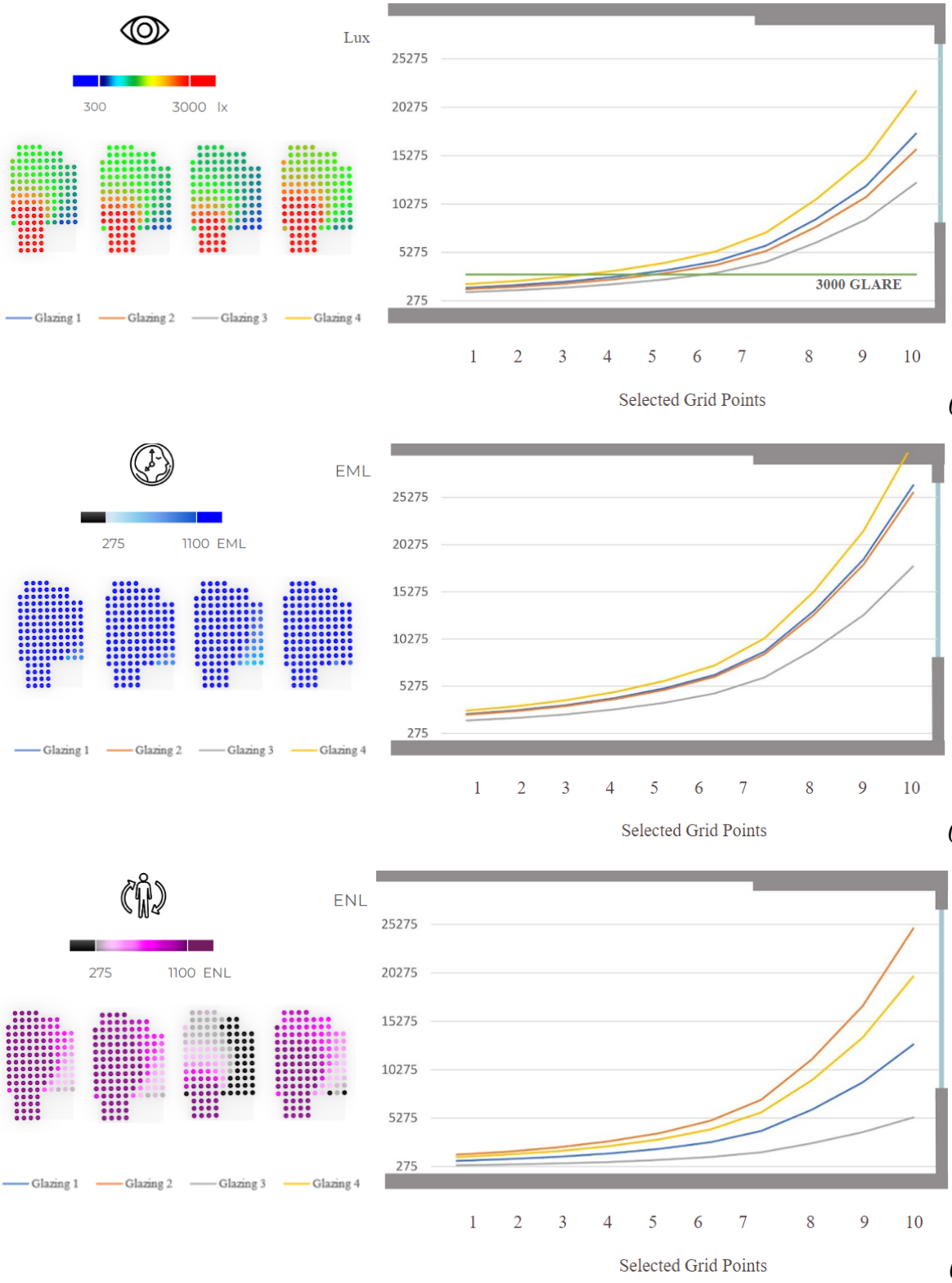

Figure 4.8 Horizontal Grid Simulation and Illuminance Curve of Selected Grids to Compare the Impact of Four Glazing Types for (a) Photopic, (b) Melanopic, and (c) Neuropic Light Simulation Results

4.1.4 Surface Material

To compare how surface material color can influence the performance of each opsin, this section compares three wall surface materials, white, blue, and red walls. Glazing 4 is selected for setup, and the simulations are performed for June 21st, clear sky with a CCT of 25000K. Figure 4.9 shows that using white satisfies the photopic (OPN1), melanopic (OPN4) and neuropic (OPN5) stimulation under their respective criteria for the majority of the room, followed by the blue wall and red wall. These results should be evaluated carefully. The wall colors were based on their color, and they have different photopic reflectance. They are not equally reflective (0.92, 0.35, 0.12, respectively for white, blue, and red as discussed in 3.3.6). The unstimulated area for neuropsin (OPN5) is restricted to one corner of the room with the white wall. The unstimulated area expands further when using the blue wall, alongside the entire side wall when using the red wall. The variations are based on both the wall reflectance and spectral selectivity of each material. The patient bed zone qualified the criteria for all opsins when using these three materials.

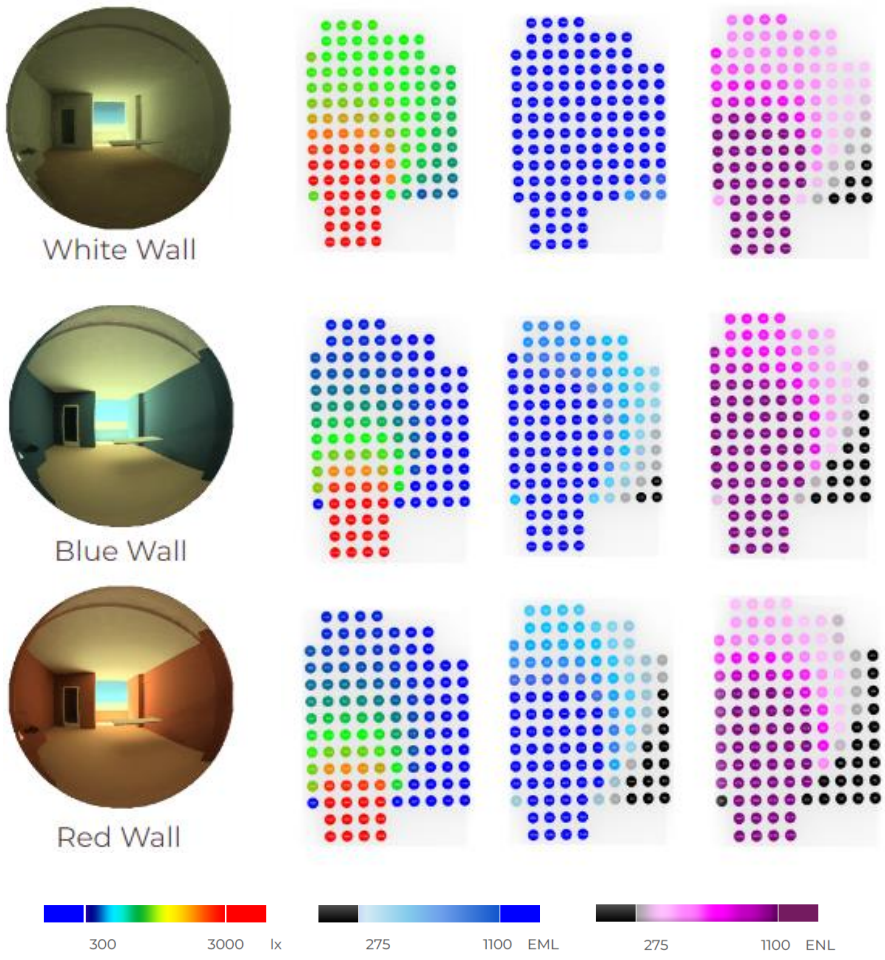

Figure 4.9 (a)Fisheye Rendering of the Room using White, Blue and Red Wall Surfaces (b)Grid Simulations for Comparing the Effect of Surface Materials on Photopic, Melanopic, and Neuropic light

4.2 Period Analysis with Measured Sky Parameters

CCT varies from 5000 K to 20000K daily based on the measured data as mentioned in Section 3.3.2.2. To compare how irradiance and CCT influence the final performance, simulations were run for one day in June (June 9) when the window was oriented to the South. Shading was not simulated. A point nearby the glazing was selected (Figure 4.10) to see how the opsin values changed throughout the day.

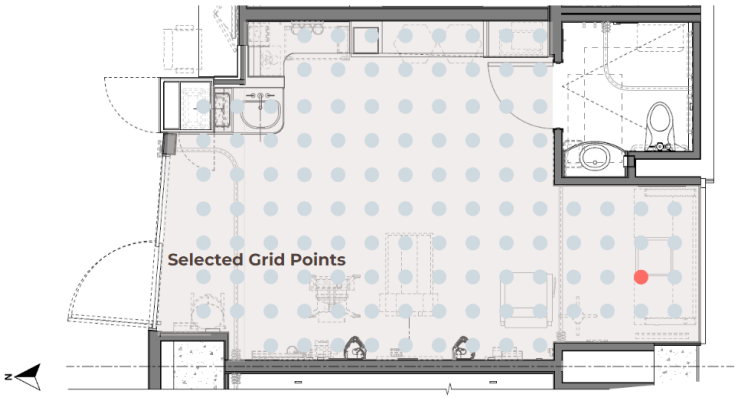

Figure 4.10 Selected Grid Point for Comparison

4.2.1 CCT and Irradiance

4.2.1.1 Irradiance

To compare the impact of irradiance on opsin levels, five time points were selected from the scatter diagram in Section 3.3.2.2. Irradiance values are variant with a range between 50 to 805 W/m^2, and the CCT values are relatively constant (ranges from 5637K to 5744K). Figures 4.11 and 4.12 show that, with similar CCTs, OPN1, 4, and 5 all increase with the increase of irradiance value.

Table 8. Irradiance, CCT and One-point Opsin Values that Compare the Effect of Irradiance.

	Point 1	Point 2	Point 3	Point 4	Point 5
CCT (K)	5744	5664	5673	5647	5637
Irradiance (W/m2)	50	164	436	622	805
OPN1(Lux)	1588	5368	14792	24278	35212
OPN4 (EML)	1837	6493	16452	26839	39401
OPN5 (ENL)	1054	4331	9985	19357	31925

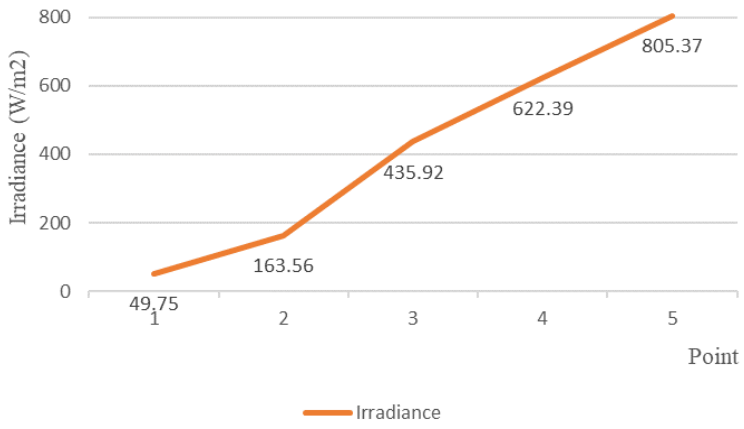

Figure 4.11 Selected Time Point with Varying Measured Sky Irradiance Value (CCT Values Are Relatively Constant)

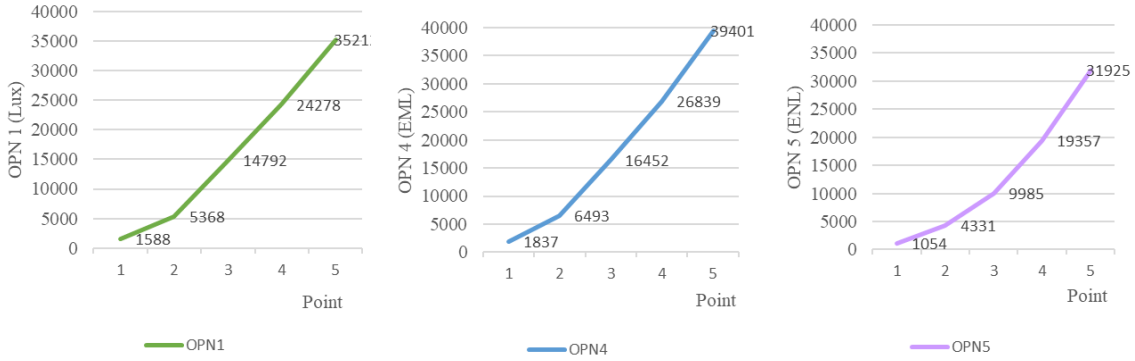

(a) *(b)* *(c)*

Figure 4.12 (a) Photopic, (b) Melanopic, and (c) Neuropic Light Simulation Results of One Select Point with Varying Measured Sky Irradiance Value (CCT Values Are Relatively)

Figure 4.13 shows the positive relationship between irradiance and opsin stimulation value. It indicates a more striking change in how the entire patient room was affected with the increased sky irradiance. From 50 W/m^2 to 164 W/m^2, there is a significant improvement for photopsin. Non-visual stimulation increased significantly when sky irradiance changed from 154 W/m^{2}to 436 W/m^2.

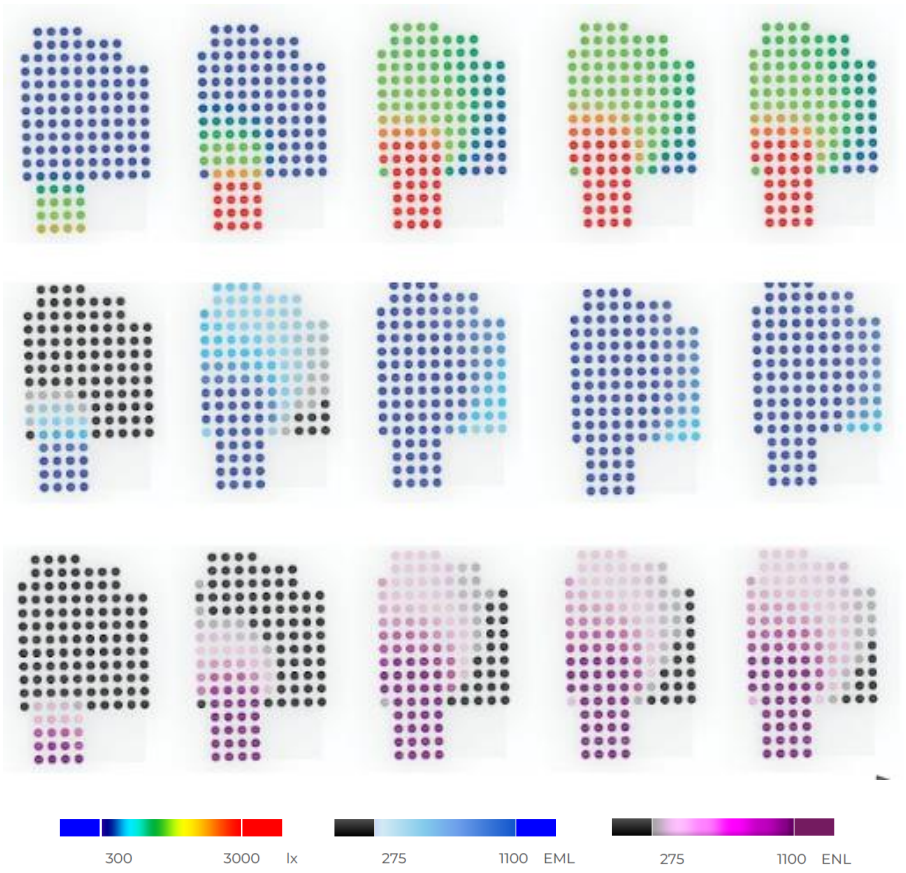

Figure 4.13 Grid Simulations for Comparing the Effect of Sky Irradiance Value on (a) Photopic, (b) Melanopic, and (c) Neuropic Light Simulation Results

4.2.1.2 CCT

To compare how CCT impacts the opsin values, three time points with similar irradiances (ranging from 46 W/m^2 to 48 W/m^2) were selected from the scatter diagram in Section 3.3.2.2. CCT values are between 6000K and 16000K (Table 6). Simulations are done using white wall and south facing window with glazing 4. Figures 4.14 and 4.15 show that, with similar irradiance, photopsin (OPN1) stimulation remains the same regardless of the CCT value. This is expected. In contrast, melanopsin (OPN4) and neuropsin (OPN5) have a clear increase with higher CCT value, as higher CCT points to higher blue content of daylight.

Table 9. Irradiance, CCT and One-Grid Opsin Stimulation Value of Selected Points to Compare the Effect of CCT.

	Point 1	Point 2	Point 3
CCT (K)	6002	10842	16739
Irradiance (W/m^2)	47	48	46
OPN1 (Lux)	1534	1588	1520
OPN4 (EML)	1752	1837	2081
OPN5 (ENL)	981	1054	1532

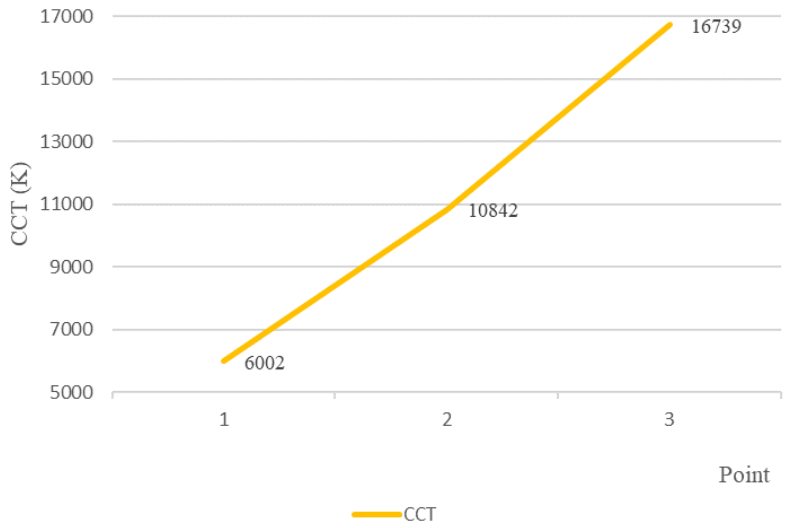

Figure 4.14 Selected Time Point with Varying Sky CCT Value (Irradiance Value Are Relatively Constant)

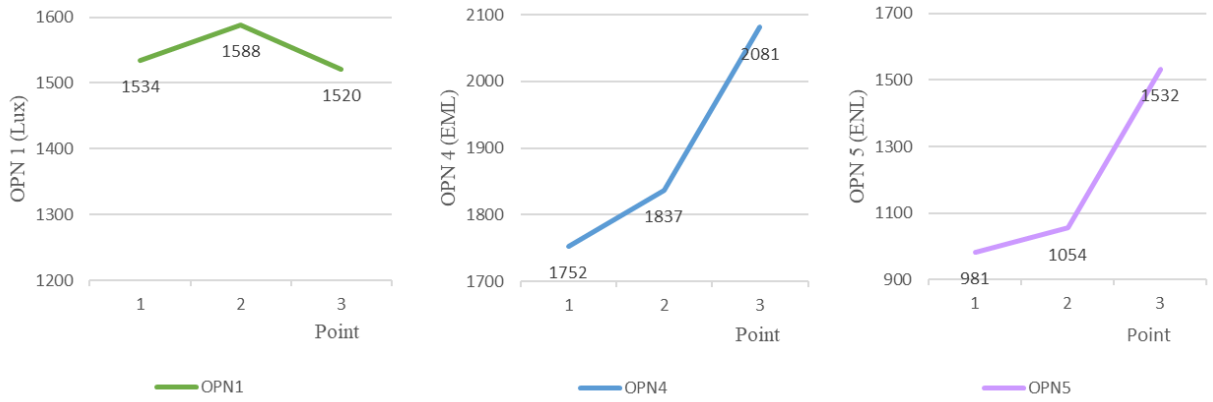

(a) *(b)* *(c)*

Figure 4.15 (a) Photopsin, (b) Melanopsin, and (c) Neuropsin Simulation Results of A Select Point with Varying Sky CCT Value (Irradiance Value Are Relatively Constant)

When the illuminance distribution is studied in the patient room, Figure 4.16 shows no difference between the photopsin (OPN1) values found between selected time spots with different CCT values. Non-visual system results, including melanopsin (OPN4) and neuropsin (OPN5) were mainly satisfactory in the family resting area. Even with high CCT values in this set of simulations, the visual and non-visual performance are still low under studied sky conditions.

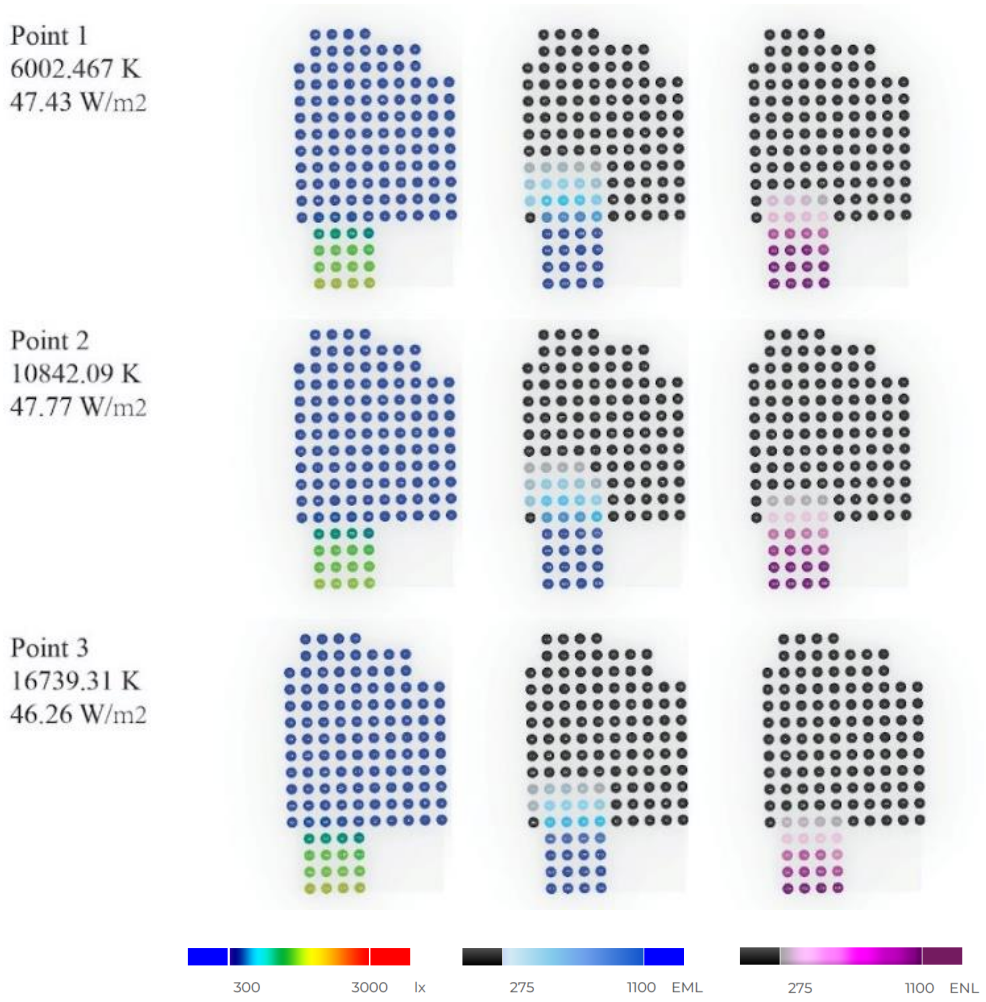

Figure 4.16 Grid Simulations for Compare the Impact of CCT on (a) Photopic, (b) Melanopic, and (c) Neuropic Light Simulation Results

4.2.2 Change Over a Day

As mentioned in Section 3.3.2.2, June 9th, 2021, was selected as a day with variable CCT values in June 2021. It is only representative of a limited time frame, and the changes over time can be more muted or more substantial. To study the dynamic of the day, hourly simulations are performed for June 9 (Table 7). Simulations utilize white wall surfaces and a south facing window with glazing 4.

Table 10. Measured Hourly CCT, Irradiance, and Percentage of the Room Area Under the Criteria of Photopsin, Melanopsin and Neuropsin on June 9, 2021

Time	CCT (K)	Irradiance (W/m^2)	OPN 1 (%)	OPN 4 (%)	OPN 5 (%)
7:00	5836	136	46.4	46.4	15.2
8:00	9710	307	84	61.6	51.2
9:00	5768	680	79.2	39.2	60
10:00	5695	173	75.2	69.6	33.6
11:00	8740	389	81.6	28.4	57.6
12:00	7294	114	50.4	62.4	25.6
13:00	5631	718	78.4	28.8	63.2
14:00	5619	672	79.2	41.6	58.4
15:00	5638	638	78.4	37.6	57.6
16:00	5652	584	80.8	42.4	57.6
17:00	5694	527	79.2	36	56
18:00	5773	395	25.6	18.4	11.2
19:00	5835	56	23.2	17.6	12.8
20:00	16714	22	12.8	18.4	16
20:59	13737	5	0	4	0

Figures 4.17 and 4.18 shows that CCT and irradiance values during daytime are quite dynamic. It also demonstrates the result of how each opsin was stimulated over a day as a combined result of the irradiance and CCT values. The results show that irradiance and CCT are not correlated to each other. The visual system, photopsin (OPN1), which is the green dashed curve mainly follows the irradiance curve, while the non-visual systems melanopsin (OPN4), which is the blue dashed curve, and neuropsin (OPN5), which is the purple dashed curve, are affected by both irradiance and CCT values.

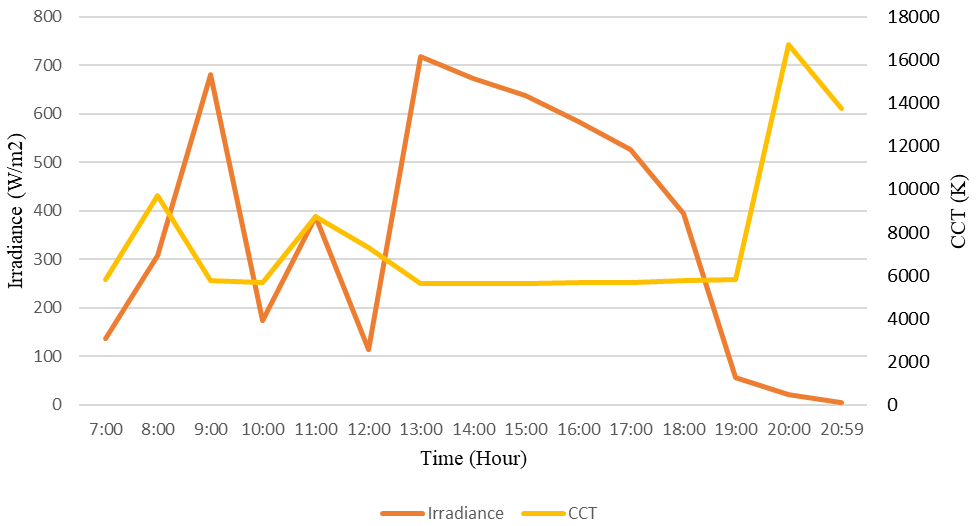

Figure 4.17 Curve Graphs of Measured Hourly CCT and Irradiance on June 9, 2021

(a)

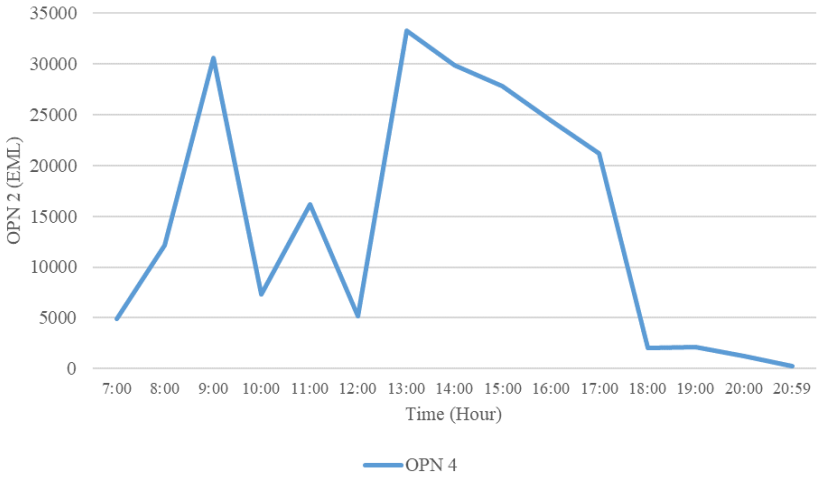

(b)

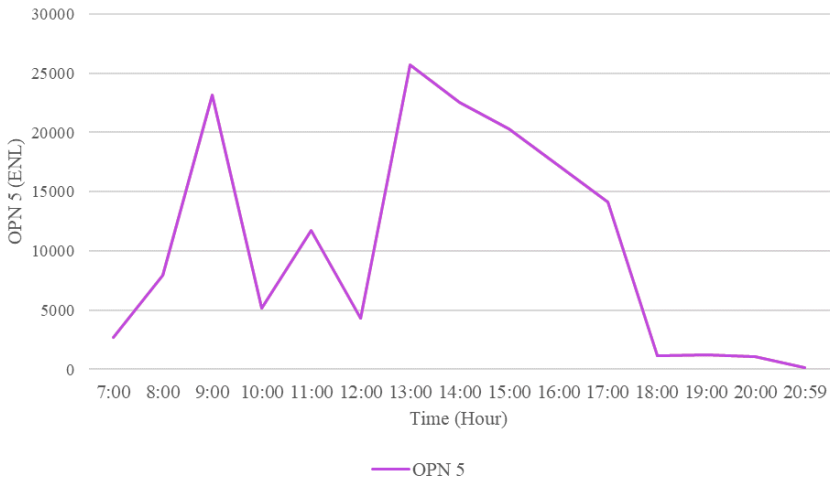

(c)

Figure 4.18 Percentage of the Room Area Under the Criteria of (a) Photopsin, (b) Melanopsin, and (c) Neuropsin Using Measured Sky Spectral Data on June 9, 2021

The horizontal grid simulation for the entire room (Figure 4.19) provides similar results; the red area for opsin1, the dark blue area for opsin 4 and the dark violet area for opsin 5 have similar patterns with the single point simulations in Figure 4.18. Comparing a situation when the irradiance is high and CCT is low, the stimulation can still be high as seen at 9:00 a.m. or 1:00 p.m. Sunset hour, such as 8:00 pm, exhibits a high CCT value and an extremely low irradiance value. As a result, the stimulation result is low. Opsin stimulation booms during sunrise hours and drops significantly during sunset hours. During daytime, the result can vary due to the sky conditions.

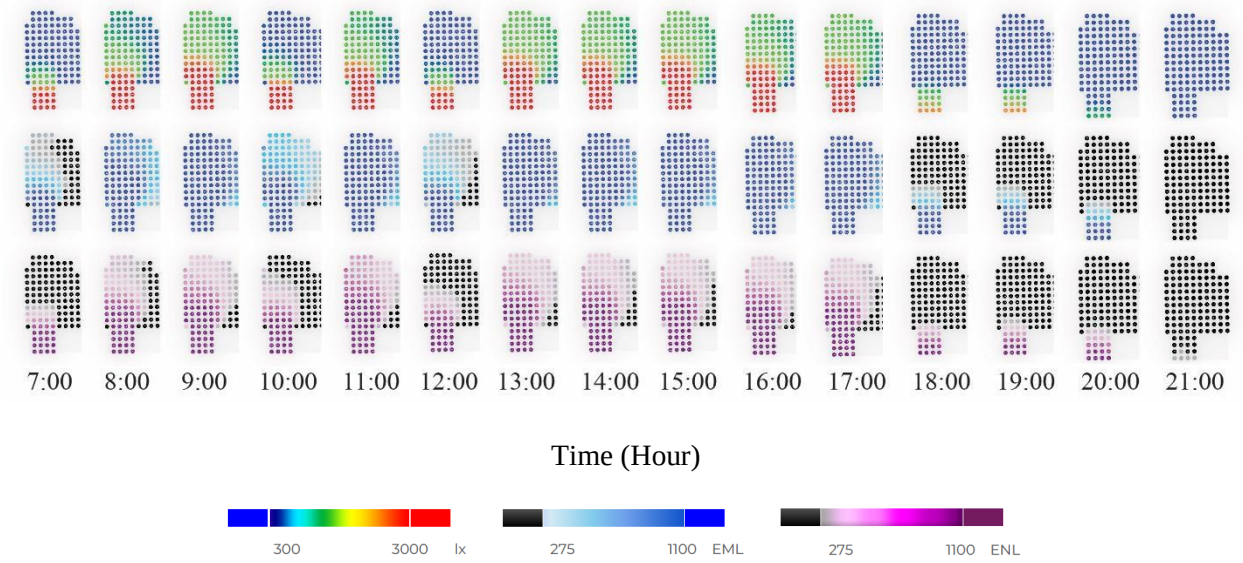

Figure 4.19 Grid simulations to Compare Changes Over a Day for (a) Photopic, (b) Melanopic, and (c) Neuropic Light Simulation Results on June 9, 2021

4.3 Analysis

4.3.1 Comparison of Change of Over Months, Clinician View

Figure 4.20 shows the visual and non-visual response for each opsin on March 21st (intermediate sky, 5000 K), June 21st (clear sky, 25000K) and December 21st. (overcast sky, 7000K). This scene shows the potential of daylight as a primary light source in delivering adequate light intensity in June followed

by March and December. The simulations for June (white wall and south facing window) demonstrate highest light levels for a given year, while December (white wall and south facing window) provide the lowest light levels comparing to other months. As expected, the room does not receive enough light to stimulate the visual and non-visual system with daylight only on March 21st and December 21st.

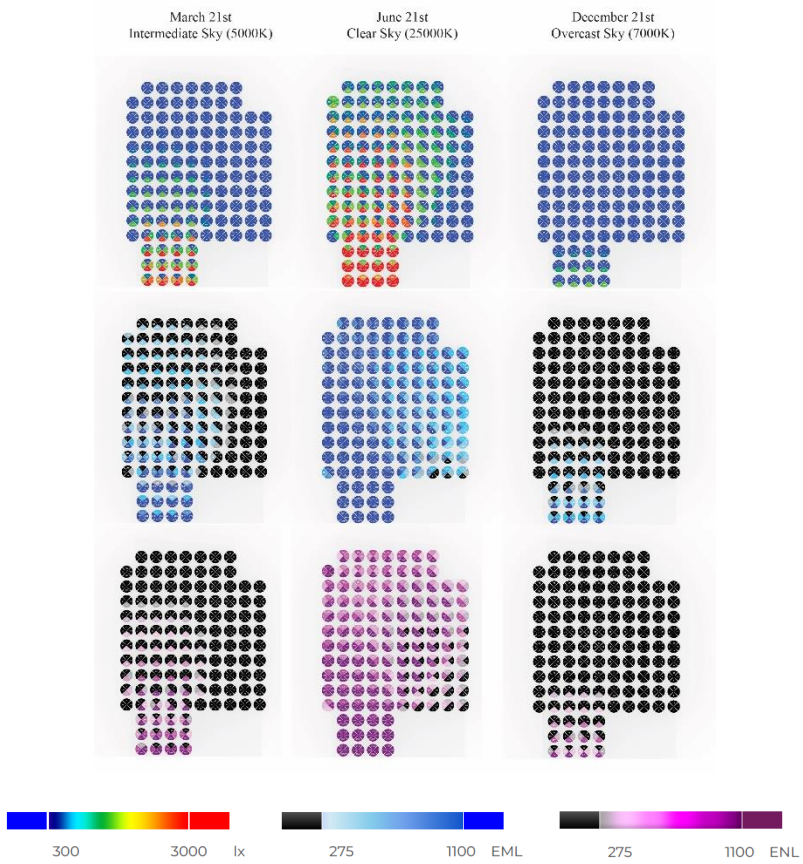

Figure 4.20 Grid simulations to Compare Changes Over Months: March 21st, June 21st , and December 21st

4.3.2 Comparison of Clinician/Family Facing Different Direction

Figure 4.21 supported that, for clinician/family view, their visual response to where the window located (south) reply on the daylight more than other directions. This difference is larger in July and it is not obviously to find in December when the entire room does not receive enough light levels. For the

melanopsin (OPN4) and neuropsin (OPN5) stimulation, north is less easier to get effected comparing to other orientations, while east and south share similar result with symmetric pattern as shown in Figure 4.21.

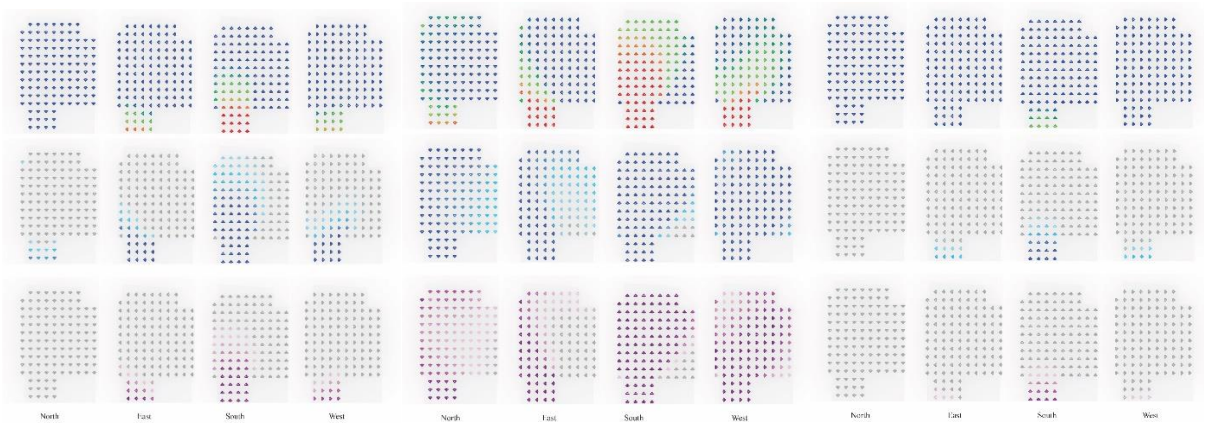

(a) *(b)* *(c)*

Figure 4.21 Photopic, Melanopic, and Neuropic Light Grid simulations to Compare Difference When Clinician/Family Facing Different Direction on (a) March 21st, 12 p.m., Intermediate Sky, 5000K, (b) June 21st, 12 p.m., Clear Sky, 25000K, (c) December 21st, 12 p.m., Overcast Sky, 5000K, Seattle, with South facing and White Wall Surfaces with Daylight Only

4.3.3 Comparison with Shade Fabric and the Supplement of Electric Light

The two sets of simulations shown in Section 4.1.4 indicate the location of the patient bed, and the program of space may take advantage of daylight for occupants' visual and non-visual health. It also shows that in general neuropic (OPN5) stimulation follows a similar pattern to melanopic (OPN4) stimulation. In June, the setting with white wall surfaces is south window orientation, the simulation assumed a strongest daylighting condition. The result shows that the room with daylight only can achieve the goals for the non-visual opsin criteria. However, this is not a realistic scenario, the glare issue needs to be resolved. The glare issue only remains in the family resting area after adding shade fabric close to the

window. The patient bed zone for their view would not be influenced by the glare issue and the family resting area glare problem can be solved by using further shading solutions. A curtain was also provided to separate the patient and family zone as shown on the plan in Section 3.3.4. However, any proposed solutions should be evaluated based on its impact on the patient bed area.

The simulations for December (white wall and south facing window) demonstrate lowest light levels for a given year. As expected, the room does not receive enough light to stimulate the visual and non-visual system with daylight only. A lighting recipe with one wall light and two ceiling lights above the patient bed was enough to provide the desired photopic and melanopic light. Neuropic light (OPN5) was also improved significantly after adding the lighting fixture. However, the entrance, sink, nurse workstation and cabin area are still lower than the recommended 275 ENL. Those areas are not closely related to patients' field of view and results can be improved by adding other lighting fixtures if needed.

These results provide important insights into NICU design. Alternative shading options (including shade fabric which is more transparent, automated venetian blinds, and separation between different function zones can be explored in single-family patient rooms) along with appropriate recipes of tunable electric lighting fixtures.

4.3.4 Comparison of the Patient View and Clinician/Family View

Although Clinicians, patient families and patients share the same room, their visual and non-visual response can be different since the previous one may move around in the patient room, and the newborns' view and position are fixed compared to them. Figure 4.22 shows the comparison of the clinician/family view and patient view using same model setting (while wall, window facing south) at the same time with same sky conditions. (June 21st, clear sky, 25000K). It can be found that these two sets of simulations share similar patterns for photopic, melanopsin (OPN4) and neuropsin (OPN5) stimulation.

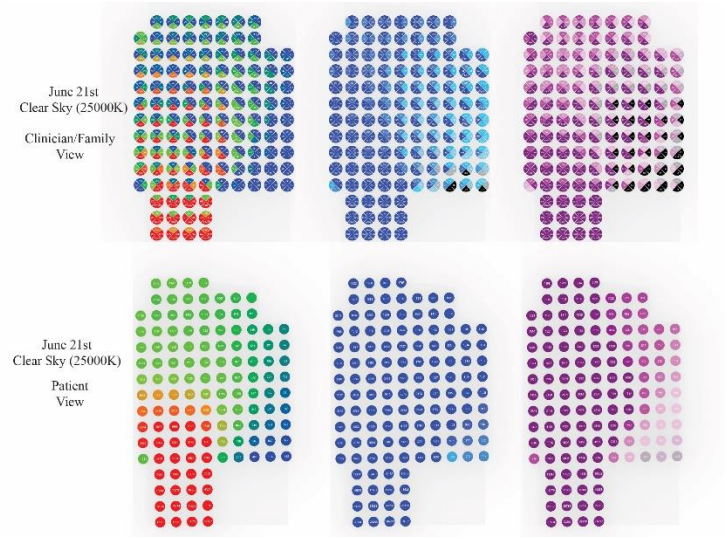

Figure 4.22 Comparison of Photopic, Melanopic, and Neuropic Light Simulation Patient and Clinician/Family View on June 21st, Clear Sky (25000K)

Since the visual and non-visual response of light with four directions of clinicians and families' view can be various. Figure 4.23 splits the stimulation result of clinician and family view from figure 4.22 into four (north, east, south and west) graphs and compare them with the patient view result as mentioned before. It was found that south (facing the window) has the most similar stimulation pattern, north (opposite to the window) was affected the least. West and east were stimulated at a very similar level and shown a symmetric pattern for the photopic stimulation result.

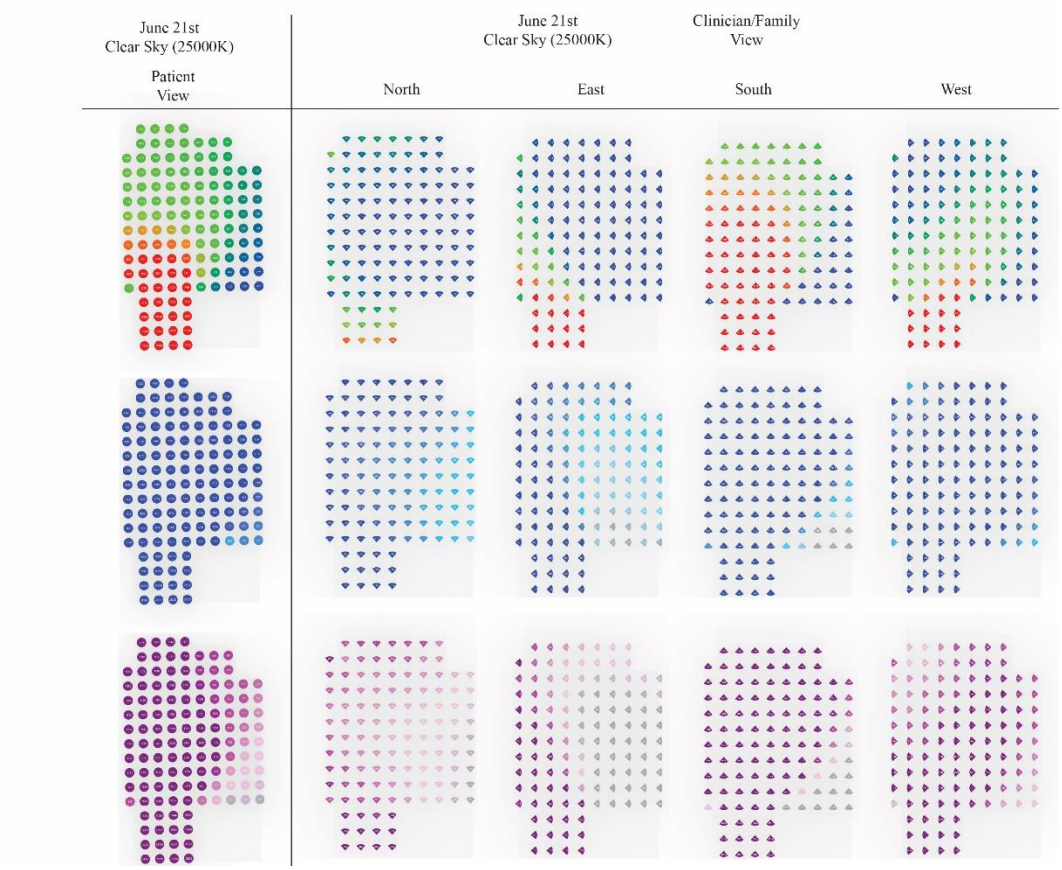

Figure 4.23 Comparison of Photopic, Melanopic, and Neuropic Light Simulation Patient and Clinician/Family (Separate Directions) View on June 21st, Clear Sky (25000K)

4.3.5 Selection of Glazing

Figure 4.24 shows the summary of each opsin performance using 4 different glazing types. The results show that the values of the neuropsin (OPN5) stimulation ranked from glazing 2, glazing 4, glazing 1 and glazing 3. This is a direct result of the spectra power distribution curves given in Section 3.3.5. The transmissivity reduction in the violet range values causes reduction in neuropic light. Glazing 4, with higher value at the peak photopic curve (555 nm), has the highest photopic value followed by Glazing 1, 2 and 3. Glazing 3, has the second highest value at the peak of the photopic curve but its performance is hampered by low transmissivity, 35.5%, which is much lower compared to other glazing.

The results highlight the need to study spectral selectivity and overall transmissivity for selecting glazing. Although all glazing types used in this study satisfy the minimum recommended criteria, since this set of the simulation is done for June, the conditions will change throughout the year. Moreover, after adding shade fabric, opsin 4 and opsin 5 will drop. Glazing 3 is not recommended in Seattle and Glazing 2 and 4 are more performative. Final decisions require a time series analysis under different conditions.

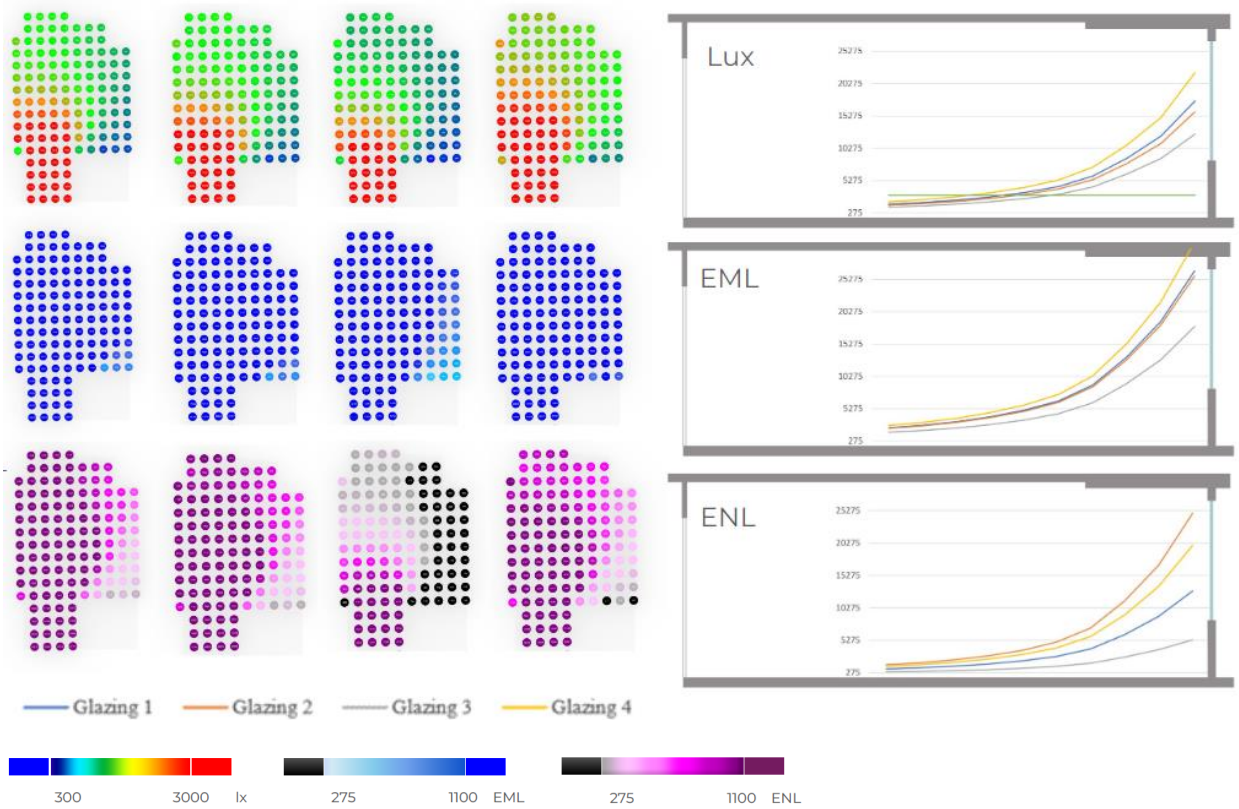

Figure 4.24 Summary of Grid Simulations and Curve Graphs of Selected Grids Points that Compare Glazing for Photopic, Melanopic, and Neuropic Light Simulation Results

4.3.6 Selection of Surface Material

When looking at selecting proper color and material for the wall surfaces in a single-family patient room. The simulation result shows that, compared with the spectra distribution curve in Section 3.3.6, the blue wall had a lower range of green and red wavelength compared to the white wall. Given its

lower overall diffuse reflectivity, it has a lower photopic stimulation. For melanopsin (OPN4) stimulation, white wall material has the highest value in the blue range, hence it comes with the highest stimulation for the circadian system. The red wall which had the lowest range on violet wavelength, and lowest overall diffuse reflection, results is the lowest neuropsin (OPN5) stimulation. When selecting wall materials, it is recommended to consider both the spectral composition and overall reflectivity of the wall.

4.3.7 Effects by Irradiance and CCT

The research demonstrates that it is necessary to use measured or plausible CCT and irradiance values in simulations. Simulations were designed to study how irradiance and CCT each have effects on the opsin performance. Based on the comparisons between different irradiances in Section 4.2.1.1, the visual and non-visual performance is affected by many factors including room shape, window size, surface materials, and distance to the window. Further design explorations should include the depth of the patient room and the location of the patient bed.

Based on the definition of photometry, photopic (OPN1) light levels do not change with CCT. Melanopsin (OPN4) and neuropsin (OPN5) results follow similar trends, and they increase as CCT increases. Photopsin (OPN1) does not increase with CCT (value jumps from 6002K to 16739K) in the close-up analysis of the area of the room closest to the window (Figure 4.25). The stimulated area for melanopsin (OPN4) and neuropsin (OPN5) increased with the increase of CCT from 10842K to 16739K.

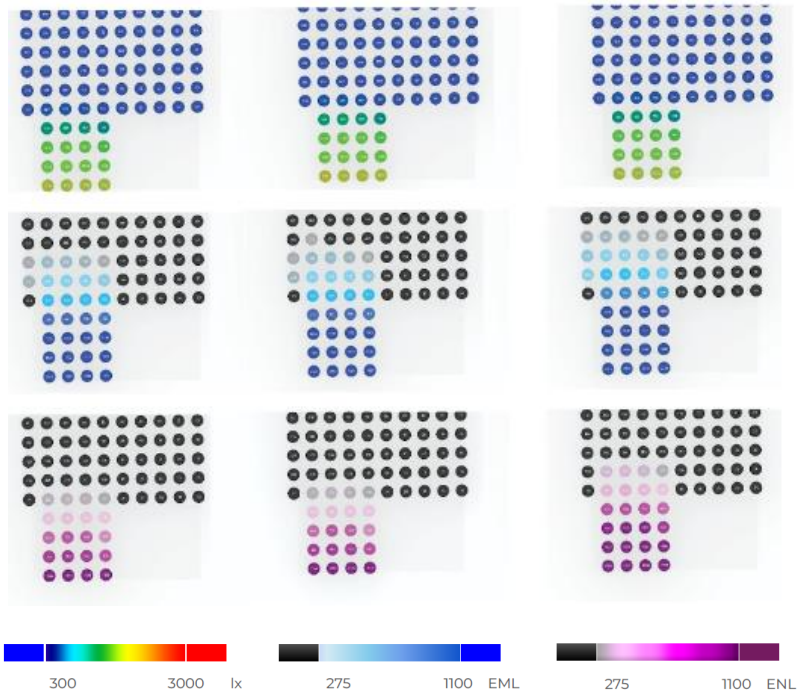

Figure 4.25 Grid Simulation to Compare Increasement of CCT for Photopsin, Melanopsin, and Neuropsin Light Simulation Results

4.3.8 Comparison with the Measured Sky Data

A quick comparison is done to illustrate the difference between a standard CIE model sky and a measured CIE sky model. Figure 4.26 compares the opsin performance of the CIE clear sky model on June 21st, 12 p.m. with 25000K, and the measured data with CCT of 5589K and irradiance of 676 W/m^2. There is a performance difference between a measured sky and the standard mathematical model. The CIE sky model is a general sky model that can be applied throughout the world, the input is latitude, date, time, and a sky type. The measurement-based sky provides a naturally occurring sky at that time. It is weather dependent. The two sets of simulations share a similar performance for photopsin (OPN1) but present a larger difference on melanopsin (OPN4) and neuropsin (OPN5) response. Collecting and using a measured sky model will improve our understanding of naturally occurring skies and their impact on visual and non-visual responses.

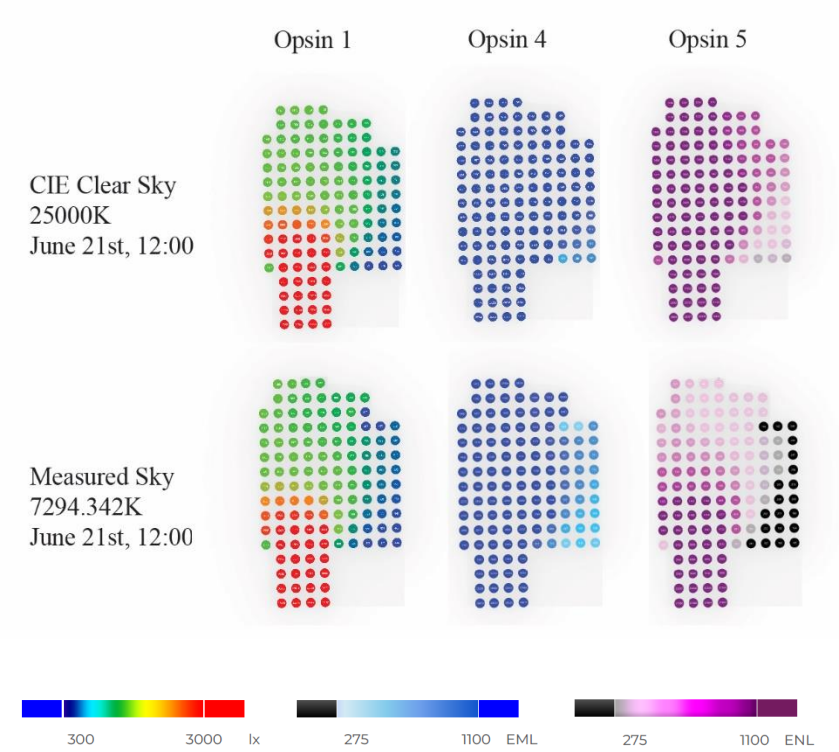

Figure 4.26 Grid Simulation to Compare CIE Clear Sky Model (25000K) and Measured Sky on June 21st, 2021

Chapter 5 Conclusion

5.1 Summary of Thesis

Photoreceptors including photopsin (OPN1), melanopsin (OPN4), and neuropsin (OPN5) impact the individuals' ability to perceive the world, physical health, behavior, and psychological health. This thesis demonstrated the workflow for a NICU setting which can be used to study the role of daylight and electric lighting in neonatal baby's development and its effects on other users in NICU, such as clinicians and families.

During the research period, Lark is revised by adding new metrics such as neuropic illuminances. The end result is a powerful simulation tool that can be used to simulate the visual and non-visual effects of light. The tool can be used to further explore the impact of various design parameters to develop design guidelines for NICUs.

The single-patient family rooms cannot always provide an ideal visual-nonvisual lighting environment with daylight only. This study revealed that along with appropriate surface materials, glazing, dynamic shading systems, and tunable electric lighting systems, the targeted range of wavelengths and intensities can be achieved and customized. Designers can provide the flexibility to control the lighting levels and spectra based on date, time, or the activity.

Existing CIE sky models are useful as they can model any location on earth, but actual sky conditions are more complex than mathematical models. Irradiance and CCT values are the two key components of the sky that varied during a day. When actual data exists, it is preferable to use measured data.

5.2 Contributions

The contributions of the thesis are as follows:

i) Lark multispectral lighting tool is revised to include neuropic light calculations.

ii) Simulation workflows are customized and exemplified for NICU settings.

iii) The workflow emphasizes the need to run multiple analyses in a given space, accounting for every occupant's field of view and needs.

5.3 Future Work

This study mainly focuses on daytime simulation and providing appropriate light levels for vision and circadian entrainment during daytime. Nighttime lighting evaluations are complex in healthcare settings. There are competing goals such as maintaining dark environments for babies and families, while providing adequate light levels for clinicians. Future research can focus on night simulation and developing the right light recipes in different parts of the healthcare facility. Another consideration is how to balance the need for clinicians to remain alert during the nightshift and the circadian phase response by delaying melatonin secretion

For the simulation tool, the future research plan is to develop time-series metrics for non-visual responses since the non-visual system adapts to changes in light intensity and spectral composition over a longer time-period than the visual system. The current maximum criteria for non-visual stimulation were set as getting stimulation for four hours and making it equal to four times of the minimum recommended level. However, responses depend on past exposure and can extend over several hours, or even days, which provides new challenges in lighting performance evaluation.

Systematic and parametric simulations can be done to develop guidelines for NICU lighting designs.

Bibliography

[1] Figueiro M. G., Brainard G. C., Lockley S. W., Revell V. L., & White R. (2008). Light and Human Health: An Overview of the Impact of Optical Radiation on Visual, Circadian, Neuroendocrine, and Neurobehavioral Responses. Illuminating Engineering Society Technical memorandum, IES TM-18-08.

[2] DiLaura D. L., Houser K. W., Mistrick R .G., & Steffy G. R. (2011). The lighting handbook. 10th ed. New York (NY): Illuminating Engineering Society of North America

[3] Bowmaker J. K., & Dartnall H. J. (1980). Visual pigments of rods and cones in a human retina." The Journal of physiology vol. 298: 501-11. doi:10.1113/jphysiol. sp013097

[4] Eichhorn J. (2007). Applications of Kernel Machines to Structured Data. 10.14279/depositonce-1547.

[5] Sandip D., & Wilson M. (2021). Spatial Mapping of Distributed Sensors Biomimicking the Human Vision System. Electronics 10, no. 12: 1443. https://doi.org/10.3390/electronics10121443

[6] Ruppertsberg A.I., & Bloj M. (2006). Rendering Complex Scenes for Psychophysics using Radiance: How Accurate can you get? Journal of Optical Society of America, 23(4), 759-768.

[7] Schanda J. (2016). CIE 1931 and 1964 Standard Colorimetric Observers: History, Data, and Recent Assessments. In: Luo M.R. (eds) Encyclopedia of Color Science and Technology. Springer, New York, NY. https://doi.org/10.1007/978-1-4419-8071-7_323

[8] George C. B., John P. H., Jeffrey M. G., Brenda B., Gena G., Edward G., & Mark D. R. (2001). Action spectrum for melatonin regulation in humans: evidence for a novel circadian photoreceptor. Journal of Neuroscience. 21(16), 6405–6412.

[9] Rea M., Figueiro M., Bullough J., & Bierman A. (2005). A model of phototransduction by the human circadian system. Brain Research Rev, 2005; 50(2):213-228

[10] Panda S., Nayak S. K., Campo B., Walker J. R., Hogenesch J. B., & Jegla T. (2005). Illumination of the melanopsin signaling pathway. Science, 307, pp. 600-604

[11] Qiu X., Kumbalasiri T., Carlson S. M., Wong K. Y., Krishna V., Provencio I., & Berson D. M. (2005). Induction of photosensitivity by heterologous expression of melanopsin. Nature, 433, pp. 745-749

[12] Koyanagi M., Kubokawa K., Tsukamoto H., Shichida Y., & Terakita A. (2005). Cephalochordate melanopsin: evolutionary linkage between invertebrate visual cells and vertebrate photosensitive retinal ganglion cells. Curr. Biol., 15 (2005), pp. 1065-1069

[13] Tori M., Kojima D., Okano T., Nakamura A., Terakita A., Shichida Y., Wada A., & Fukada Y. (2007). Two isoforms of chicken melanopsins show blue light sensitivity. FEBS Lett., 581 (2007), pp. 5327-5331

[14] Bailes H.J., & Lucas R.J. (2013). Human melanopsin forms a pigment maximally sensitive to blue light (λmax ~479 nm) supporting activation of Gq/11 and Gi/o signalling cascades. Proc. Biol. Sci., 280 (2013), p. 20122987

[15] Lucas R.J., Lall G. S., Allen A. E., & Brown T. M. (2012). How rod, cone, and melanopsin photoreceptors come together to enlighten the mammalian circadian clock. Prog. Brain Res., 199 (2012), pp. 1-18

[16] Lewy A.J., Wehr T. A., GoodwinF. K., Newsome D. A., & Markey S. P. (1980). Light suppresses melatonin secretion in humans. Science, 210, pp. 1267-1269

[17] Lucas J.R., Peirson S. N., Berson D. M., Brown T. M., Cooper H. M., Czeisler C. A., Figueiro M. G., Gamlin P. D., Lockley S. W., O'Hagan J. B., Price L. L.A., Provencio I., Skene D. J., & Brainard G. C. (2014). Measuring and using light in the melanopsin age. Trends in Neurosciences, Volume 37, Issue 1, Pages 1-9, ISSN 0166-2236, https://doi.org/10.1016/j.tins.2013.10.004.

[18] Panda S., Provencio I., Tu D. C., Pires S. S., Rollag M. D., Castrucci A. M., Pletcher M. T., Sato T. K., Wiltshire T., Andahazy M., Kay S. A., Van Gelder R. N., & Hogenesch J. B. (2003). Melanopsin is

required for non-image-forming photic responses in blind mice. Science, 301, pp. 525-527, 10.1126/science.1086179

[19] Ruby N.F. (2002). Role of Melanopsin in circadian responses to light. Science (80-.), 298, pp. 2211-2213, 10.1126/science.1076701

[20] Jagannath A., Hughes S., Abdelgany A., Pothecary C. A., Di Pretoro S., Pires S. S., Vachtsevanos A., Pilorz V., Brown L. A., Hossbach M., MacLaren R. E., Halford S., Gatti S., Hankins M. W., Wood M. J., Foster R. G., & Peirson S. N. (2015). Isoforms of Melanopsin Mediate Different Behavioral Responses to Light. Current biology: CB, 25(18), 2430–2434. https://doi.org/10.1016/j.cub.2015.07.071

[21] Cho Y., Ryu S. H., Lee B. R., Kim K. H., Lee E, & Choi J. (2015). Effects of artificial light at night on human health: A literature review of observational and experimental studies applied to exposure assessment. Chronobiol Int. 32(9):1294-310. doi: 10.3109/07420528.2015.1073158. Epub 2015 Sep 16. PMID: 26375320.

[22] Kim Y. J., Lee E., Lee H. S., Kim M., & Park M.S. (2015). High prevalence of breast cancer in light polluted areas in urban and rural regions of South Korea: An ecologic study on the treatment prevalence of female cancers based on National Health Insurance data. Chronobiol Int. Jun;32(5):657-67. doi: 10.3109/07420528.2015.1032413. Epub 2015 May 8. PMID: 25955405.

[23] Kozaki T., Kubokawa A., Taketomi R., & Hatae K. (2016). Light-induced melatonin suppression at night after exposure to different wavelength composition of morning light. Neurosci Lett. Mar 11;616:1-4. doi: 10.1016/j.neulet.2015.12.063. Epub 2016 Jan 14. PMID: 26777427.

[24] Legates T.A., Fernandez D.C., & Hattar S. (2014) Light as a central modulator of circadian rhythms, sleep and affect. Nat Rev Neurosci. 15(7):443-454. doi:10.1038/nrn3743[25] Hurley S., Goldberg D., Nelson D., Hertz A., Horn-Ross P. L., Bernstein L., & Reynolds, P. (2014). Light at night and breast cancer risk among California teachers. Epidemiology (Cambridge, Mass.), 25(5), 697–706. https://doi.org/10.1097/EDE.0000000000000137

[26] Cajochen C., Münch M., Kobialka S., Kräuchi K., Steiner R., Oelhafen P., Orgül S., & Wirz-Justice A. (2005). High sensitivity of human melatonin, alertness, thermoregulation, and heart rate to short wavelength light. J Clin Endocrinol Metab. Mar;90(3):1311-6. doi: 10.1210/jc.2004-0957. Epub 2004 Dec 7. PMID: 15585546.

[27] Vandewalle G., Maquet P., & Dijk D. J. (2009) Light as a modulator of cognitive brain function. Trends Cogn Sci. Oct;13(10):429-38. doi: 10.1016/j.tics.2009.07.004. Epub 2009 Sep 12. PMID: 19748817.

[28] Duda M., Domagalik A., Orlowska-Feuer P., Krzysztynska-Kuleta O., Beldzik E., Smyk M. K., Stachurska A., Oginska H., Jeczmien-Lazur J. S., Fafrowicz M., Marek T., Lewandowski M. H., & Sarna T. (2020) Melanopsin: From a small molecule to brain functions. Neurosci Biobehav Rev. Jun;113:190-203. doi: 10.1016/j.neubiorev.2020.03.012. Epub 2020 Mar 13. PMID: 32173405.

[29] Cajochen C., Frey S., Anders D., Späti J., Bues M., Pross A., Mager R., Wirz-Justice A., & Stefani O. (1985). Evening exposure to a light-emitting diodes (LED)-backlit computer screen affects circadian physiology and cognitive performance. J Appl Physiol. 2011 May;110(5):1432-8. doi: 10.1152/japplphysiol.00165.2011. Epub 2011 Mar 17. PMID: 21415172.

[30] Chang A. M., Aeschbach D., Duffy J. F., &Czeisler C. A. (2015) Evening use of light-emitting eReaders negatively affects sleep, circadian timing, and next-morning alertness. Proc. Natl. Acad. Sci. U. S. A., 112, pp. 1232-1237, 10.1073/pnas.1418490112

[31] Hysing M., Pallesen M., Stormark K. M., Jakobsen R., Lundervold A. J., & Sivertsen B. (2015) Sleep and use of electronic devices in adolescence: results from a large population-based study. BMJ Open, 5, Article e006748, 10.1136/bmjopen-2014-006748

[32] Van der Lely S., Frey S., Garbazza C., Wirz-Justice A., Jenni O. G., Steiner R., Wolf S., Cajochen C., Bromundt V., & Schmidt C. (2015) Blue blocker glasses as a countermeasure for alerting effects of

evening light-emitting diode screen exposure in male teenagers. J Adolesc Health. Jan;56(1):113-9. doi: 10.1016/j.jadohealth.2014.08.002. Epub 2014 Oct 3. PMID: 25287985.

[33] Kimberly B., & James R.P. (2009) Amber lenses to block blue light and improve sleep: a randomized trial. Chronobiol. Int., 26, pp. 1602 1612, 10.3109/07420520903523719

[34] Buhr E.D., Vemaraju S., Diaz N., Lang R.A., & Van Gelder R.N. (2019) Neuropsin (OPN5) Mediates Local Light-Dependent Induction of Circadian Clock Genes and Circadian Photoentrainment in Exposed Murine Skin. Curr Biol. 2019 Oct 21;29(20):3478-3487.e4. doi: 10.1016/j.cub.2019.08.063. Epub 2019 Oct 10. PMID: 31607531; PMCID: PMC6814305.

[35] Kojima D., Mori S., Torii M., Wada A.,Morishita R., & Fukada Y. (2011) UV-sensitive photoreceptor protein OPN5 in humans and mice. PLoS ONE, 6, p. e26388

[36] Jiang X., Pardue M. T., Mori K., Ikeda S. I., Torii H., D'Souza S., Lang R. A., Kurihara T., & Tsubota K. (2021). Violet light suppresses lens-induced myopia via neuropsin (OPN5) in mice. Proc Natl Acad Sci U S A. Jun 1;118(22):e2018840118. doi: 10.1073/pnas.2018840118. PMID: 34031241; PMCID: PMC8179197.

[37] Zhang K. X., D'Souza S., Upton B. A., Kernodle S., Vemaraju S., Nayak G., Gaitonde K. D., Holt A. L., Linne C. D., Smith A. N., Petts N. T., Batie M., Mukherjee R., Tiwari D., Buhr E. D., Van Gelder R. N., Gross C., Sweeney A., Sanchez-Gurmaches J., Seeley R. J., & Lang R. A. (2020). Violet-light suppression of thermogenesis by opsin 5 hypothalamic neurons. Nature. 2020 Sep;585(7825):420-425. doi: 10.1038/s41586-020-2683-0. Epub Sep 2. PMID: 32879486; PMCID: PMC8130195.

[38] Buhr E. D., Yue W. W., Ren X., Jiang Z., Liao H. W., Mei X., Vemaraju S., Nguyen M. T., Reed R. R., Lang R. A., Yau K. W., & Van Gelder R. N. (2015). Neuropsin (OPN5)-mediated photoentrainment of local circadian oscillators in mammalian retina and cornea. Proc Natl Acad Sci U S A. 2015 Oct 20;112(42):13093-8. doi: 10.1073/pnas.1516259112. Epub Sep 21. PMID: 26392540; PMCID: PMC4620855.

[39] IES (Illuminating Engineering Society). (2016). “Lighting for Hospitals and Healthcare Facilities.” ANSI/IES RP-28–16, Revised. New York, NY.

[40] DiLaura D. L., Houser K. W., Mistrick R. G., Steffy G. R. (2011) The Lighting Handbook, 10th Ed, IES.

[41] Illuminating Engineering Society. (2020). IES RP-29 RECOMMENDED PRACTICE: LIGHTING HOSPITAL AND HEALTHCARE FACILITIES.11 October 2020

[42] Consensus Committee on Recommended Design Standards for Advanced Neonatal Care. (2019). Recommended Standards for Newborn ICU Design, Ninth Edition. Report of the Ninth Consensus Conference on Newborn ICU Design, Clearwater Beach, Florida. March 5.

[43] International WELL Building Institute. (2018). Melanopic Ratio.xls. http://standard.wellcertified.com/tables# melanopic Ratio.

[44] Mardaljevic J., Andersen M., Roy N., & Christoffersen J. (2013). A framework for predicting the non-visual effects of daylight – Part II: The simulation model. Lighting Research and Technology, 46(4), 388-406.

[45] Anderson G. P., Clough S. A., Kneizys F. X., Chetwynd J. H., & Shettle E. P. (1986). AFGL (Air Force Geophysical Laboratory) atmospheric constituent profiles (0. 120km), Environmental research papers, United States. https://www.osti.gov/biblio/6862535.

[46] Lucas R., Peirson S., Berson D., Brown T., Cooper H., Czeisler C., Figueiro M., Gamlin P., Lockley S., O’Hagan J., Price L., Provencio I., Skene D., & Brainard G. (2014). “Irradiance Toolbox” . http://lucasgroup.lab.manchester.ac.uk/research/me asuringmelanopicilluminance/.

[47] International WELL Building Institute. (2017) The WELL Performance Verification Guidebook, Q1, 2022. https://v2.wellcertified.com/en/wellv2/overview

[48] Honsberg C.B, & Bowden S.G. (2019) Photovoltaics Education Website. www.pveducation.org.

[49] Walker P., & & United States. National Aeronautics Space Administration. (1989). Measurement of the light flux density patterns from luminaires proposed as photon sources for photosynthesis during space travel. NASA contractor report; NASA CR-186124. Washington, DC, United States. National Aeronautics Space Administration.

[50] Consensus Committee on Recommended Design Standards for Advanced Neonatal Care. (2019). Recommended Standards for Newborn ICU Design, Ninth Edition. Report of the Ninth Consensus Conference on Newborn ICU Design, Clearwater Beach, Florida. March 5.

[51] Wilkerson A., Safranek S., Irvin L., & Tredinnick L. (2022): Lighting System Control Data to Improve Design and Operation: Tunable Lighting System Data from NICU Patient Rooms, LEUKOS, DOI: 10.1080/15502724.2022.2059669

[52] Neonatology Today. (2021) Peer Reviewed Research, News and Information in Neonatal and Perinatal Medicine. Volume 16, Issue 9, September.

[53] Duarte I., Rotter, A., Malvestiti A., & Hafner M. (2009). The role of glass as a barrier against the transmission of ultraviolet radiation: An experimental study. Photodermatology, photoimmunology & photomedicine. 25. 181-4. 10.1111/j.1600-0781.2009.00434.x.

[54] Wyszecki G., & Stiles W.S. (2000) Color Science: Concepts and Methods, Quantitative Data and Formulae, New York: John Wiley and Sons.

[55] Berns R., & Reiman D. (2002). Color managing the 3rd edition of Billmeyer and Saltzman's Principles of Color Technology. Color Research & Application. 27. 360 - 373. 10.1002/col.10083.

[56] Hall R. (1989). Illumination and Color in Computer Generated Imagery, New York: Springler-Verlag.

[57] Inanici M. (2004). Transformations in Architectural Lighting Analysis: Virtual Lighting Laboratory. Dissertation: The University of Michigan, College of Architecture and Urban Planning. Available from: ProQuest Information and Learning, Ann Arbor, MI; AAT 3121949.

[58] Rea M., (Ed.) (1999). Lighting Handbook Reference & Application, Illuminating Engineering Society of North America.

[59] Devlin K., Chalmers A., Wilkie A., & Purgathofer W. (2002). Tone reproduction and physically based spectral rendering. Eurographics.

[60] Ward, G. (1994). The RADIANCE Lighting Simulation and Rendering System. Computer Graphics. July.

[61] *Lars*on G.W., Shakespeare R. A., Bennewitz P.A., Ehrlich C. , Mardaljevic J., & Phillips E. (1998). Rendering with Radiance, The Art and Science of Lighting Visualization. Morgan Kaufmann Publishers.ISBN 0-9745381-0-8 replaces the now out-of-print first edition ISBN 1-55860-499-5

[62] Inanici M, Brennan M, & Clark E. (2015). Multispectral Lighting Simulations: Computing Circadian Light. International Building Performance Simulation Association (IBPSA) 2015 Conference, Hyderabad, India.

[63] Inanici M., & ZGF Architects LLP. (2015). Lark spectral lighting. https://faculty.washington.edu/inanici/Lark/Lark_home_page.html

[64] Solemma, ALFA (Adaptive Lighting for Alertness). (2017). Retrieved June 15 2021 from https://www.solemma.com/Alfa.html.

[65] McNeel, R. et al. (2010). Grasshopper generative modeling for rhino. Computer software (2011b),12 http://www.grasshopper3d.com.

[66] Balakrishnan P., Jakubiec J. A. (2019). Spectral Rendering with Daylight: A Comparison of Two Spectral Daylight Simulation Platforms. Singapore University of Technology and Design, Singapore. University of Toronto, Toronto, Canada.

[67] Ruppertsberg A. I., & Bloj M. (2008). Creating Physically Accurate Visual Stimuli for Free: Spectral Rendering with Radiance. Behaviour and Research methods, 40(1), 304-308.

[68] Inanici M., Abboushi B., & Safranek S. (in print, 2022). Evaluation of Sky Spectra and Sky Models in Daylighting Simulations. Lighting Research & Technology.

[69] Pierson C., Aarts M., & Andersen M. (2021). Validation of Spectral Simulation Tools for the Prediction of Indoor Daylight Exposure. 17th International IBPSA Building Simulation Conference Book of Abstracts. P8

[70] Balakrishnan P., & Jakubiec A. (2019). Spectral Rendering with Daylight: A Comparison of Two Spectral Daylight Simulation Platforms. Singapore University of Technology and Design, Singapore. University of Toronto, Toronto, Canada.

[71] Jakubiec A. (2021). Evaluating the use of photobiology-driven alertness and health measures for circadian lighting design. IBPSA.

[72] Mayer B, & Kylling A. (2005). Technical note: The libRadtran software package for radiative transfer calculations - description and examples of use. Atmospheric Chemistry and Physics, 5 (7). 1855-1877 doi:10.5194/acp-5-1855-2005

[73] Pechacek C. S., Andersen M., & Lockley S. W. (2008). Prospective evaluation of the Circadian Efficacy of (Day)Light in Rooms. Leukos, the Journal of the Illuminating Engineering Society, 5(1), 1-26.

[74] U.S. Environmental Protection Agency. (1989). Report to Congress on indoor air quality: Volume 2. EPA/400/1-89/001C. Washington, DC.

[75] Spectral sky models for advanced daylight simulations. IEA SHC Task 61 / EBC Annex 77: Integrated Solutions for Daylighting and Electric Lighting. https://www.iea-shc.org/Data/Sites/1/publications/IEA-SHC-Task61--Technical-Report-C3-Spectral-sky-models.pdf

[76] Klepeis N. E., Nelson W. C., Ott W. R., Robinson J. P., Tsang A.M., Switzer P., Behar J.V., Hern S.C., & Engelmann W.H. (2001). The National Human Activity Pattern Survey (NHAPS): A Resource for Assessing Exposure to Environmental Pollutants. Lawrence Berkeley National Laboratory.

[77] Diakite-Kortlever A., Balakrishnan P., Darula S., Geisler-Moroder D., Jakubiec J., Knoop M., Luo T., Seckmeyer G., Tobar M., Wang T., Wienold J., & Ward G. (2022). Spectral sky models for advanced daylight simulations. IEA SHC Task 61 / EBC Annex 77 Subtask C3. 10.18777/ieashc-task61-2021-0005.

[78] Mansencal T., Mauderer M., Parsons M., Shaw N., Wheatley K., Cooper S., Vandenberg J.D., Canavan L., Crowson K., Lev O., Leinweber K., Sharma S., Sobotka T.J., Moritz D., Pppp M., Rane C., Eswaramoorthy P., Mertic J., Pearlstine B., Leonhardt M., Niemitalo O., Szymanski M., Schambach M., Huang S., Wei M., Joywardhan N., Wagih O., Redman P., Goldstone J., Hill S., Smith J., Savoir F., Saxena G., Chopra S., Sibiryakov I., Gates T., Pal G., Tessore N., & Pierre A. (2020) Colour Science for Python. https://www.colour-science.org/

[79] Berkeley Lab. Optics 6. Windows and Daylighting, Berkeley LaBuilding Technology & Urban System. https://windows.lbl.gov/software/optics.

[80] Spectral Material Database. https://www.spectraldb.com/

[81] Personal communication with Mehlika Inanici

[82] Inanici M., Brennan M., & Clark E. (2015) Spectral Daylighting Simulations: Computing Circadian Light.

[83] ATG rooftop data for June 2021. Department of Atmosphere. University of Washington. https://a.atmos.washington.edu/data/data.php?loc=local